Theoretical Aspects of Higgs Physics

V. Ravindran

Institute of Mathematical Sciences, Chennai

- Higgs phenomenon
- Unitarity, vacuum stability ...
- Why N^iLO for Higgs
- Higgs with Jets, tops
- Higgs Characterisation
- Conclusion

What is next at LHC, TIFR, Jan 6-9, 2014.

Scalar field and Yukawa sectors in the SM

- Gauge principle in Quantum field theory provides framework to study interaction of elementary particles
- Gauge symmetry severely constraints the mass terms of gauge fields and matter fields.
- Higgs mechanism provides a recipe to understand why $\boldsymbol{Ws}$ and $\boldsymbol{Z}$ have masses without spoiling gauge symmetry

Scalar field and Yukawa sectors in the SM

- Gauge principle in Quantum field theory provides framework to study interaction of elementary particles
- Gauge symmetry severely constraints the mass terms of gauge fields and matter fields.
- Higgs mechanism provides a recipe to understand why Ws and Z have masses without spoiling gauge symmetry

- It is done through the introduction of complex scalar field through $SU(2)_L \times U(1)_Y$ gauge invariant Lagrangian:

$$\mathcal{L}_\Phi = (\mathcal{D}_\mu \Phi)^\dagger \mathcal{D}^\mu \Phi - V(\Phi), \qquad \Phi = \begin{pmatrix} \Phi^+ \\ \Phi^0 \end{pmatrix}$$

Scalar field and Yukawa sectors in the SM

- Gauge principle in Quantum field theory provides framework to study interaction of elementary particles
- Gauge symmetry severely constraints the mass terms of gauge fields and matter fields.
- Higgs mechanism provides a recipe to understand why Ws and Z have masses without spoiling gauge symmetry

● It is done through the introduction of complex scalar field through $SU(2)_L \times U(1)_Y$ gauge invariant Lagrangian:

$$\mathcal{L}_\Phi = (\mathcal{D}_\mu \Phi)^\dagger \mathcal{D}^\mu \Phi - V(\Phi), \qquad \Phi = \begin{pmatrix} \Phi^+ \\ \Phi^0 \end{pmatrix}$$

where

$$\mathcal{D}_\mu \Phi = \left(\partial_\mu - \frac{i}{2} g \tau \cdot \mathcal{A}_\mu - \frac{i}{2} g' B_\mu\right)\Phi$$

$$V(\Phi) = -\mu^2 \Phi^\dagger \Phi + \lambda (\Phi^\dagger \Phi)^2 \qquad \mu^2 > 0$$

Scalar field and Yukawa sectors in the SM

- Gauge principle in Quantum field theory provides framework to study interaction of elementary particles

- Gauge symmetry severely constraints the mass terms of gauge fields and matter fields.

- Higgs mechanism provides a recipe to understand why $W s$ and Z have masses without spoiling gauge symmetry

- It is done through the introduction of complex scalar field through $SU(2)_L \times U(1)_Y$ gauge invariant Lagrangian:

$$\mathcal{L}_\Phi = (\mathcal{D}_\mu \Phi)^\dagger \mathcal{D}^\mu \Phi - V(\Phi), \qquad \Phi = \begin{pmatrix} \Phi^+ \\ \Phi^0 \end{pmatrix}$$

where

$$\mathcal{D}_\mu \Phi = \left(\partial_\mu - \frac{i}{2} g \tau \cdot \mathcal{A}_\mu - \frac{i}{2} g' B_\mu \right) \Phi$$

$$V(\Phi) = -\mu^2 \Phi^\dagger \Phi + \lambda (\Phi^\dagger \Phi)^2 \qquad \mu^2 > 0$$

- The $SU(2)_L \times U(1)_Y$ invariant Yukawa interaction Lagrangian is given by

$$\mathcal{L}_Y = Y_e \overline{L} \Phi e_R + Y_u \overline{Q}_L \tilde{\Phi} u_R + Y_d \overline{Q}_L \Phi d_R + h.c$$

where $\tilde{\Phi} = i\tau_2 \Phi^*$ with $Y(\tilde{\Phi}) = -1$

Spontaneous Symmetry Breaking in the SM

Scalar potential $\mu^2 > 0$ derives the vacuum to have non-zero vacuum expectation value

$$|<\Omega|\Phi|\Omega>| = \begin{pmatrix} 0 \\ \frac{v}{\sqrt{2}} \end{pmatrix} \qquad v = \sqrt{\frac{\mu^2}{\lambda}}$$

Spontaneous Symmetry Breaking in the SM

Scalar potential $\mu^2 > 0$ derives the vacuum to have non-zero vacuum expectation value

$$| < \Omega|\Phi|\Omega > | = \begin{pmatrix} 0 \\ \frac{v}{\sqrt{2}} \end{pmatrix} \qquad v = \sqrt{\frac{\mu^2}{\lambda}}$$

Parameterise $\Phi(x)$ in terms of four real fields $h(x), \zeta^1(x), \zeta^2(x), \zeta^3(x)$ as

$$\Phi(x) \quad = \quad U^{-1}(\zeta) \begin{pmatrix} 0 \\ \frac{v+h(x)}{\sqrt{2}} \end{pmatrix}, \qquad U(\zeta) = \exp(-i\zeta(x) \cdot \tau/v)$$

Spontaneous Symmetry Breaking in the SM

Scalar potential $\mu^2 > 0$ derives the vacuum to have non-zero vacuum expectation value

$$|<\Omega|\Phi|\Omega>| = \begin{pmatrix} 0 \\ \frac{v}{\sqrt{2}} \end{pmatrix} \qquad v = \sqrt{\frac{\mu^2}{\lambda}}$$

Parameterise $\Phi(x)$ in terms of four real fields $h(x), \zeta^1(x), \zeta^2(x), \zeta^3(x)$ as

$$\Phi(x) \quad = \quad U^{-1}(\zeta)\begin{pmatrix} 0 \\ \frac{v+h(x)}{\sqrt{2}} \end{pmatrix}, \qquad U(\zeta) = \exp(-i\zeta(x)\cdot\tau/v)$$

such that

$$<\Omega|\zeta_i|\Omega> = <\Omega|h|\Omega> = 0$$

Spontaneous Symmetry Breaking in the SM

Scalar potential $\mu^2 > 0$ derives the vacuum to have non-zero vacuum expectation value

$$|<\Omega|\Phi|\Omega>| = \begin{pmatrix} 0 \\ \frac{v}{\sqrt{2}} \end{pmatrix} \qquad v = \sqrt{\frac{\mu^2}{\lambda}}$$

Parameterise $\Phi(x)$ in terms of four real fields $h(x), \zeta^1(x), \zeta^2(x), \zeta^3(x)$ as

$$\Phi(x) \quad = \quad U^{-1}(\zeta) \begin{pmatrix} 0 \\ \frac{v+h(x)}{\sqrt{2}} \end{pmatrix}, \qquad U(\zeta) = \exp(-i\zeta(x) \cdot \tau/v)$$

such that

$$<\Omega|\zeta_i|\Omega>=<\Omega|h|\Omega>= 0$$

The $\zeta_i(x)$ fields can be gauged away by the unitary gauge transformations

$$\Phi^U = U(\zeta)\Phi = \begin{pmatrix} 0 \\ \frac{v+h(x)}{\sqrt{2}} \end{pmatrix} = \frac{v+h(x)}{\sqrt{2}}\ \chi \qquad \chi = \begin{pmatrix} 0 \\ 1 \end{pmatrix}$$

Spontaneous Symmetry Breaking in the SM

Scalar potential $\mu^2 > 0$ derives the vacuum to have non-zero vacuum expectation value

$$|<\Omega|\Phi|\Omega>| = \begin{pmatrix} 0 \\ \frac{v}{\sqrt{2}} \end{pmatrix} \qquad v = \sqrt{\frac{\mu^2}{\lambda}}$$

Parameterise $\Phi(x)$ in terms of four real fields $h(x), \zeta^1(x), \zeta^2(x), \zeta^3(x)$ as

$$\Phi(x) \quad = \quad U^{-1}(\zeta) \begin{pmatrix} 0 \\ \frac{v+h(x)}{\sqrt{2}} \end{pmatrix}, \qquad U(\zeta) = \exp(-i\zeta(x) \cdot \tau/v)$$

such that

$$<\Omega|\zeta_i|\Omega> = <\Omega|h|\Omega> = 0$$

The $\zeta_i(x)$ fields can be gauged away by the unitary gauge transformations

$$\Phi^U = U(\zeta)\Phi = \begin{pmatrix} 0 \\ \frac{v+h(x)}{\sqrt{2}} \end{pmatrix} = \frac{v + h(x)}{\sqrt{2}} \chi \qquad \chi = \begin{pmatrix} 0 \\ 1 \end{pmatrix}$$

- $\zeta_i(x)$ are called Goldstone bosons (massless,spinless)
- $h(x)$ is called the Higgs boson.

Masses of the Higgs boson and the fermions

- Scalar potential $V(\Phi)$ in the unitary gauge becomes

$$V(\Phi) = V(h) = \mu^2 h^2 + \lambda v h^3 + \frac{\lambda}{4} h^4$$

Masses of the Higgs boson and the fermions

- Scalar potential $V(\Phi)$ in the unitary gauge becomes

$$V(\Phi) = V(h) = \mu^2 h^2 + \lambda v h^3 + \frac{\lambda}{4} h^4$$

The mass of the h field (Higgs boson) is given by

$$\boxed{m_h^2 = 2\mu^2 = 2\lambda v^2}$$

Masses of the Higgs boson and the fermions

- Scalar potential $V(\Phi)$ in the unitary gauge becomes

$$V(\Phi) = V(h) = \mu^2 h^2 + \lambda v h^3 + \frac{\lambda}{4} h^4$$

The mass of the h field (Higgs boson) is given by

$$\boxed{m_h^2 = 2\mu^2 = 2\lambda v^2}$$

- The Yukawa part of the Lagrangian in the Unitary gauge is given by

$$\mathcal{L}_Y \quad = \quad \left(\frac{h(x)+v}{\sqrt{2}}\right)\left(Y_e\, \overline{e}_L^U\, e_R^U + Y_u\, \overline{u}_L^U\, u_R^U + Y_d\, \overline{d}_L^U\, d_R^U\right) + h.c$$

Masses of the Higgs boson and the fermions

- Scalar potential $V(\Phi)$ in the unitary gauge becomes

$$V(\Phi) = V(h) = \mu^2 h^2 + \lambda v h^3 + \frac{\lambda}{4} h^4$$

The mass of the h field (Higgs boson) is given by

$$\boxed{m_h^2 = 2\mu^2 = 2\lambda v^2}$$

- The Yukawa part of the Lagrangian in the Unitary gauge is given by

$$\mathcal{L}_Y \quad = \quad \left(\frac{h(x) + v}{\sqrt{2}}\right)\left(Y_e\, \overline{e}_L^U e_R^U + Y_u\, \overline{u}_L^U u_R^U + Y_d\, \overline{d}_L^U d_R^U\right) + h.c$$

The fermions masses and their interaction with $h(x)$

$$\boxed{m_i = \frac{Y_i v}{\sqrt{2}}}, \qquad i = e, u, d, \qquad h(x)\overline{Q}Q \Longrightarrow i\,\frac{m_Q}{v} \qquad Q = \tau, b, t$$

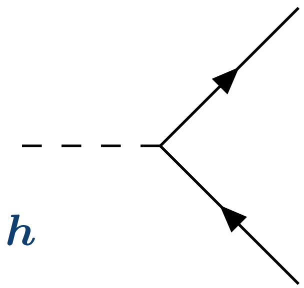

Masses of the Higgs boson and the fermions

- Scalar potential $V(\Phi)$ in the unitary gauge becomes

$$V(\Phi) = V(h) = \mu^2 h^2 + \lambda v h^3 + \frac{\lambda}{4} h^4$$

The mass of the h field (Higgs boson) is given by

$$\boxed{m_h^2 = 2\mu^2 = 2\lambda v^2}$$

- The Yukawa part of the Lagrangian in the Unitary gauge is given by

$$\mathcal{L}_Y \quad = \quad \left(\frac{h(x) + v}{\sqrt{2}}\right)\left(Y_e\, \overline{e}_L^U e_R^U + Y_u\, \overline{u}_L^U u_R^U + Y_d\, \overline{d}_L^U d_R^U\right) + h.c$$

The fermions masses and their interaction with $h(x)$

$$\boxed{m_i = \frac{Y_i v}{\sqrt{2}}}, \qquad i = e, u, d, \qquad h(x)\overline{Q}Q \Longrightarrow i\,\frac{m_Q}{v} \qquad Q = \tau, b, t$$

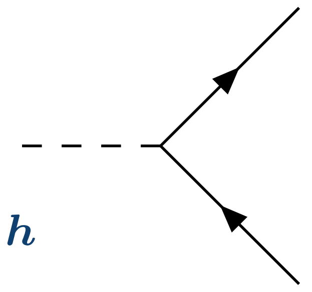

Masses and Vertices of $W^{\pm}, Z, \gamma$ bosons

$$|\mathcal{D}_\mu \Phi|^2 \quad \Longrightarrow \quad \frac{v^2}{8}\left(1+\frac{h(x)}{v}\right)^2\left(g^2\left[(\mathcal{A}_\mu^{U1})^2+(\mathcal{A}_\mu^{U2})^2\right]+\left[g\mathcal{A}_\mu^{U3}-g'B_\mu^{U})^2\right]\right)$$

Masses and Vertices of $W^{\pm}, Z, \gamma$ bosons

$$|\mathcal{D}_\mu \Phi|^2 \quad \Longrightarrow \quad \frac{v^2}{8}\left(1+\frac{h(x)}{v}\right)^2 \left(g^2\left[(\mathcal{A}_\mu^{U1})^2+(\mathcal{A}_\mu^{U2})^2\right]+\left[g\mathcal{A}_\mu^{U3}-g' B_\mu^U)^2\right]\right)$$

$$W_\mu^{\pm}=\frac{1}{\sqrt{2}}(\mathcal{A}_\mu^{U1}\mp i\mathcal{A}_\mu^{U2}), \qquad Z_\mu = \cos\theta_W \mathcal{A}_\mu^{U3}-\sin\theta_W B_\mu^U \qquad \theta_W - \text{Weinberg} \quad \text{ang}$$

$$A_\mu = \sin\theta_W \mathcal{A}_\mu^{U3}+\cos\theta_W B_\mu^U\,, \qquad \tan\theta_W=\frac{g'}{g},$$

Masses and Vertices of $W^\pm, Z, \gamma$ bosons

$$|\mathcal{D}_\mu \Phi|^2 \quad \Longrightarrow \quad \frac{v^2}{8}\left(1+\frac{h(x)}{v}\right)^2 \left(g^2\left[(\mathcal{A}_\mu^{U1})^2+(\mathcal{A}_\mu^{U2})^2\right]+\left[g\mathcal{A}_\mu^{U3}-g' B_\mu^U)^2\right]\right)$$

$$W_\mu^\pm = \frac{1}{\sqrt{2}}(\mathcal{A}_\mu^{U1} \mp i\mathcal{A}_\mu^{U2}), \qquad Z_\mu = \cos\theta_W \mathcal{A}_\mu^{U3} - \sin\theta_W B_\mu^U \qquad \theta_W - \text{Weinberg} \quad \text{ang}$$

$$A_\mu = \sin\theta_W \mathcal{A}_\mu^{U3} + \cos\theta_W B_\mu^U\,, \qquad \tan\theta_W = \frac{g'}{g},$$

$$|\mathcal{D}_\mu \Phi|^2 \quad \Longrightarrow \quad \frac{1}{2} M_W^2 W_\mu^+ W^{-\mu}\left(1+\frac{h(x)}{v}\right)^2$$

$$+\left[\frac{1}{2} M_Z^2\, Z^\mu Z_\mu + \frac{1}{2} \quad \text{“0”} \quad A_\mu A^\mu\right]\left(1+\frac{h(x)}{v}\right)^2$$

Masses and Vertices of $W^\pm, Z, \gamma$ bosons

$$|\mathcal{D}_\mu \Phi|^2 \quad \Longrightarrow \quad \frac{v^2}{8}\left(1+\frac{h(x)}{v}\right)^2 \left(g^2\left[(\mathcal{A}_\mu^{U1})^2 + (\mathcal{A}_\mu^{U2})^2\right] + \left[g\mathcal{A}_\mu^{U3} - g' B_\mu^U)^2\right]\right)$$

$$W_\mu^\pm = \frac{1}{\sqrt{2}}(\mathcal{A}_\mu^{U1} \mp i\mathcal{A}_\mu^{U2}), \qquad Z_\mu = \cos\theta_W \mathcal{A}_\mu^{U3} - \sin\theta_W B_\mu^U \qquad \theta_W - \text{Weinberg ang}$$

$$A_\mu = \sin\theta_W \mathcal{A}_\mu^{U3} + \cos\theta_W B_\mu^U, \qquad \tan\theta_W = \frac{g'}{g},$$

$$|\mathcal{D}_\mu \Phi|^2 \quad \Longrightarrow \quad \frac{1}{2} M_W^2 W_\mu^+ W^{-\mu} \left(1+\frac{h(x)}{v}\right)^2 + \left[\frac{1}{2} M_Z^2 \, Z^\mu Z_\mu + \frac{1}{2} \quad \text{“0”} \quad A_\mu A^\mu\right]\left(1+\frac{h(x)}{v}\right)^2$$

where the masses of $W^\pm, Z, \gamma$ bosons:

$$\boxed{M_W^2 = \frac{g^2 v^2}{4}, \qquad M_Z^2 = \frac{v^2}{4}(g^2 + g'^2), \qquad M_\gamma = 0}$$

The vertices are

$$h(x) V_{i\mu} V_i^{*\mu} \quad \Longrightarrow \quad 2i\frac{M_i^2}{v} g_{\mu\nu}, \qquad h(x)h(x) V_{i\mu} V_i^{*\mu} \quad \Longrightarrow \quad 2i\frac{M_{V_i}^2}{v^2} g_{\mu\nu}$$

Standard Model today

Standard Model today

- Tests of Standard Model of Strong,Electroweak interactions:

$$SU(3)_C \otimes SU(2)_L \otimes U(1)_Y$$

have been incredibly successful.

Standard Model today

- Tests of Standard Model of Strong,Electroweak interactions:

$$SU(3)_C \otimes SU(2)_L \otimes U(1)_Y$$

have been incredibly successful.

1) Discovery of all the gauge bosons ($W^{\pm}, Z, gluon$), all the fermions ($c, b, t, \tau...$),

2) Precise measurements of SM parameters at 0.1% level effects($\alpha_{em}, g-2, m_W, m_t$,....).

Standard Model today

- Tests of Standard Model of Strong,Electroweak interactions:

$$SU(3)_C \otimes SU(2)_L \otimes U(1)_Y$$

have been incredibly successful.

1) Discovery of all the gauge bosons ($W^{\pm}, Z, gluon$), all the fermions ($c, b, t, \tau...$),

2) Precise measurements of SM parameters at 0.1% level effects($\alpha_{em}, g-2, m_W, m_t$,....).

- The $3/4$ of this Higgs field, called "would be Goldstone bosons":

$$w_1(x), w_2(x), z(x)$$

reappear as longitudinal components of $W^{\pm}$ and Z respectively.

- The remaining $1/4$ is nothing but the Higgs boson, $h(x)$ and it has been observed at the LHC.

Standard Model today

- Tests of Standard Model of Strong,Electroweak interactions:

$$SU(3)_C \otimes SU(2)_L \otimes U(1)_Y$$

  have been incredibly successful.

  1) Discovery of all the gauge bosons ($W^{\pm}, Z, gluon$), all the fermions ($c, b, t, \tau...$),

  2) Precise measurements of SM parameters at 0.1% level effects($\alpha_{em}, g-2, m_W, m_t$,....).

- The $3/4$ of this Higgs field, called "would be Goldstone bosons":

$$w_1(x), w_2(x), z(x)$$

  reappear as longitudinal components of $W^{\pm}$ and Z respectively.

- The remaining $1/4$ is nothing but the Higgs boson, $h(x)$ and it has been observed at the LHC.

- But this particle has to pass all the tests to be called Higgs Boson of the SM

Standard Model today

- Tests of Standard Model of Strong,Electroweak interactions:

$$SU(3)_C \otimes SU(2)_L \otimes U(1)_Y$$

have been incredibly successful.

1) Discovery of all the gauge bosons ($W^{\pm}, Z, gluon$), all the fermions ($c, b, t, \tau...$),

2) Precise measurements of SM parameters at 0.1% level effects($\alpha_{em}, g-2, m_W, m_t$,....).

- The $3/4$ of this Higgs field, called "would be Goldstone bosons":

$$w_1(x), w_2(x), z(x)$$

reappear as longitudinal components of $W^{\pm}$ and Z respectively.

- The remaining $1/4$ is nothing but the Higgs boson, $h(x)$ and it has been observed at the LHC.

- But this particle has to pass all the tests to be called Higgs Boson of the SM

Standard Model today

- Tests of Standard Model of Strong,Electroweak interactions:

$$SU(3)_C \otimes SU(2)_L \otimes U(1)_Y$$

  have been incredibly successful.

  1) Discovery of all the gauge bosons ($W^{\pm}, Z, gluon$), all the fermions ($c, b, t, \tau ...$),

  2) Precise measurements of SM parameters at 0.1% level effects($\alpha_{em}, g-2, m_W, m_t$,....).

- The $3/4$ of this Higgs field, called "would be Goldstone bosons":

$$w_1(x), w_2(x), z(x)$$

  reappear as longitudinal components of $W^{\pm}$ and Z respectively.

- The remaining $1/4$ is nothing but the Higgs boson, $h(x)$ and it has been observed at the LHC.

- But this particle has to pass all the tests to be called Higgs Boson of the SM
- I will restrict myself to SM higgs in the rest of the talk and discuss the physics that revolves around it.

Standard Model today

- Tests of Standard Model of Strong,Electroweak interactions:

$$SU(3)_C \otimes SU(2)_L \otimes U(1)_Y$$

have been incredibly successful.

1) Discovery of all the gauge bosons ($W^{\pm}, Z, gluon$), all the fermions ($c, b, t, \tau...$),

2) Precise measurements of SM parameters at 0.1% level effects($\alpha_{em}, g-2, m_W, m_t$,....).

- The $3/4$ of this Higgs field, called "would be Goldstone bosons":

$$w_1(x), w_2(x), z(x)$$

reappear as longitudinal components of $W^{\pm}$ and Z respectively.

- The remaining $1/4$ is nothing but the Higgs boson, $h(x)$ and it has been observed at the LHC.

- But this particle has to pass all the tests to be called Higgs Boson of the SM
- I will restrict myself to SM higgs in the rest of the talk and discuss the physics that revolves around it.

Unitarity and Landau pole

- Longitudinal polarisation of Ws and Zs spoil high energy behaviour of gauge theories without Higgs boson.

Unitarity and Landau pole

- Longitudinal polarisation of Ws and Zs spoil high energy behaviour of gauge theories without Higgs boson.
- When $s \gg M_W^2, m_h^2,\qquad a_0 \to -m_h^2/(8\pi v^2)$

$$\left| -\frac{m_h^2}{8\pi v^2} \right| \leq \frac{1}{2} \quad \Longrightarrow \quad m_h < 2v\sqrt{\pi} = 870 GeV \qquad \text{combined} \quad \text{with} \quad \text{Z} \Longrightarrow \quad 710\; GeV$$

Unitarity and Landau pole

- Longitudinal polarisation of Ws and Zs spoil high energy behaviour of gauge theories without Higgs boson.
- When $s \gg M_W^2, m_h^2,$ $\qquad a_0 \to -m_h^2/(8\pi v^2)$

$$\left| -\frac{m_h^2}{8\pi v^2} \right| \leq \frac{1}{2} \quad \Longrightarrow \quad m_h < 2v\sqrt{\pi} = 870 GeV \quad \text{combined} \quad \text{with} \quad \text{Z} \Longrightarrow \quad 710\ GeV$$

- Finiteness of λ coupling upto a cut off scale of the theory: Droping gauge and Yukawa contributions,

$$\lambda(Q^2) = \frac{\lambda(Q_0^2)}{1 - \frac{3}{4\pi^2}\lambda(Q_0^2)\log\frac{Q^2}{Q_0^2}}$$

Unitarity and Landau pole

- Longitudinal polarisation of Ws and Zs spoil high energy behaviour of gauge theories without Higgs boson.
- When $s \gg M_W^2, m_h^2,\qquad a_0 \to -m_h^2/(8\pi v^2)$

$$\left| -\frac{m_h^2}{8\pi v^2} \right| \leq \frac{1}{2} \quad \Longrightarrow \quad m_h < 2v\sqrt{\pi} = 870 GeV \quad \text{combined} \quad \text{with} \quad Z \Longrightarrow \quad 710\ GeV$$

- Finiteness of λ coupling upto a cut off scale of the theory: Droping gauge and Yukawa contributions,

$$\lambda(Q^2) = \frac{\lambda(Q_0^2)}{1 - \frac{3}{4\pi^2}\lambda(Q_0^2)\log\frac{Q^2}{Q_0^2}}$$

- The Landau pole gives the scale Λ_P given by (choose $Q = \Lambda_P, Q_0 = v$)

$$\Lambda_P = v\exp\left(\frac{2\pi^2}{3\lambda(v^2)}\right) = v\exp\left(\frac{4\pi^2 v^2}{3m_h^2}\right)$$

Unitarity and Landau pole

- Longitudinal polarisation of Ws and Zs spoil high energy behaviour of gauge theories without Higgs boson.
- When $s \gg M_W^2, m_h^2$, $\quad a_0 \to -m_h^2/(8\pi v^2)$

$$\left| -\frac{m_h^2}{8\pi v^2} \right| \leq \frac{1}{2} \quad \Longrightarrow \quad m_h < 2v\sqrt{\pi} = 870 GeV \quad \text{combined} \quad \text{with} \quad \text{Z} \Longrightarrow \quad 710\ GeV$$

- Finiteness of λ coupling upto a cut off scale of the theory: Droping gauge and Yukawa contributions,

$$\lambda(Q^2) = \frac{\lambda(Q_0^2)}{1 - \frac{3}{4\pi^2}\lambda(Q_0^2)\log\frac{Q^2}{Q_0^2}}$$

- The Landau pole gives the scale Λ_P given by (choose $Q = \Lambda_P, Q_0 = v$)

$$\Lambda_P = v \exp\left(\frac{2\pi^2}{3\lambda(v^2)}\right) = v \exp\left(\frac{4\pi^2 v^2}{3m_h^2}\right)$$

- If $\Lambda_P = 10^{19}$ GeV, the higgs has to be light $m_h \leq 145$ GeV.
- If $\Lambda_P = 10^3$ GeV, the higgs has to be heavy $m_h \leq 750$ GeV.

Precision measurements and top mass

Precision measurements and top mass

- Longitudinal polarisations of Ws and Z can give new UV divergences which can not be renormalised away without Higgs field.

Precision measurements and top mass

- Longitudinal polarisations of Ws and Z can give new UV divergences which can not be renormalised away without Higgs field.

- Quantum corrections modify tree level relations among gauge masses and gauge couplings:

$$G_F = \frac{\pi\alpha_{em}}{\sqrt{2}M_W^2(1 - M_W^2/M_Z^2)}\left(1 - \Delta\rho\right)^{-1}$$

$$\Delta\rho_{top} = -\frac{3G_F m_t^2}{8\sqrt{2}\pi^2}\cot^2(\theta_W), \qquad \Delta\rho_W = \frac{11 G_F M_W^2}{24\sqrt{2}\pi^2}\log\left(\frac{m_h^2}{M_W^2}\right)$$

Precision measurements and top mass

- Longitudinal polarisations of Ws and Z can give new UV divergences which can not be renormalised away without Higgs field.

- Quantum corrections modify tree level relations among gauge masses and gauge couplings:

$$G_F = \frac{\pi \alpha_{em}}{\sqrt{2} M_W^2 (1 - M_W^2/M_Z^2)} \Big(1 - \Delta\rho\Big)^{-1}$$

$$\Delta\rho_{top} = -\frac{3 G_F m_t^2}{8\sqrt{2}\pi^2} \cot^2(\theta_W), \qquad \Delta\rho_W = \frac{11 G_F M_W^2}{24\sqrt{2}\pi^2} \log\left(\frac{m_h^2}{M_W^2}\right)$$

- Precision measurements can give bounds on Higgs boson mass.

Precision measurements and top mass

- Longitudinal polarisations of Ws and Z can give new UV divergences which can not be renormalised away without Higgs field.

- Quantum corrections modify tree level relations among gauge masses and gauge couplings:

$$G_F = \frac{\pi \alpha_{em}}{\sqrt{2} M_W^2 (1 - M_W^2/M_Z^2)} \left(1 - \Delta\rho\right)^{-1}$$

$$\Delta\rho_{top} = -\frac{3 G_F m_t^2}{8\sqrt{2}\pi^2} \cot^2(\theta_W), \qquad \Delta\rho_W = \frac{11 G_F M_W^2}{24\sqrt{2}\pi^2} \log\left(\frac{m_h^2}{M_W^2}\right)$$

- Precision measurements can give bounds on Higgs boson mass.

- Bounds are sensitive to top quark mass m_t

Vacuum stability

Vacuum stability

- NNLO computation of various couplings in the SM by Degrassi et.al:

$$m_h \geq 129.2 + 1.8 \times \left(\frac{m_t^{\rm pole} - 173.2\ {\rm GeV}}{0.9\ {\rm GeV}} \right) - 0.5 \times \left(\frac{\alpha_s(M_Z) - 0.1184}{0.0007} \right) \pm 1.0\ {\rm GeV}\,.$$

Vacuum stability

- NNLO computation of various couplings in the SM by Degrassi et.al:

$$\boldsymbol{m_h \geq 129.2 + 1.8 \times \left(\frac{m_t^{\rm pole} - 173.2\ \rm GeV}{0.9\ \rm GeV} \right) - 0.5 \times \left(\frac{\alpha_s(M_Z) - 0.1184}{0.0007} \right) \pm 1.0\ \ \rm GeV\ .}$$

- m_t dependence:

$$\boldsymbol{\Delta m_t = 1\, GeV \qquad \longrightarrow \qquad \Delta m_h = \pm 2\, GeV}$$

2σ variation of the top quark mass allows the upper bound $m_h \geq \mathbf{125.6}$ GeV.

Vacuum stability

- NNLO computation of various couplings in the SM by Degrassi et.al:

$$m_h \geq 129.2 + 1.8 \times \left(\frac{m_t^{\rm pole} - 173.2 \text{ GeV}}{0.9 \text{ GeV}} \right) - 0.5 \times \left(\frac{\alpha_s(M_Z) - 0.1184}{0.0007} \right) \pm 1.0 \text{ GeV} .$$

- m_t dependence:

$$\Delta m_t = 1\, GeV \qquad \longrightarrow \qquad \Delta m_h = \pm 2\, GeV$$

2σ variation of the top quark mass allows the upper bound $m_h \geq 125.6$ GeV.

- Top quark production measurements at Tevatron and NNLO (approx) results give (Alekhin et al):

$$m_t^{\overline{\rm MS}}(m_t) = 163.3 \pm 2.7 \text{ GeV} \qquad \longrightarrow \qquad m_t^{\rm pole} = 173.3 \pm 2.8 \text{ GeV} ,$$

The upper bound for vacuum stability can be realized

$$m_h \geq 129.4 \pm 5.6 \text{ GeV} ,$$

consistent with the recent measurements by ATLAS and CMS thanks to larger error.

Vacuum stability

- NNLO computation of various couplings in the SM by Degrassi et.al:

$$m_h \geq 129.2 + 1.8 \times \left(\frac{m_t^{\text{pole}} - 173.2 \text{ GeV}}{0.9 \text{ GeV}} \right) - 0.5 \times \left(\frac{\alpha_s(M_Z) - 0.1184}{0.0007} \right) \pm 1.0 \text{ GeV} .$$

- m_t dependence:

$$\Delta m_t = 1\, GeV \qquad \longrightarrow \qquad \Delta m_h = \pm 2\, GeV$$

2σ variation of the top quark mass allows the upper bound $m_h \geq 125.6$ GeV.
- Top quark production measurements at Tevatron and NNLO (approx) results give (Alekhin et al):

$$m_t^{\overline{\text{MS}}}(m_t) = 163.3 \pm 2.7 \text{ GeV} \qquad \longrightarrow \qquad m_t^{\text{pole}} = 173.3 \pm 2.8 \text{ GeV} ,$$

The upper bound for vacuum stability can be realized

$$m_h \geq 129.4 \pm 5.6 \text{ GeV} ,$$

consistent with the recent measurements by ATLAS and CMS thanks to larger error.
- Global average has small error

$$m_t^{\text{exp}} = 173.2 \pm 0.9 \text{ GeV} .$$

which can give stringiant condition on vacuum stability with small error on the higgs mass.

Vacuum stability

Vacuum stability

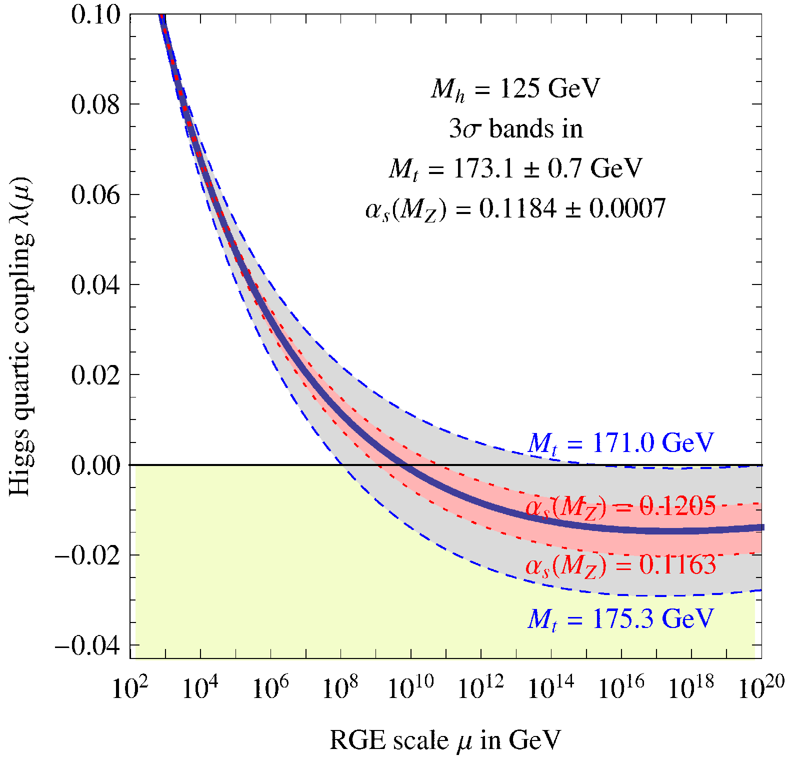

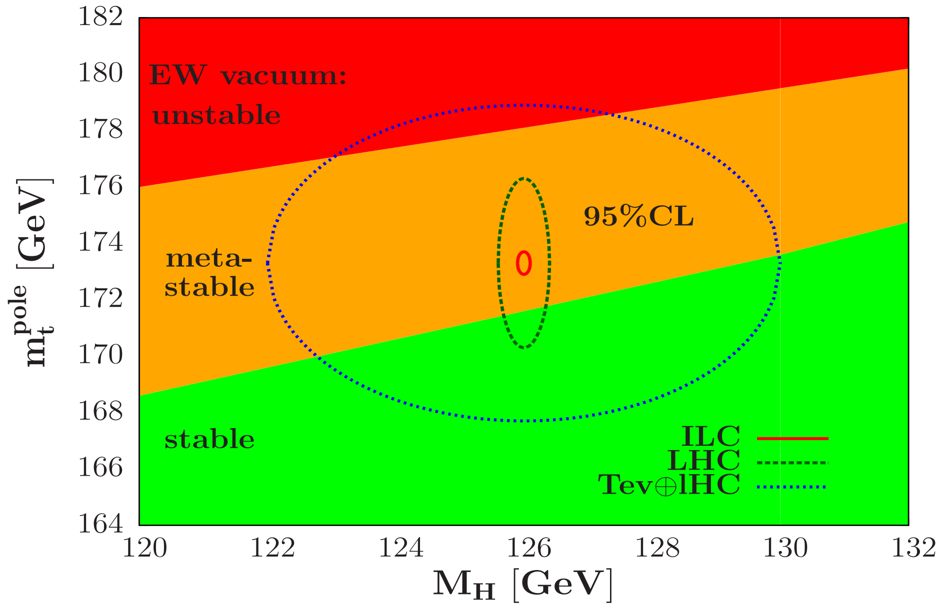

Vacuum stability

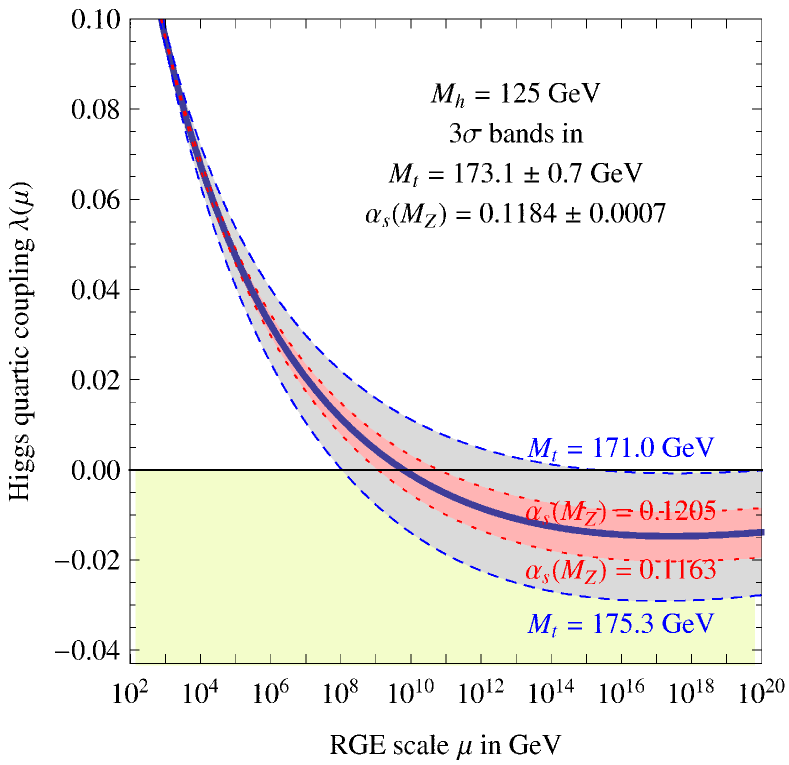

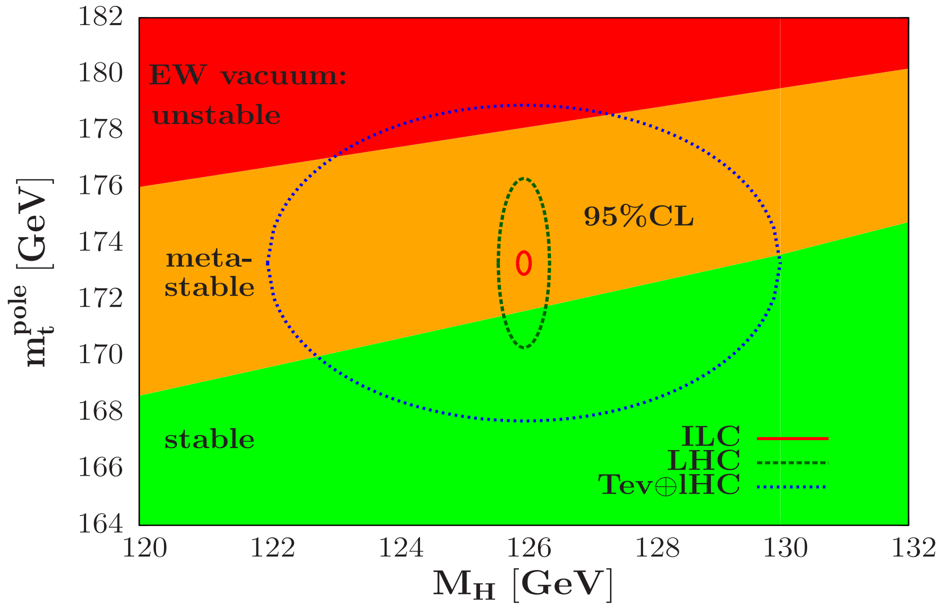

- $\boldsymbol{\lambda}$ is sensitive to top mass
- Stability of vacuum can be answered only if the error on the top mass goes down significantly.
- e^+e^- machine can give better measurement of top mass

Higgs Production at the LHC ($8\ TeV$)

Higgs Production at the LHC ($8\ TeV$)

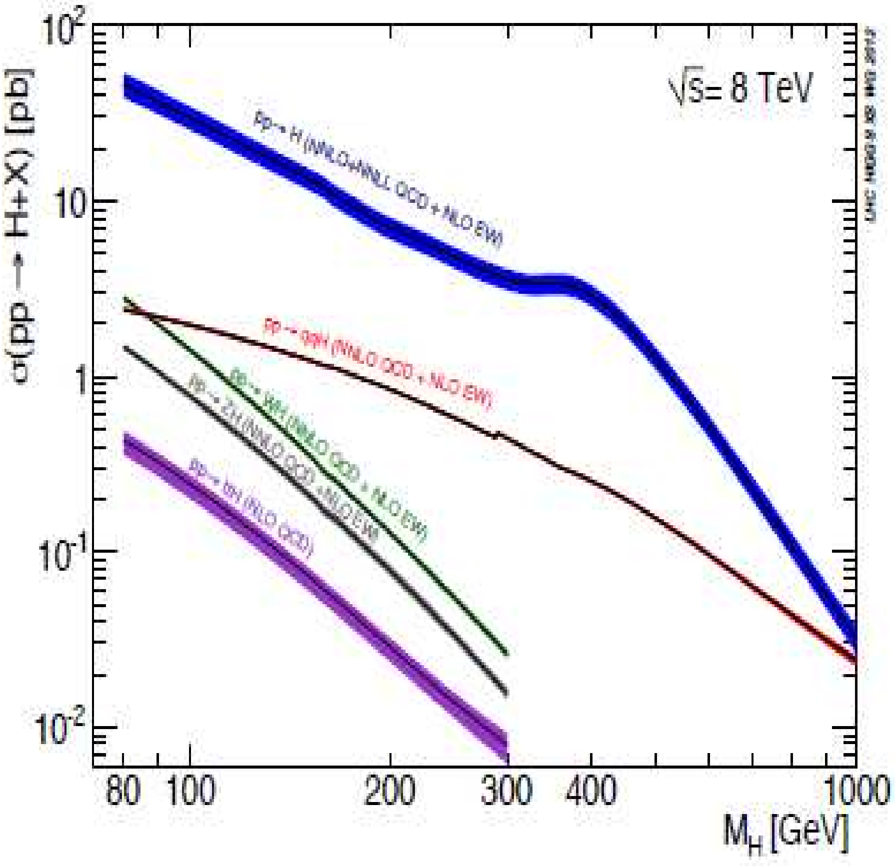

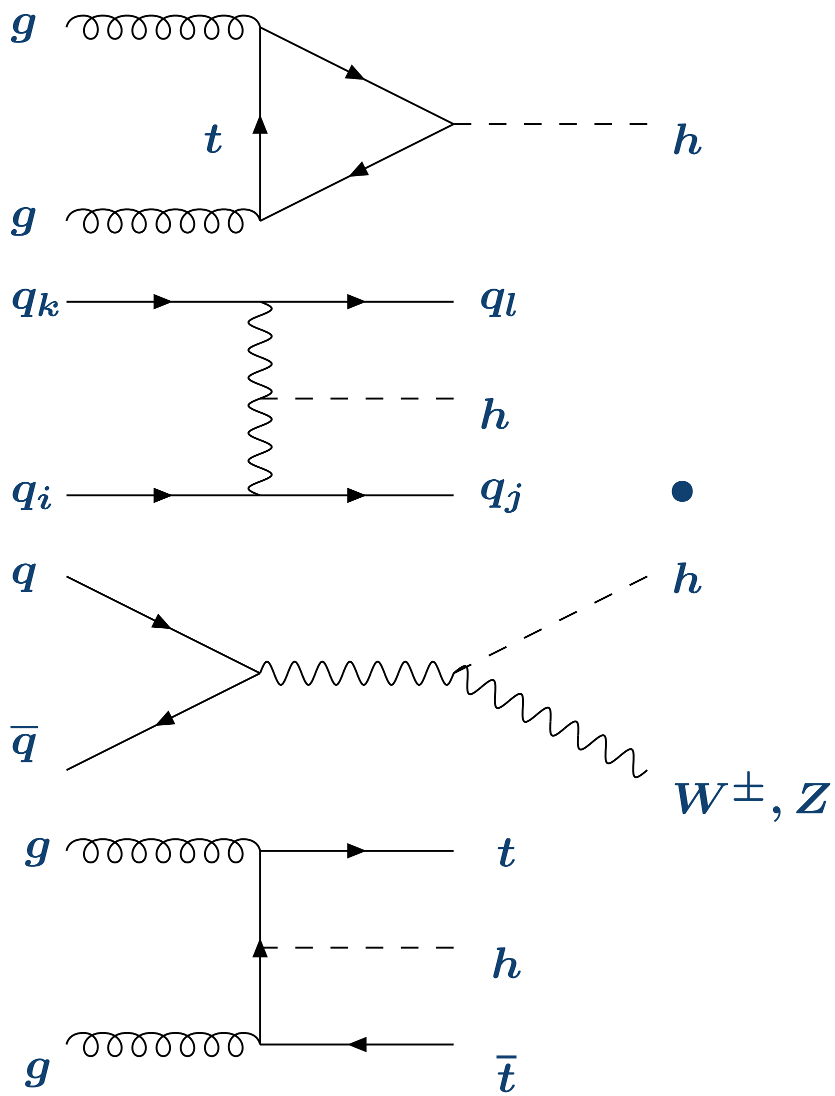

First three productions are known to NNLO level in QCD

● the last one is known only upto NLO level.

Theory influence on the rates

Theory influence on the rates

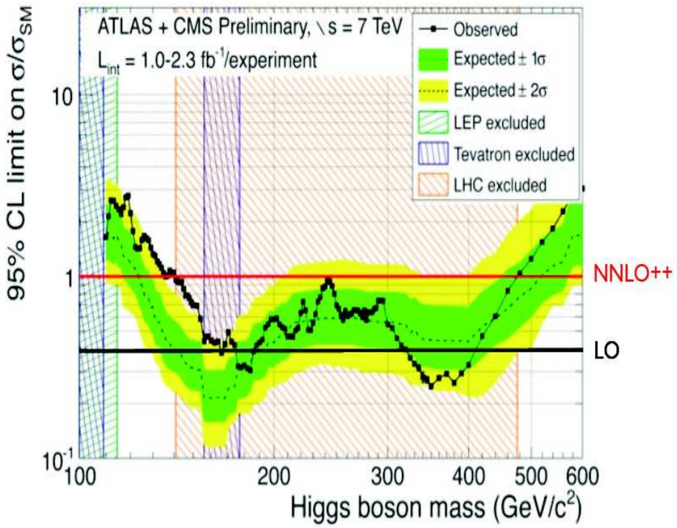

Theory influence on the rates

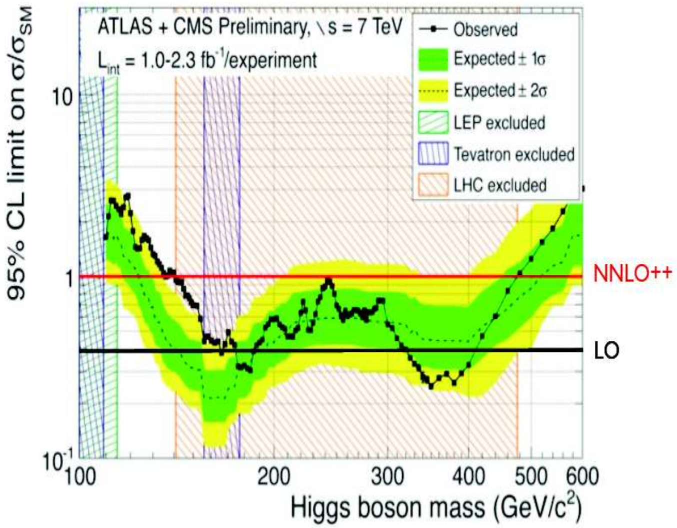

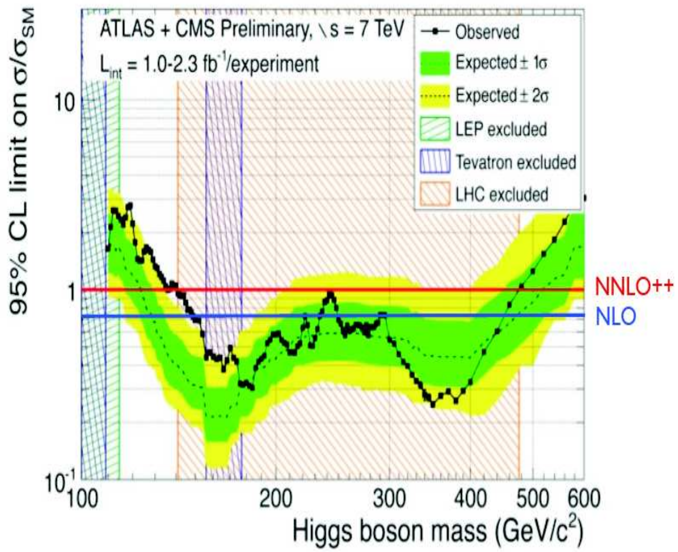

Theory influence on the rates

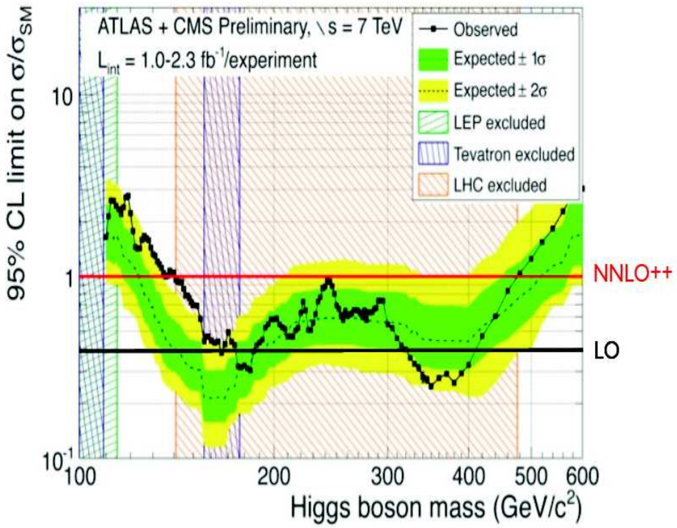

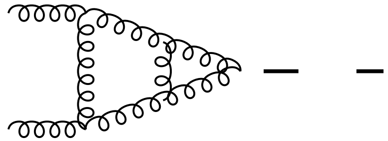

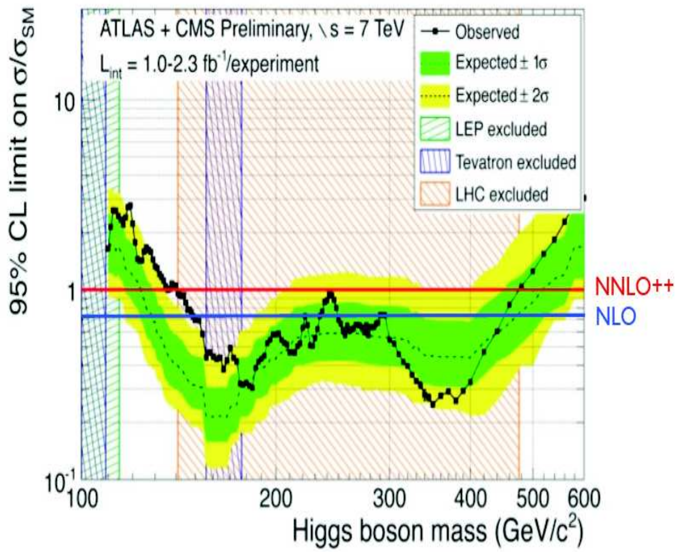

Theory influence on the rates

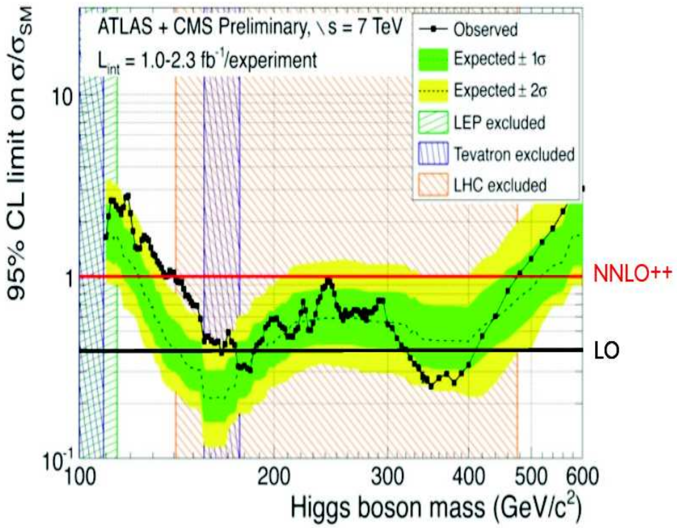

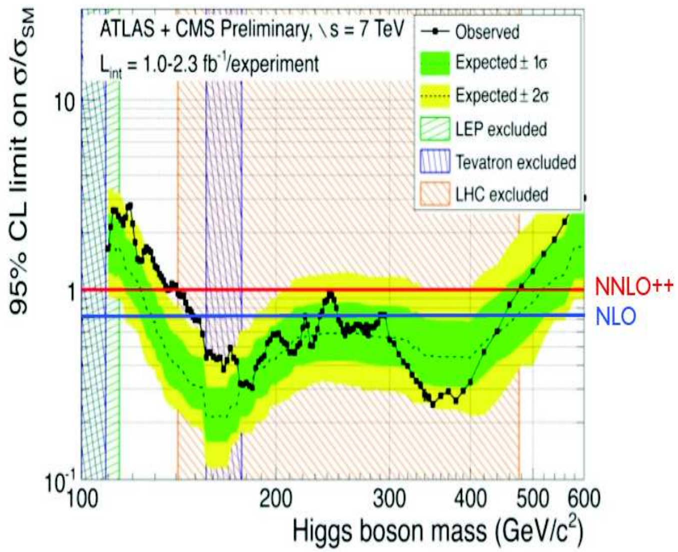

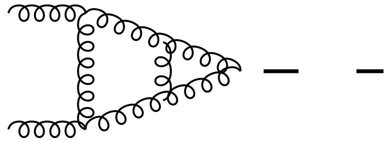

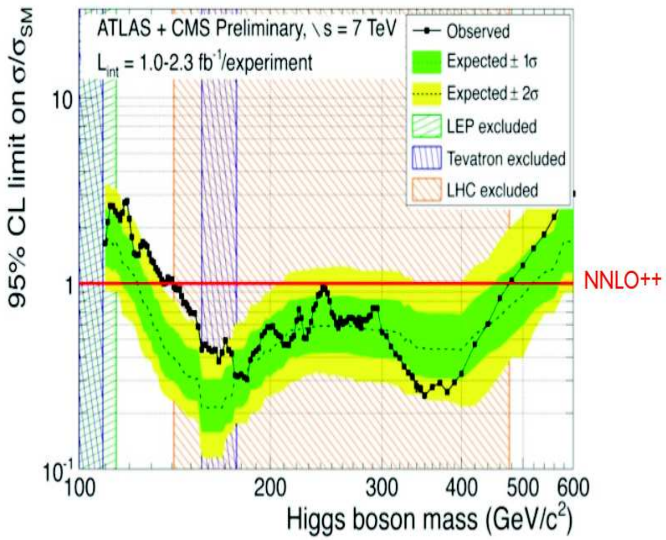

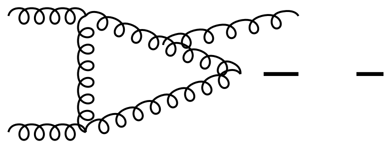

Theory influence on the rates

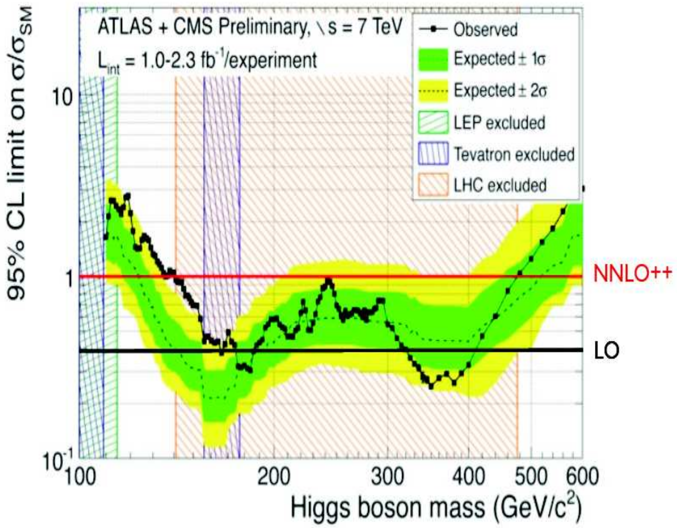

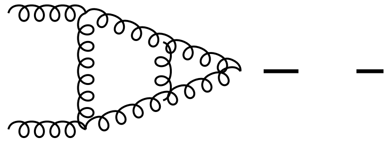

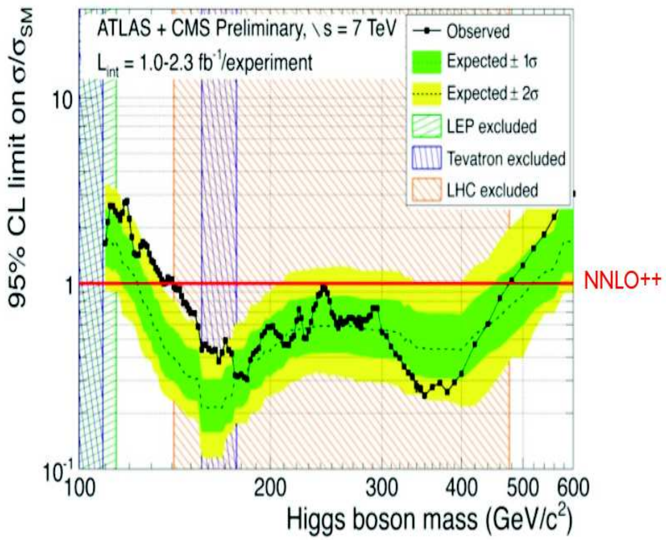

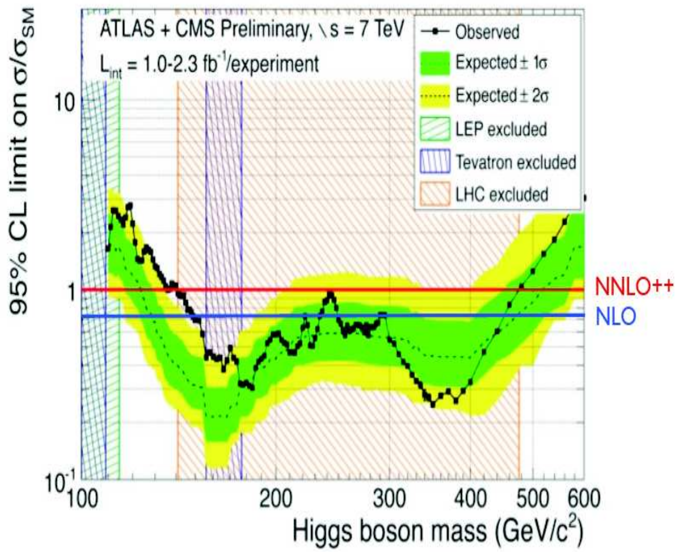

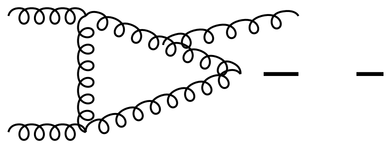

- To exclude something we need to understand the signal well
- To discover something we need to understand the background well

R.Harlander

Why LO, NLO and NNLO for Higgs production

$$P_1 + P_2 \to higgs + X$$

Why LO, NLO and NNLO for Higgs production

$$P_1 + P_2 \to higgs + X$$

$$2S\, d\sigma^{P_1 P_2}\left(\tau, m_h^2\right) = \sum_{ab} f_{a/P_1}\left(\tau, \mu_F\right) \otimes f_{b/P_2}\left(\tau, \mu_F\right) \otimes 2\hat{s}\, d\hat{\sigma}^{ab}\left(\tau, m_h^2, \mu_F\right), \qquad \tau = \frac{m_h^2}{S}$$

Why LO, NLO and NNLO for Higgs production

$$P_1 + P_2 \to higgs + X$$

$$2S\, d\sigma^{P_1 P_2}\left(\tau, m_h^2\right) = \sum_{ab} f_{a/P_1}\left(\tau, \mu_F\right) \otimes f_{b/P_2}\left(\tau, \mu_F\right) \otimes 2\hat{s}\, d\hat{\sigma}^{ab}\left(\tau, m_h^2, \mu_F\right), \qquad \tau = \frac{m_h^2}{S}$$

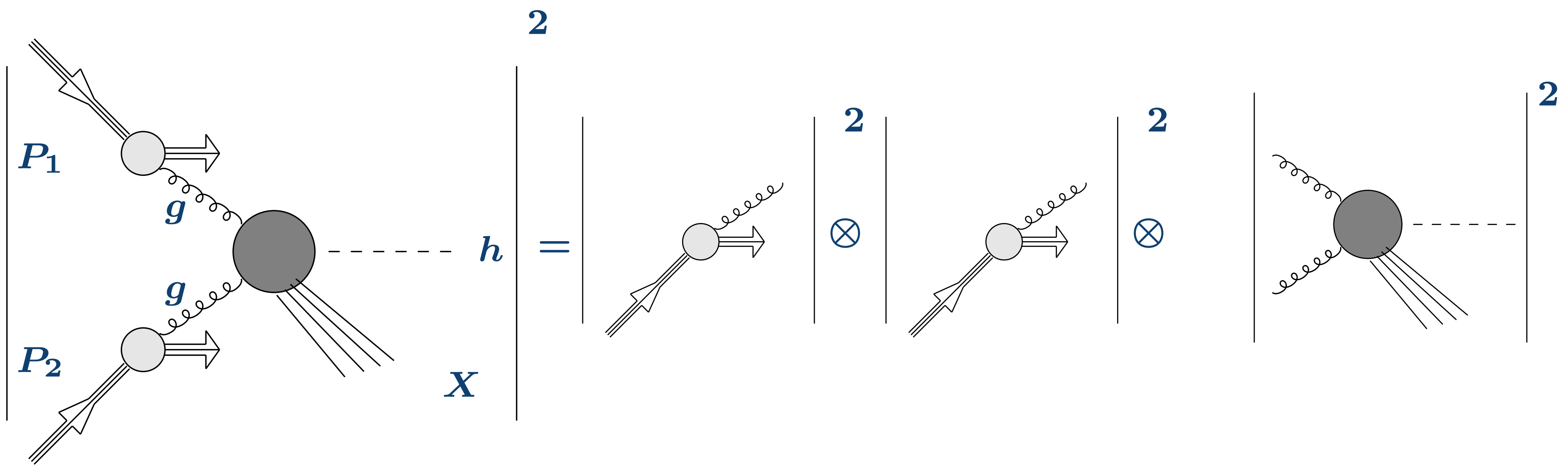

Why LO, NLO and NNLO for Higgs production

$$P_1 + P_2 \to higgs + X$$

$$2S\, d\sigma^{P_1 P_2}\left(\tau, m_h^2\right) = \sum_{ab} f_{a/P_1}\left(\tau, \mu_F\right) \otimes f_{b/P_2}\left(\tau, \mu_F\right) \otimes 2\hat{s}\, d\hat{\sigma}^{ab}\left(\tau, m_h^2, \mu_F\right), \qquad \tau = \frac{m_h^2}{S}$$

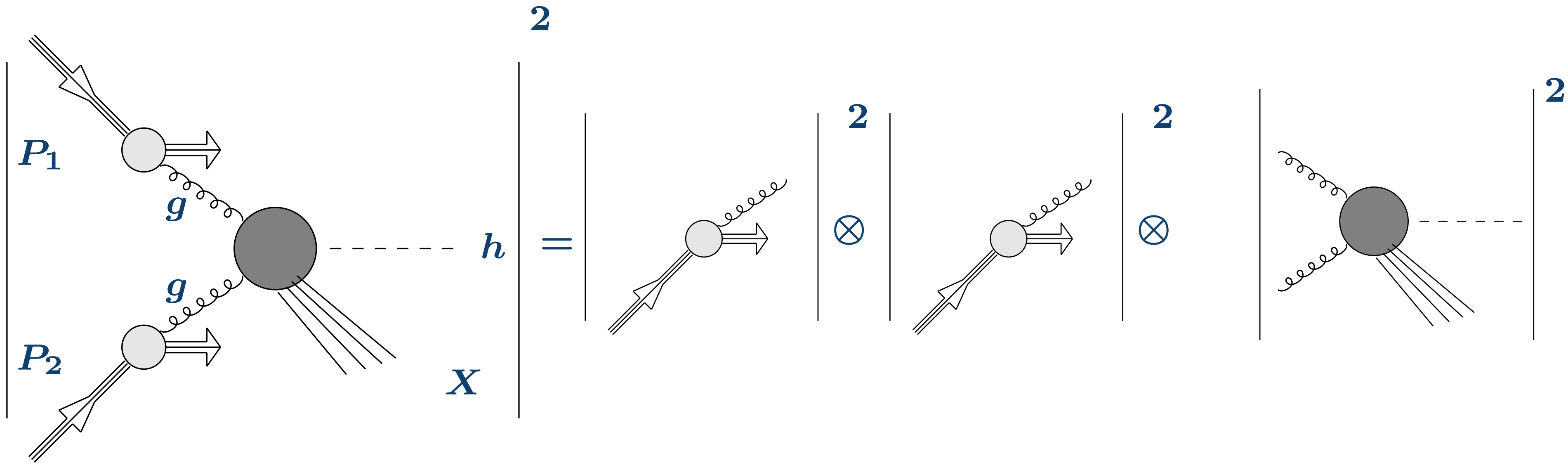

Extraction of non-perturbative functions:

- $f_a(x)$ are parton distribution functions inside the hadron P.
- Non-perturbative in nature and process independent.

Why LO, NLO and NNLO for Higgs production

$$P_1 + P_2 \to higgs + X$$

$$2S\, d\sigma^{P_1 P_2}\left(\tau, m_h^2\right) = \sum_{ab} f_{a/P_1}(\tau, \mu_F) \otimes f_{b/P_2}(\tau, \mu_F) \otimes 2\hat{s}\, d\hat{\sigma}^{ab}\left(\tau, m_h^2, \mu_F\right), \qquad \tau = \frac{m_h^2}{S}$$

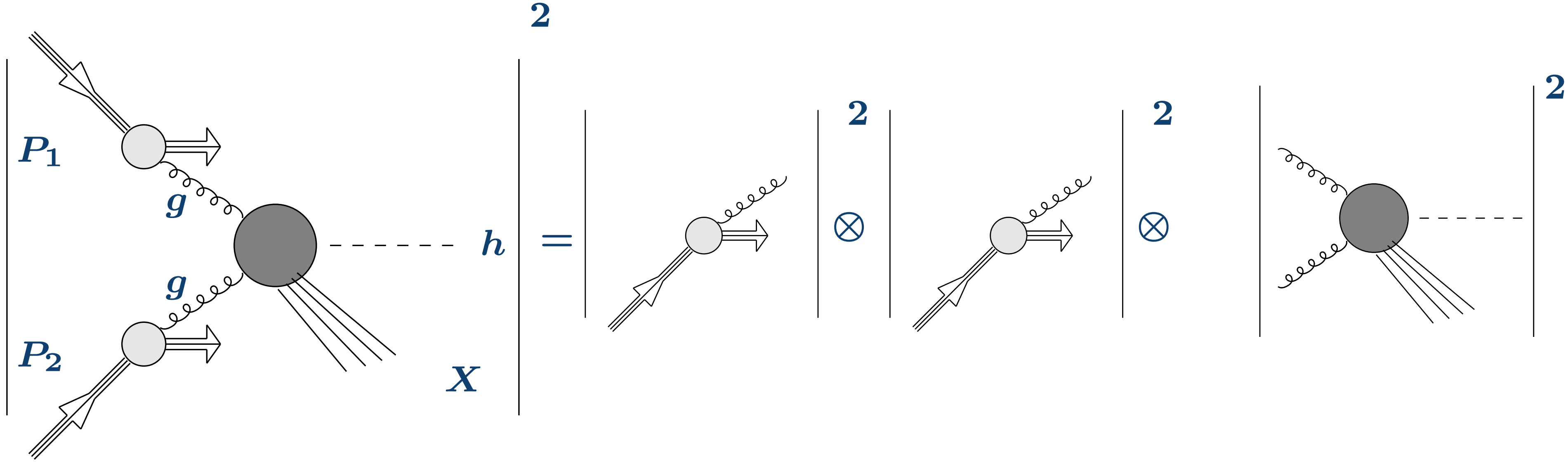

Extraction of non-perturbative functions:

- $f_a(x)$ are parton distribution functions inside the hadron P.
- Non-perturbative in nature and process independent.

Large Perturbative corrections:

- $\hat{\sigma}_{ab}$ are the partonic cross sections.
- Perturbatively calculable.

Why LO, NLO and NNLO for Higgs production

$$P_1 + P_2 \to higgs + X$$

$$2S\, d\sigma^{P_1 P_2}\left(\tau, m_h^2\right) = \sum_{ab} f_{a/P_1}\left(\tau, \mu_F\right) \otimes f_{b/P_2}\left(\tau, \mu_F\right) \otimes 2\hat{s}\, d\hat{\sigma}^{ab}\left(\tau, m_h^2, \mu_F\right), \qquad \tau = \frac{m_h^2}{S}$$

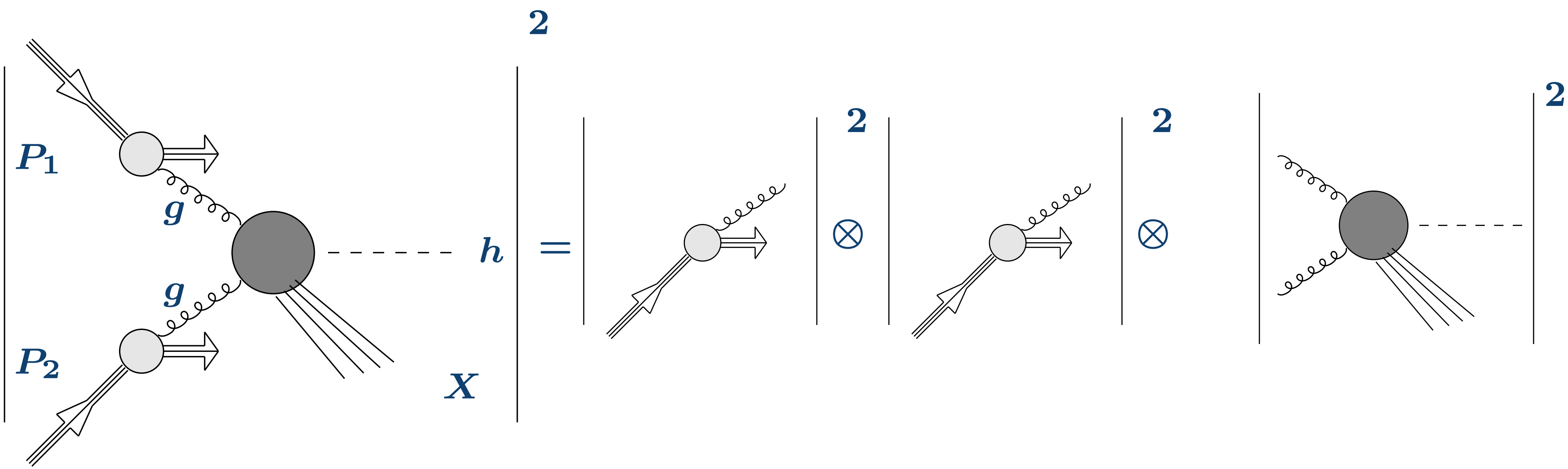

Extraction of non-perturbative functions:

- $f_a(x)$ are parton distribution functions inside the hadron P.
- Non-perturbative in nature and process independent.

Large Perturbative corrections:

- $\hat{\sigma}_{ab}$ are the partonic cross sections.
- Perturbatively calculable.

PDF from LHC

[Martin, Roberts, Stirling, Thorne]

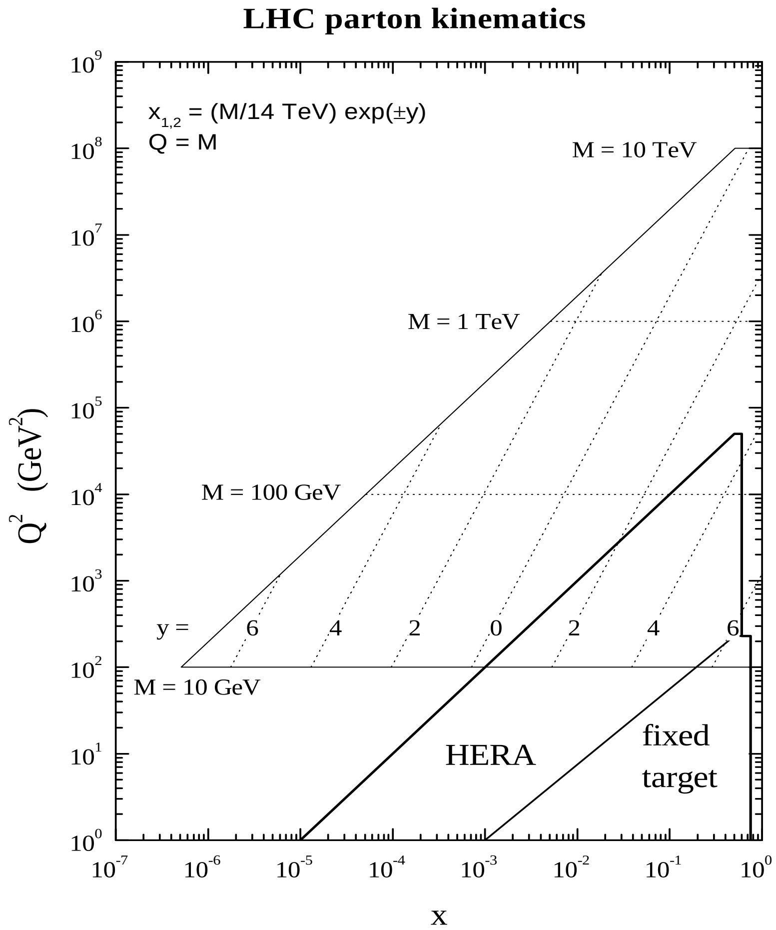

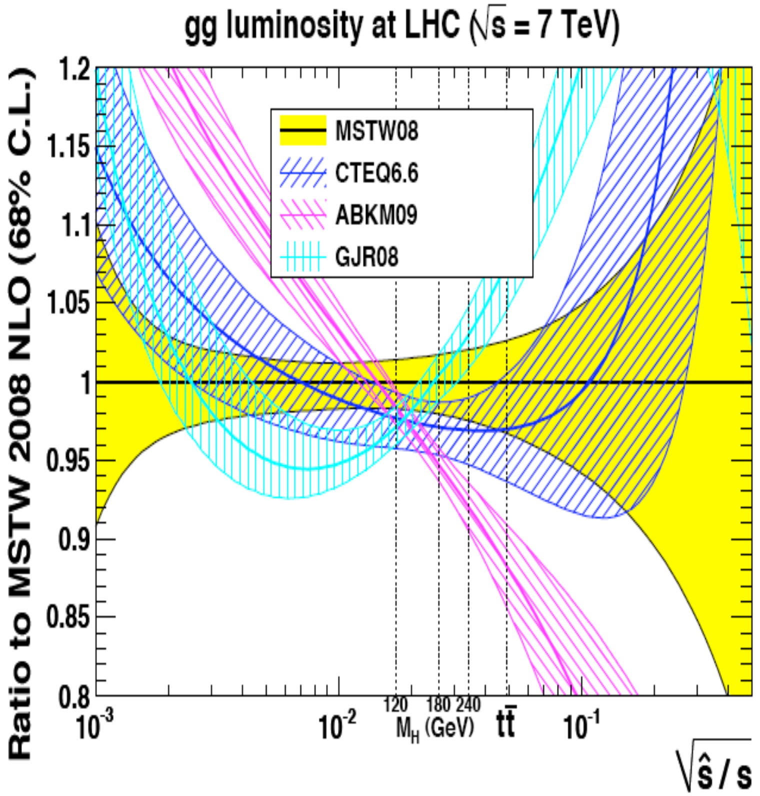

PDF from LHC

[*Martin, Roberts, Stirling, Thorne*]

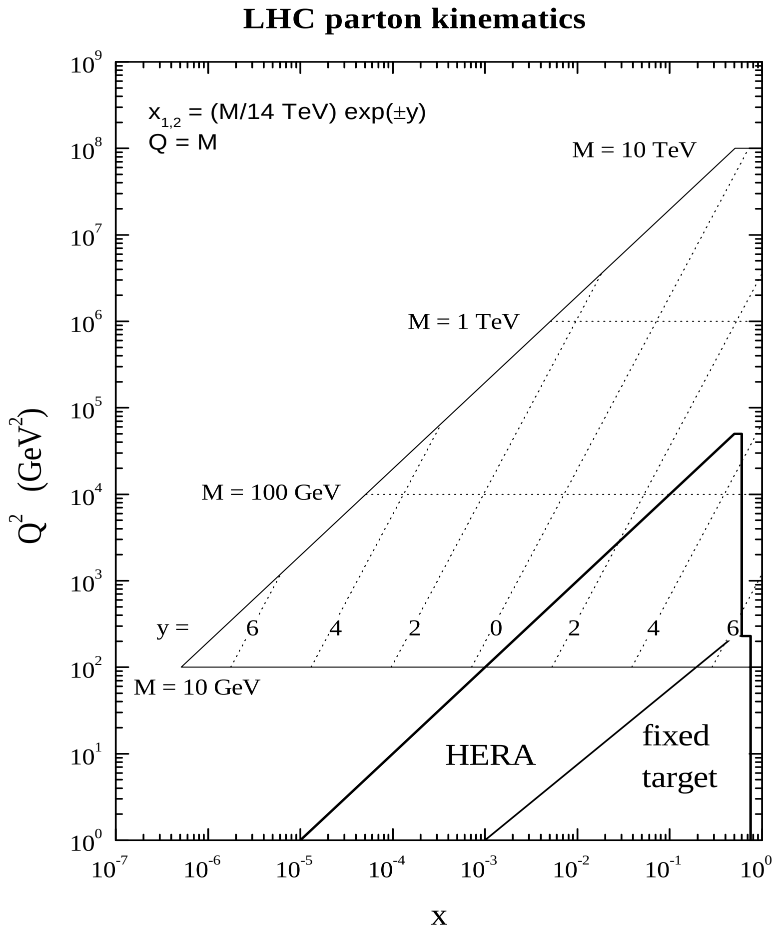

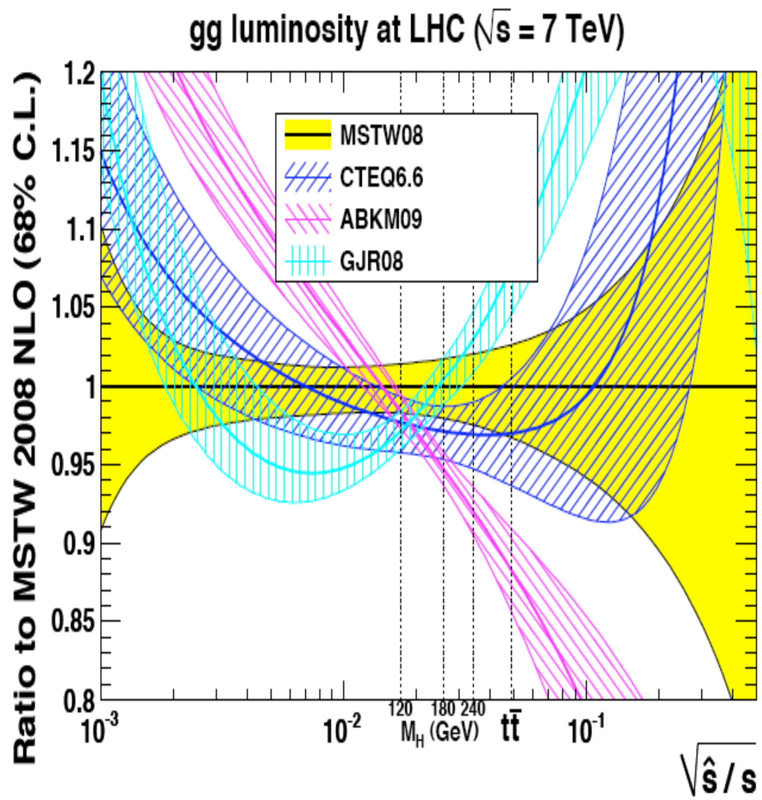

- MSTW, ABM and NNPDF come with different PDF sets with different choices of α_s, m_c, m_b

PDF from LHC

[Martin, Roberts, Stirling, Thorne]

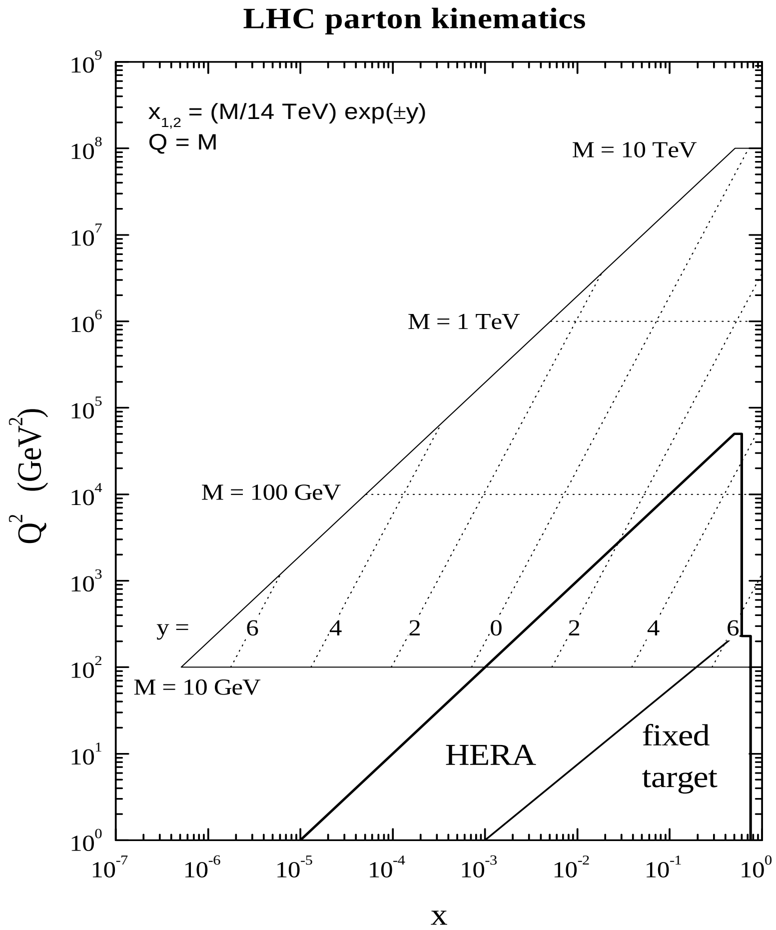

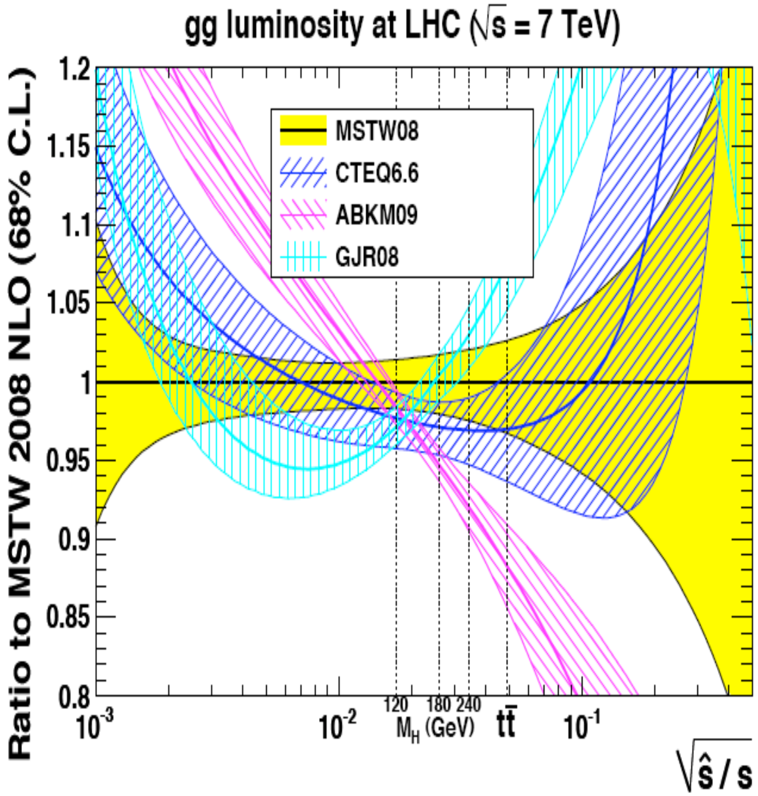

- MSTW, ABM and NNPDF come with different PDF sets with different choices of α_s, m_c, m_b

- Choice of PDF set can bring in significant uncertainty of the order 10 to 20%

Partonic Cross section

Partonic Cross section

$$2S\,d\sigma^{P_1P_2}\left(\tau, m_h^2\right) = \sum_{ab}\int_\tau^1 \frac{dx}{x}\Phi_{ab}\left(x,\mu_F\right)2\hat{s}\,d\hat{\sigma}^{ab}\left(\frac{\tau}{x}, m_h^2, \mu_F\right)$$

Partonic Cross section

$$2S\, d\sigma^{P_1 P_2}\left(\tau, m_h^2\right) = \sum_{ab} \int_\tau^1 \frac{dx}{x} \Phi_{ab}\left(x, \mu_F\right) 2\hat{s}\, d\hat{\sigma}^{ab}\left(\frac{\tau}{x}, m_h^2, \mu_F\right)$$

Partonic Cross section

$$2S\, d\sigma^{P_1 P_2}\left(\tau, m_h^2\right) = \sum_{ab} \int_\tau^1 \frac{dx}{x} \Phi_{ab}\left(x, \mu_F\right) 2\hat{s}\, d\hat{\sigma}^{ab}\left(\frac{\tau}{x}, m_h^2, \mu_F\right)$$

- $d\hat{\sigma}^{ab}$ is perturbatively computable as a power series in $\alpha_s(\mu_R)$, where μ_R is the

renormalisation scale.

$$d\hat{\sigma}^{ab}\left(\mu_F\right) = \alpha_s^d(\mu_R) \sum_{i=0} \alpha_s^i(\mu_R) d\hat{\sigma}^{ab,(i)}\left(\mu_F, \mu_R\right)$$

- Renormalisation group equation:

$$\boxed{\mu_R^2 \frac{d}{d\mu_R^2} \alpha_s(\mu_R) = \beta\left(\alpha_s(\mu_R)\right)}$$

- Fixed order results are often sensitive to μ_R. • Many new production channels open up

beyond LO.

Gluon fusion to Higgs at Leading Order(LO)

Hinchcliff, many others

Gluon fusion to Higgs at Leading Order(LO)

Hinchcliff, many others

$$2S\, d\sigma^{PP}(x, m_h) = \int_x^1 \frac{dz}{z} \Phi_{gg}^{(0)}(z, m_h, \mu_F)\, 2\hat{s}\, d\hat{\sigma}_{gg}^{(0)}\left(\frac{x}{z}, m_h^2, \mu_R\right) + \cdots$$

Gluon fusion to Higgs at Leading Order(LO)

Hinchcliff, many others

$$2S\, d\sigma^{PP}(x, m_h) = \int_x^1 \frac{dz}{z} \Phi_{gg}^{(0)}(z, m_h, \mu_F)\, 2\hat{s}\, d\hat{\sigma}_{gg}^{(0)}\left(\frac{x}{z}, m_h^2, \mu_R\right) + \cdots$$

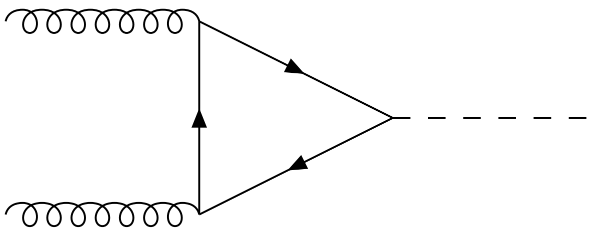

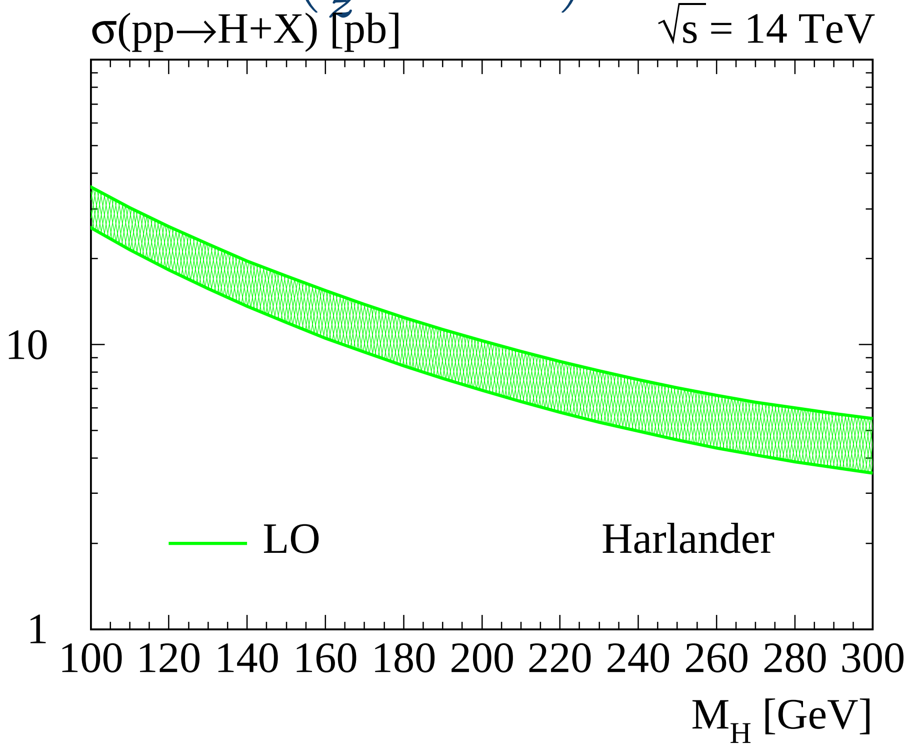

$$\hat{\sigma}_{gg}^{(0)}(\hat{s}, \mu_R) \sim \alpha_s^2(\mu_R) \left[F(G_F, m_t, m_h)\right],$$

Gluon fusion to Higgs at Leading Order(LO)

Hinchcliff, many others

$$2S\, d\sigma^{PP}(x, m_h) = \int_x^1 \frac{dz}{z} \Phi_{gg}^{(0)}(z, m_h, \mu_F)\, 2\hat{s}\, d\hat{\sigma}_{gg}^{(0)}\left(\frac{x}{z}, m_h^2, \mu_R\right) + \cdots$$

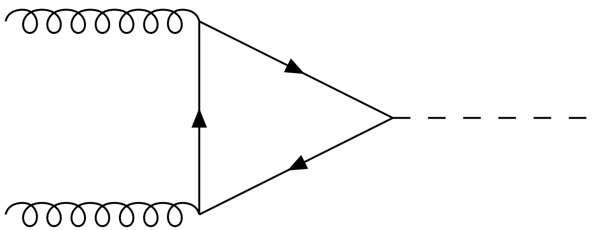

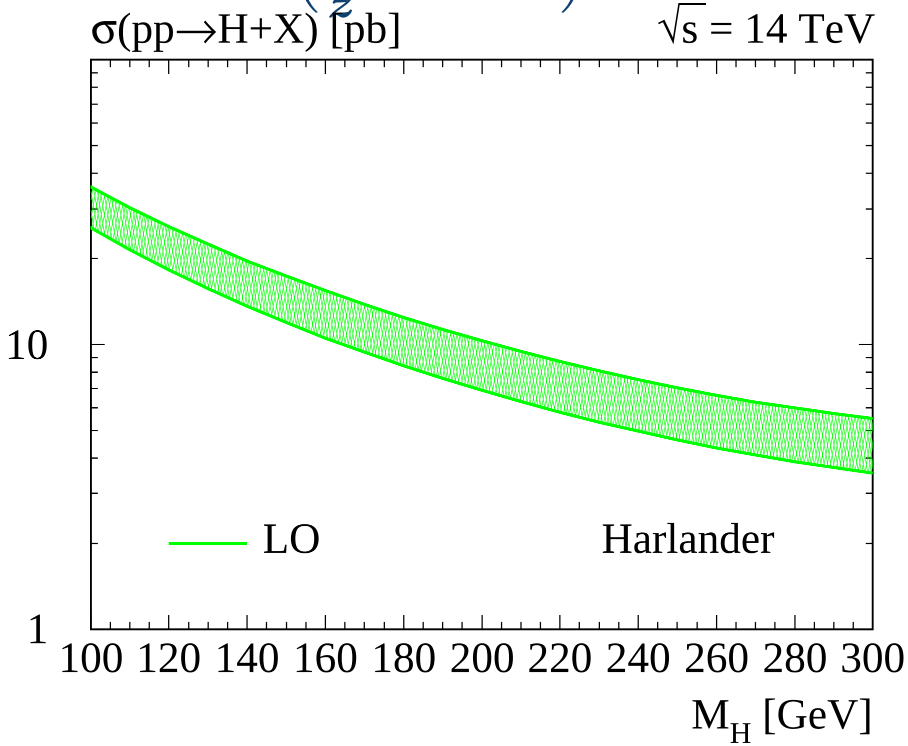

$$\hat{\sigma}_{gg}^{(0)}(\hat{s}, \mu_R) \sim \alpha_s^2(\mu_R) \left[F(G_F, m_t, m_h) \right],$$

- Leading order is uncontrolable due to μ_R scale and can not be used for any study in the present form.
- Only higher order corrections can provide sensible result thanks to RG equation

$$\mu^2 \frac{d}{d\mu^2} \sigma = 0$$

NNLO QCD corrected Higgs Cross section at $\sqrt{S} = 14$ TeV

$m_H/2 < \mu_F = \mu_R < 2m_H$

NNLO QCD corrected Higgs Cross section at $\sqrt{S} = 14$ TeV

$$m_H/2 < \mu_F = \mu_R < 2m_H$$

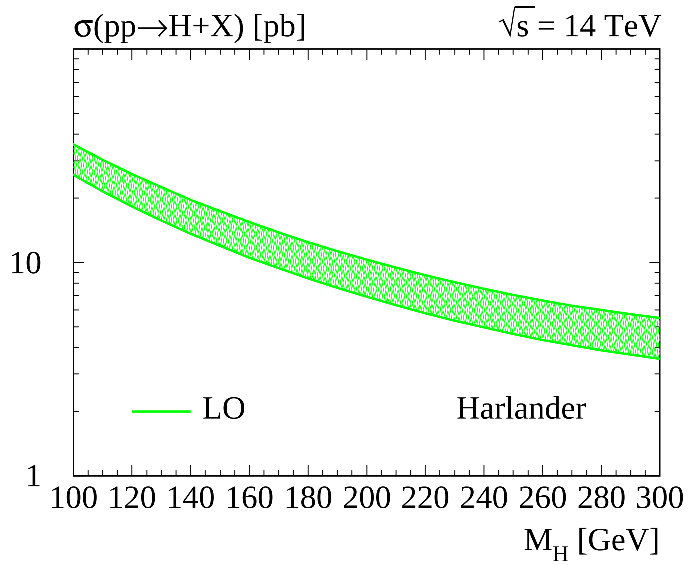

NNLO QCD corrected Higgs Cross section at $\sqrt{S} = 14$ TeV

$$m_H/2 < \mu_F = \mu_R < 2m_H$$

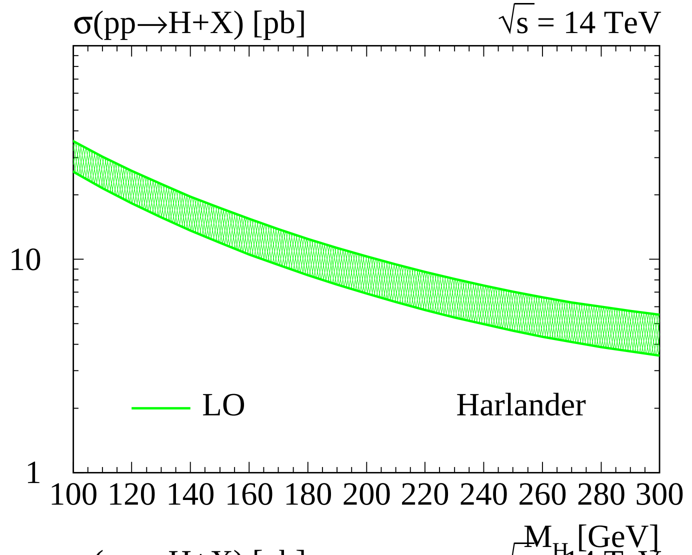

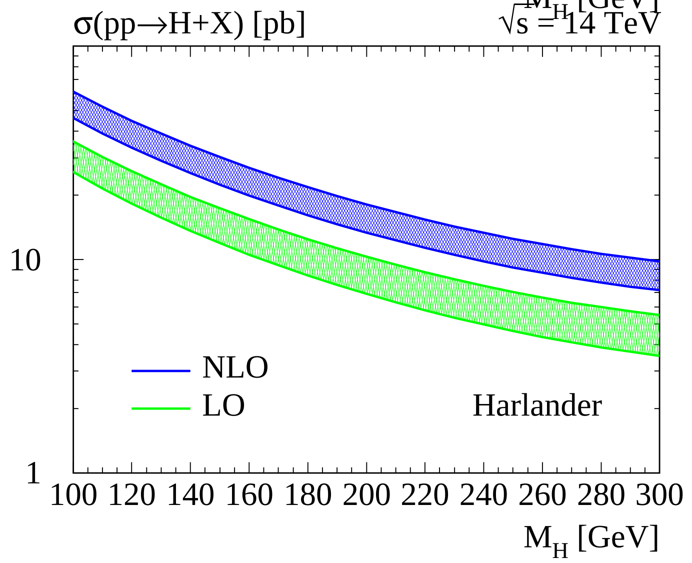

NNLO QCD corrected Higgs Cross section at $\sqrt{S} = 14$ TeV

$$m_H/2 < \mu_F = \mu_R < 2m_H$$

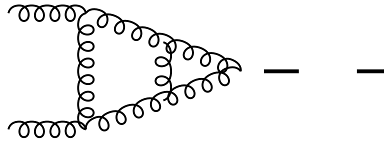

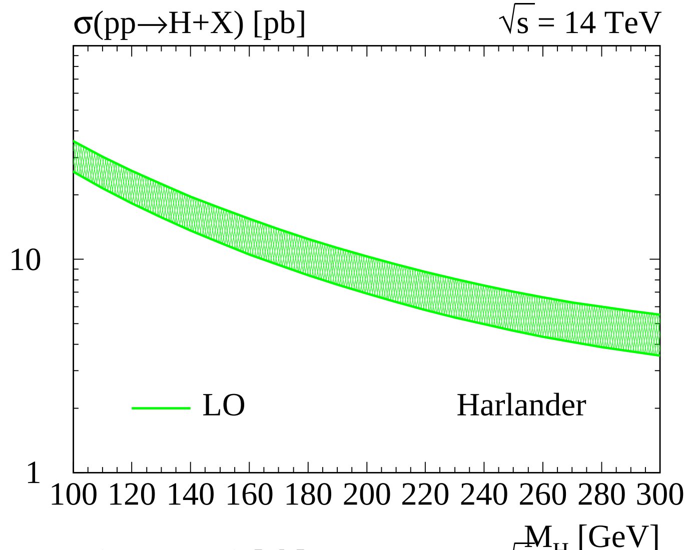

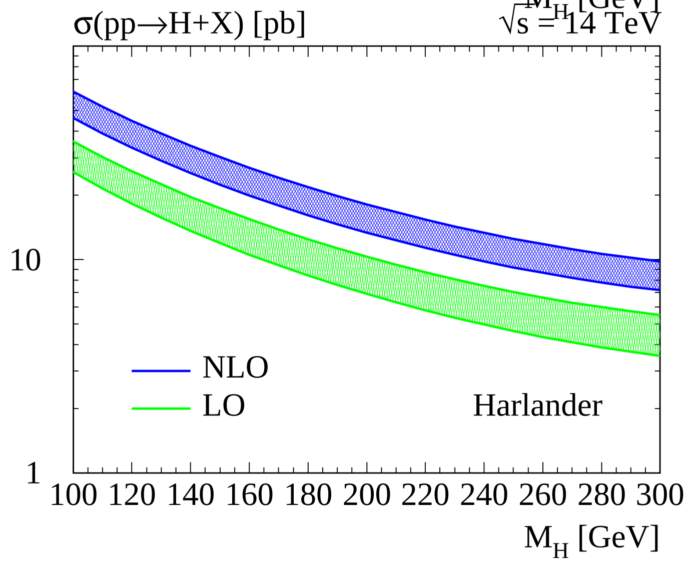

NNLO QCD corrected Higgs Cross section at $\sqrt{S} = 14$ TeV

$m_H/2 < \mu_F = \mu_R < 2m_H$

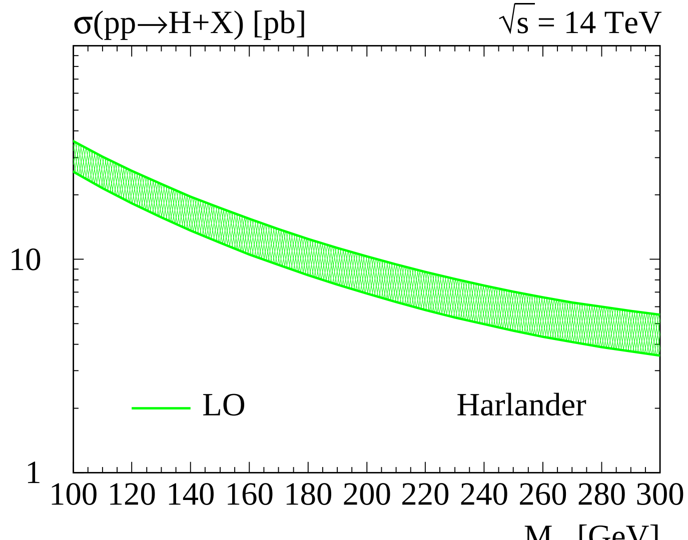

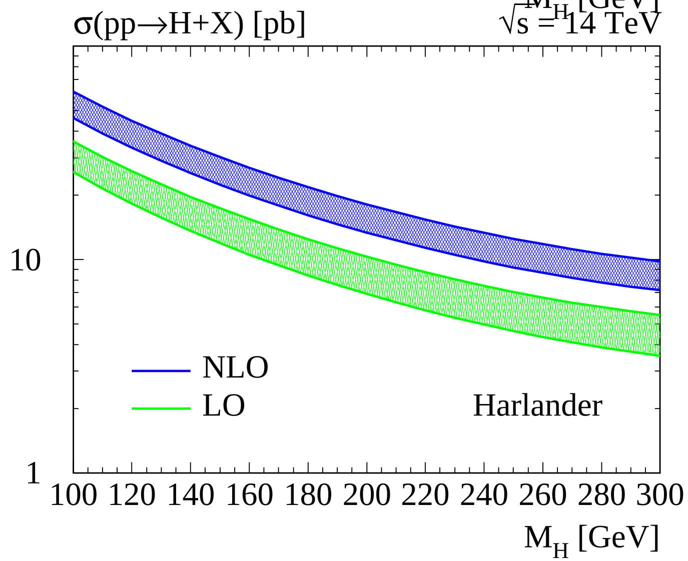

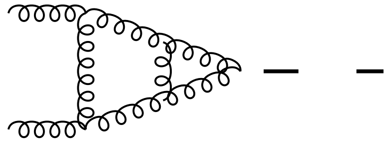

A.Djouadi,D.Grandenz,M.Spira,P.Zerwas

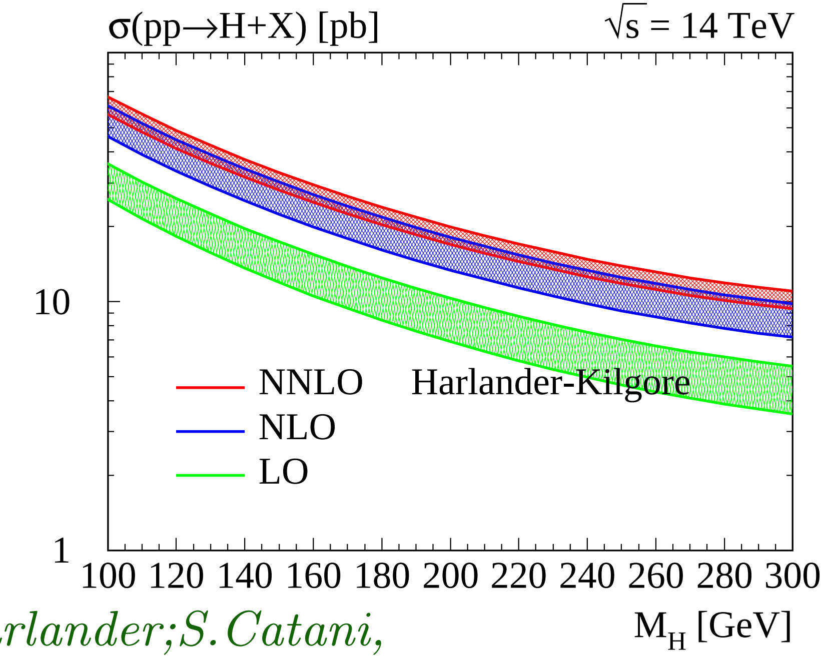

R.Harlander;S.Catani,
D.DeFlorian,M.Grazzini;
R.Harlander,B.Kilgore;C.Anastasiou,Melnikov;
VR,J.Smith,W.L.van Neerven

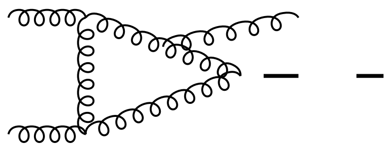

Soft gluons dominate!

$S.Catani, P.Nason, M.Grazzini, D.DeFlorian; R.Harlander,$
$B.Kilgore; E.Laenen, L.Magnea, Moch, Vogt$, VR

Soft gluons dominate!

S. Catani, P. Nason, M. Grazzini, D. DeFlorian; R. Harlander, B. Kilgore; E. Laenen, L. Magnea, Moch, Vogt, VR

$$2S\, d\sigma^{P_1 P_2}(\tau, m_H) = \sum_{ab} \int_\tau^1 \frac{dx}{x} \Phi_{ab}(x)\, 2\hat{s}\, d\hat{\sigma}^{ab}\left(\frac{\tau}{x}, m_H\right) \qquad \tau = \frac{m_H^2}{S}$$

Soft gluons dominate!

S.Catani, P.Nason, M.Grazzini, D.DeFlorian; R.Harlander, B.Kilgore; E.Laenen, L.Magnea, Moch, Vogt, VR

$$2S\, d\sigma^{P_1 P_2}(\tau, m_H) = \sum_{ab} \int_\tau^1 \frac{dx}{x} \Phi_{ab}(x)\, 2\hat{s}\, d\hat{\sigma}^{ab}\left(\frac{\tau}{x}, m_H\right) \qquad \tau = \frac{m_H^2}{S}$$

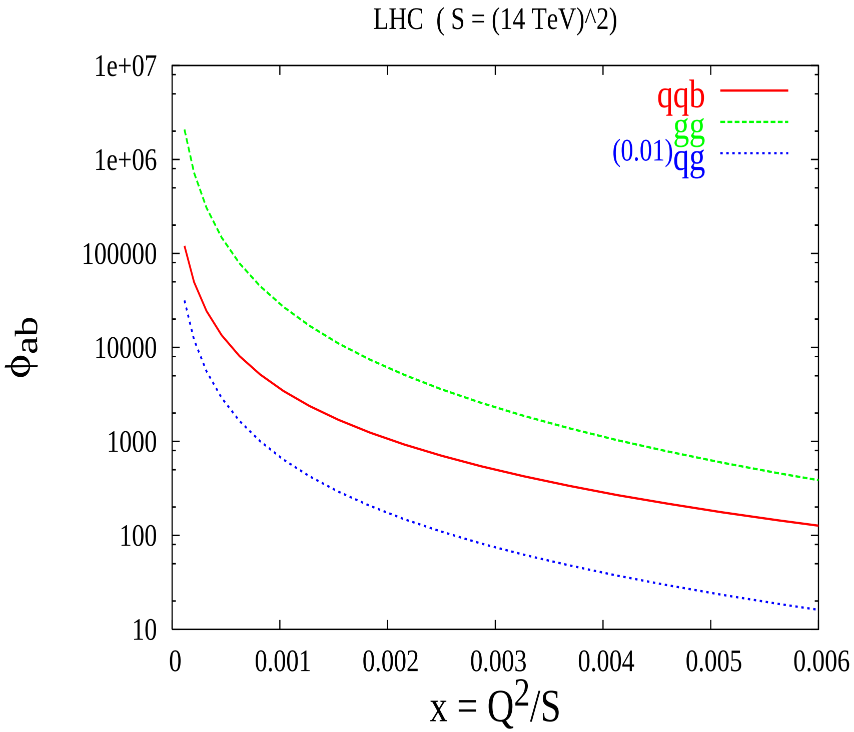

Gluon flux is largest at LHC ●
Soft gluon NNLL resummation gives less than 9% correction at the LHC

S.Catani, D.DeFlorian, P.Nason, M.Grazzini

Soft gluons dominate!

S.Catani, P.Nason, M.Grazzini, D.DeFlorian; R.Harlander, B.Kilgore; E.Laenen, L.Magnea, Moch, Vogt, VR

$$2S\, d\sigma^{P_1 P_2}(\tau, m_H) = \sum_{ab} \int_\tau^1 \frac{dx}{x} \Phi_{ab}(x)\, 2\hat{s}\, d\hat{\sigma}^{ab}\left(\frac{\tau}{x}, m_H\right) \qquad \tau = \frac{m_H^2}{S}$$

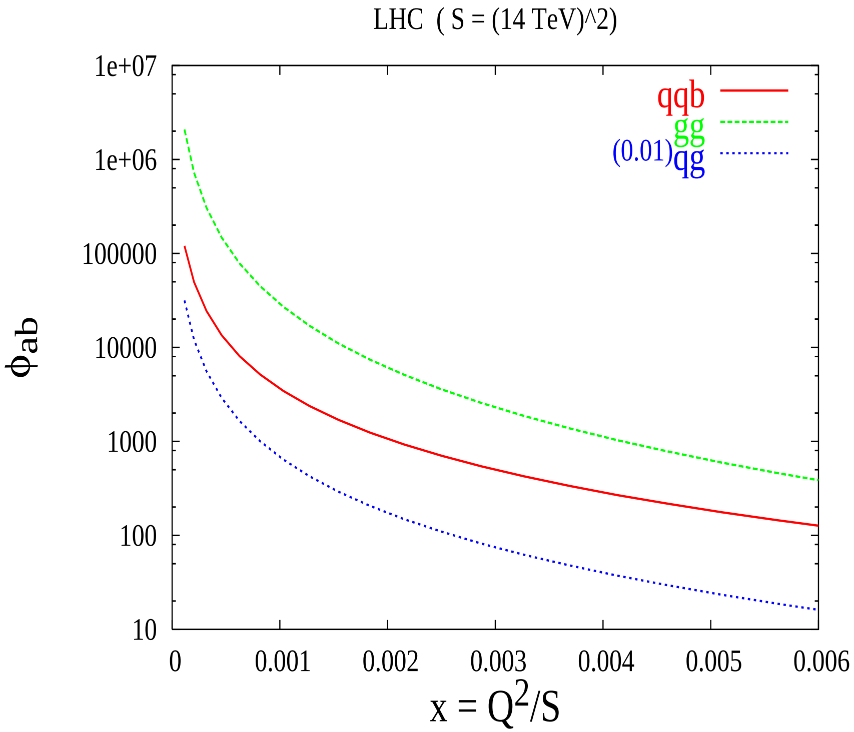

- $\Phi_{ab}(x)$ becomes large when $x \to x_{min} = \tau$

- Gluon flux is largest at LHC
- Soft gluon NNLL resummation gives less than 9% correction at the LHC
  S.Catani, D.DeFlorian, P.Nason, M.Grazzini

Soft gluons dominate!

*S.Catani,P.Nason,M.Grazzini,D.DeFlorian;R.Harlander, B.Kilgore;E.Laenen,L.Magnea,Moch,Vogt,*VR

$$2S\, d\sigma^{P_1 P_2}(\tau, m_H) = \sum_{ab} \int_\tau^1 \frac{dx}{x} \Phi_{ab}(x)\, 2\hat{s}\, d\hat{\sigma}^{ab}\left(\frac{\tau}{x}, m_H\right) \qquad \tau = \frac{m_H^2}{S}$$

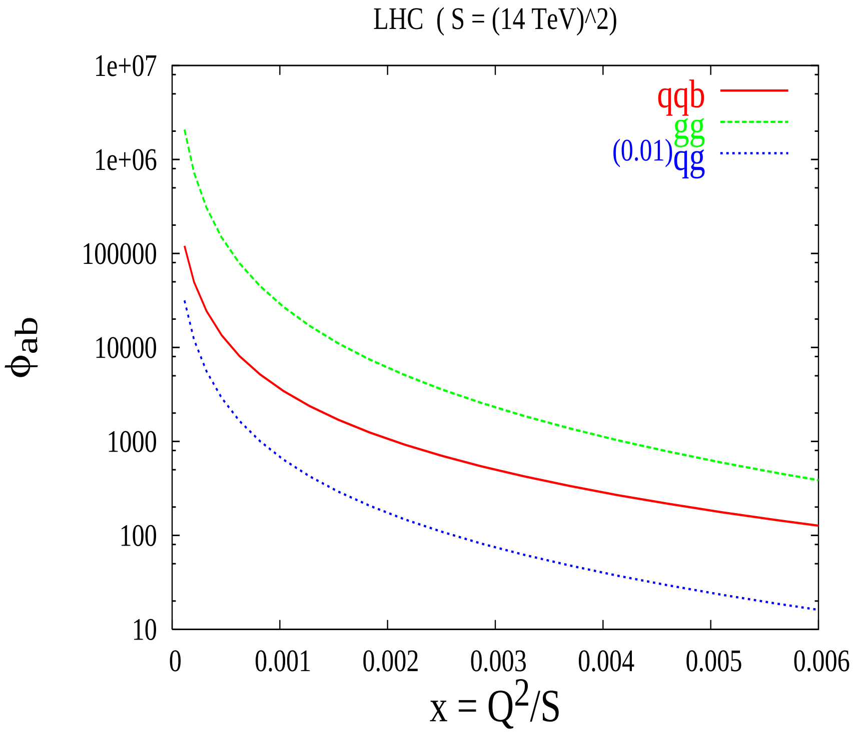

- $\Phi_{ab}(x)$ becomes large when $x \to x_{min} = \tau$
- Dominant contribution to Higgs production comes from the region when $x \to \tau$
- Gluon flux is largest at LHC

Soft gluon NNLL resummation gives less than 9% correction at the LHC

S.Catani,D.DeFlorian,P.Nason,M.Grazzini

Soft gluons dominate!

S. Catani, P. Nason, M. Grazzini, D. DeFlorian; R. Harlander, B. Kilgore; E. Laenen, L. Magnea, Moch, Vogt, VR

$$2S\, d\sigma^{P_1 P_2}(\tau, m_H) = \sum_{ab} \int_\tau^1 \frac{dx}{x} \Phi_{ab}(x)\, 2\hat{s}\, d\hat{\sigma}^{ab}\left(\frac{\tau}{x}, m_H\right) \qquad \tau = \frac{m_H^2}{S}$$

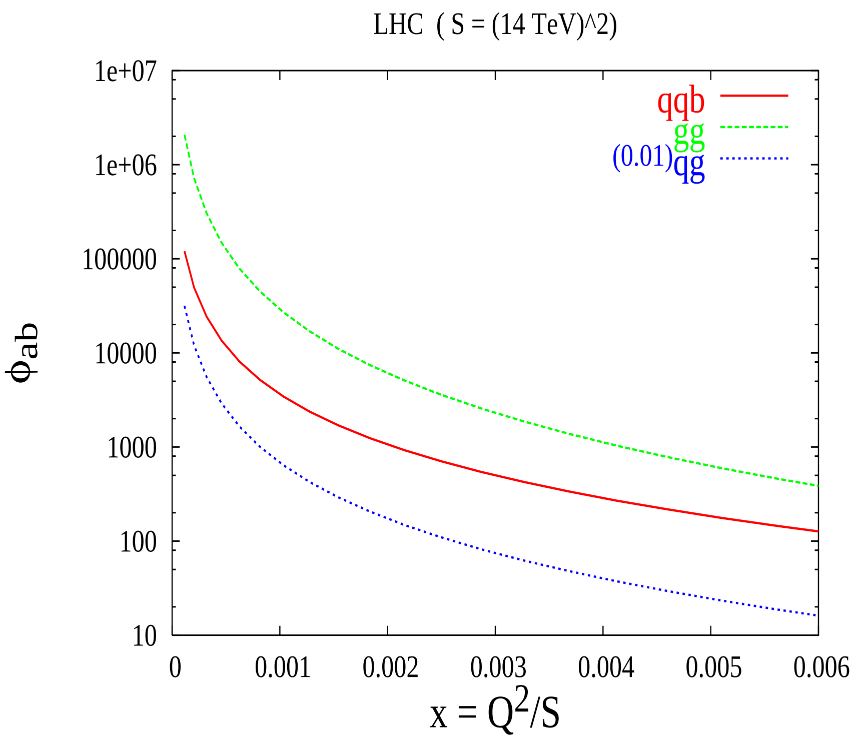

- $\Phi_{ab}(x)$ becomes large when $x \to x_{min} = \tau$
- Dominant contribution to Higgs production comes from the region when $x \to \tau$
- It is sufficient if we know the partonic cross section when $x \to \tau$

- Gluon flux is largest at LHC
- Soft gluon NNLL resummation gives less than 9% correction at the LHC

S. Catani, D. DeFlorian, P. Nason, M. Grazzini

Soft gluons dominate!

S.Catani, P.Nason, M.Grazzini, D.DeFlorian; R.Harlander, B.Kilgore; E.Laenen, L.Magnea, Moch, Vogt, VR

$$2S\, d\sigma^{P_1 P_2}(\tau, m_H) = \sum_{ab} \int_\tau^1 \frac{dx}{x} \Phi_{ab}(x)\, 2\hat{s}\, d\hat{\sigma}^{ab}\left(\frac{\tau}{x}, m_H\right) \qquad \tau = \frac{m_H^2}{S}$$

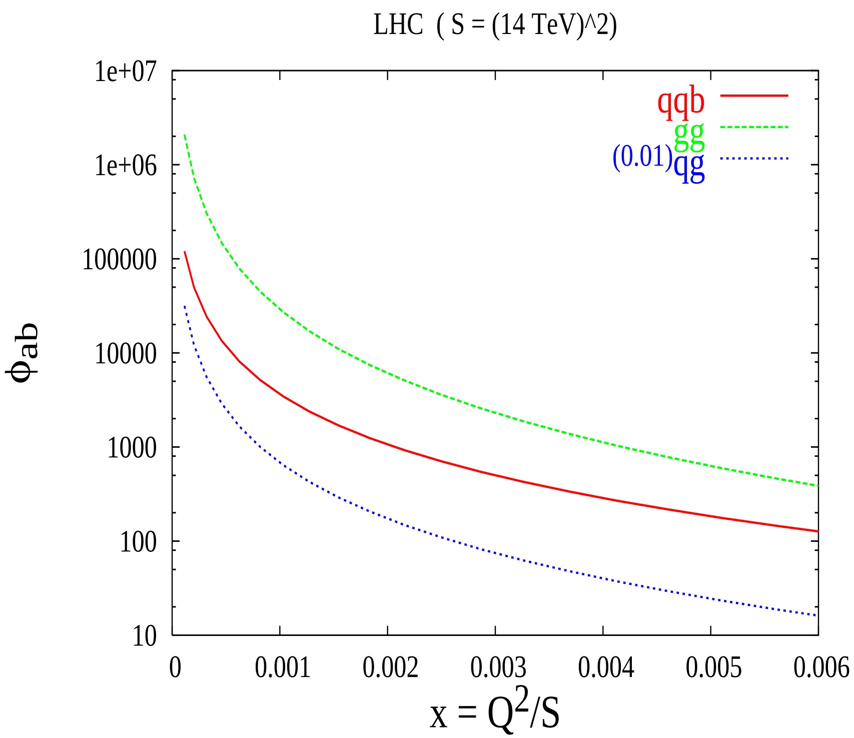

- $\Phi_{ab}(x)$ becomes large when $x \to x_{min} = \tau$
- Dominant contribution to Higgs production comes from the region when $x \to \tau$
- It is sufficient if we know the partonic cross section when $x \to \tau$
- $x \to \tau$ is called *soft limit*.

- Gluon flux is largest at LHC

Soft gluon NNLL resummation gives less than 9% correction at the LHC

S.Catani, D.DeFlorian, P.Nason, M.Grazzini

Soft gluons dominate!

S.Catani, P.Nason, M.Grazzini, D.DeFlorian; R.Harlander, B.Kilgore; E.Laenen, L.Magnea, Moch, Vogt, VR

$$2S\, d\sigma^{P_1 P_2}(\tau, m_H) = \sum_{ab} \int_\tau^1 \frac{dx}{x} \Phi_{ab}(x)\, 2\hat{s}\, d\hat{\sigma}^{ab}\left(\frac{\tau}{x}, m_H\right) \qquad \tau = \frac{m_H^2}{S}$$

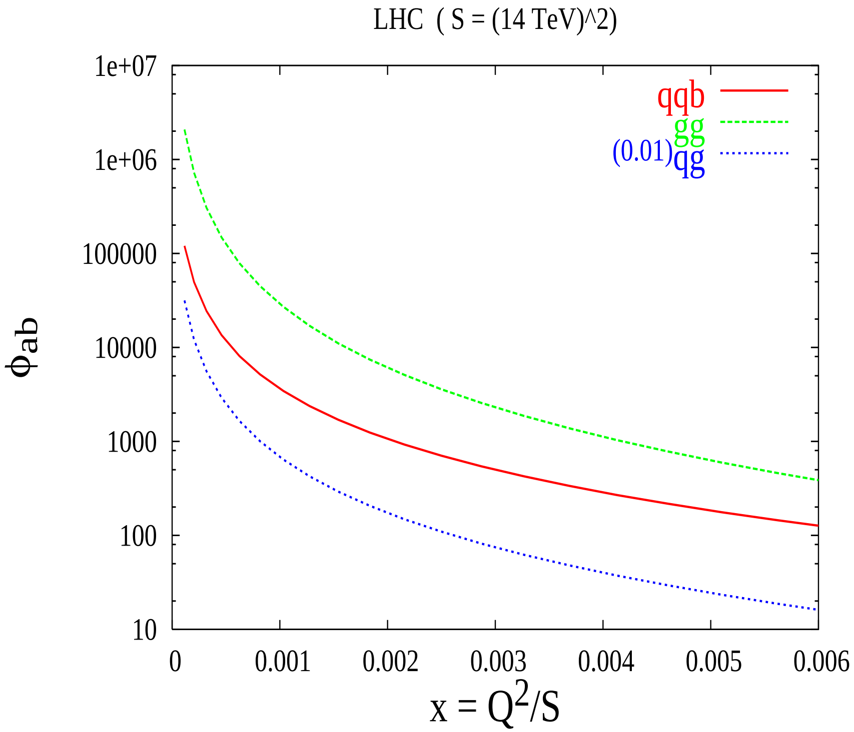

- $\Phi_{ab}(x)$ becomes large when $x \to x_{min} = \tau$
- Dominant contribution to Higgs production comes from the region when $x \to \tau$
- It is sufficient if we know the partonic cross section when $x \to \tau$
- $x \to \tau$ is called $soft\ limit$.
- Expand the partonic cross section around $x = \tau$.

- Gluon flux is largest at LHC
- Soft gluon NNLL resummation gives less than 9% correction at the LHC

S.Catani, D.DeFlorian, P.Nason, M.Grazzini

Soft gluon Resummation beyond $NNLL$ for Higgs production

$S.Catani, P.Nason, D.DeFlorian, M.Grazzini;\ S.Moch, A.Vogt; E.Laenen, L.Magnea$

Soft gluon Resummation beyond $NNLL$ for Higgs production

S.Catani, P.Nason, D.DeFlorian, M.Grazzini; S.Moch, A.Vogt; E.Laenen, L.Magnea

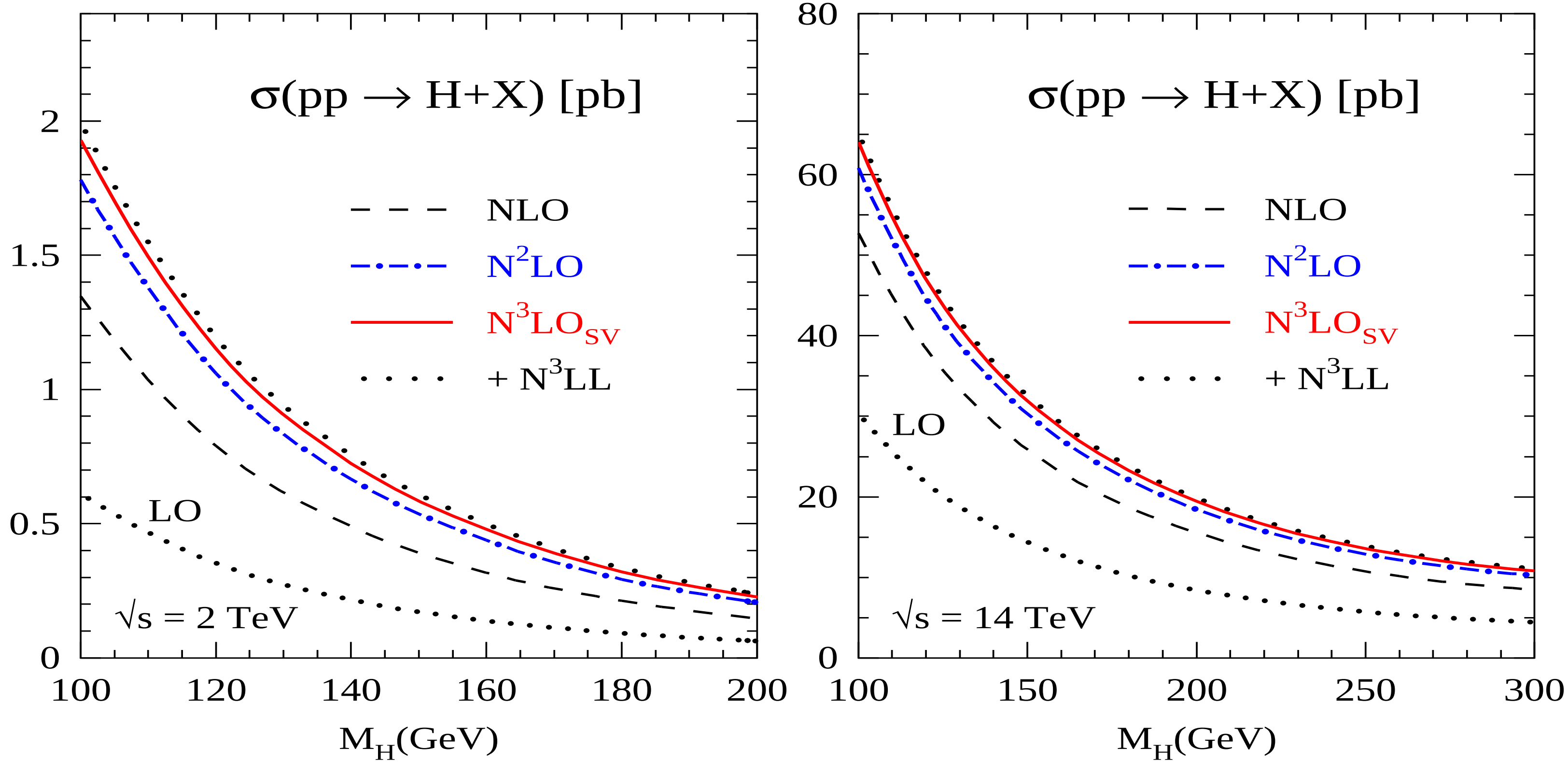

Soft gluon Resummation beyond $NNLL$ for Higgs production

S.Catani, P.Nason, D.DeFlorian, M.Grazzini; S.Moch, A.Vogt; E.Laenen, L.Magnea

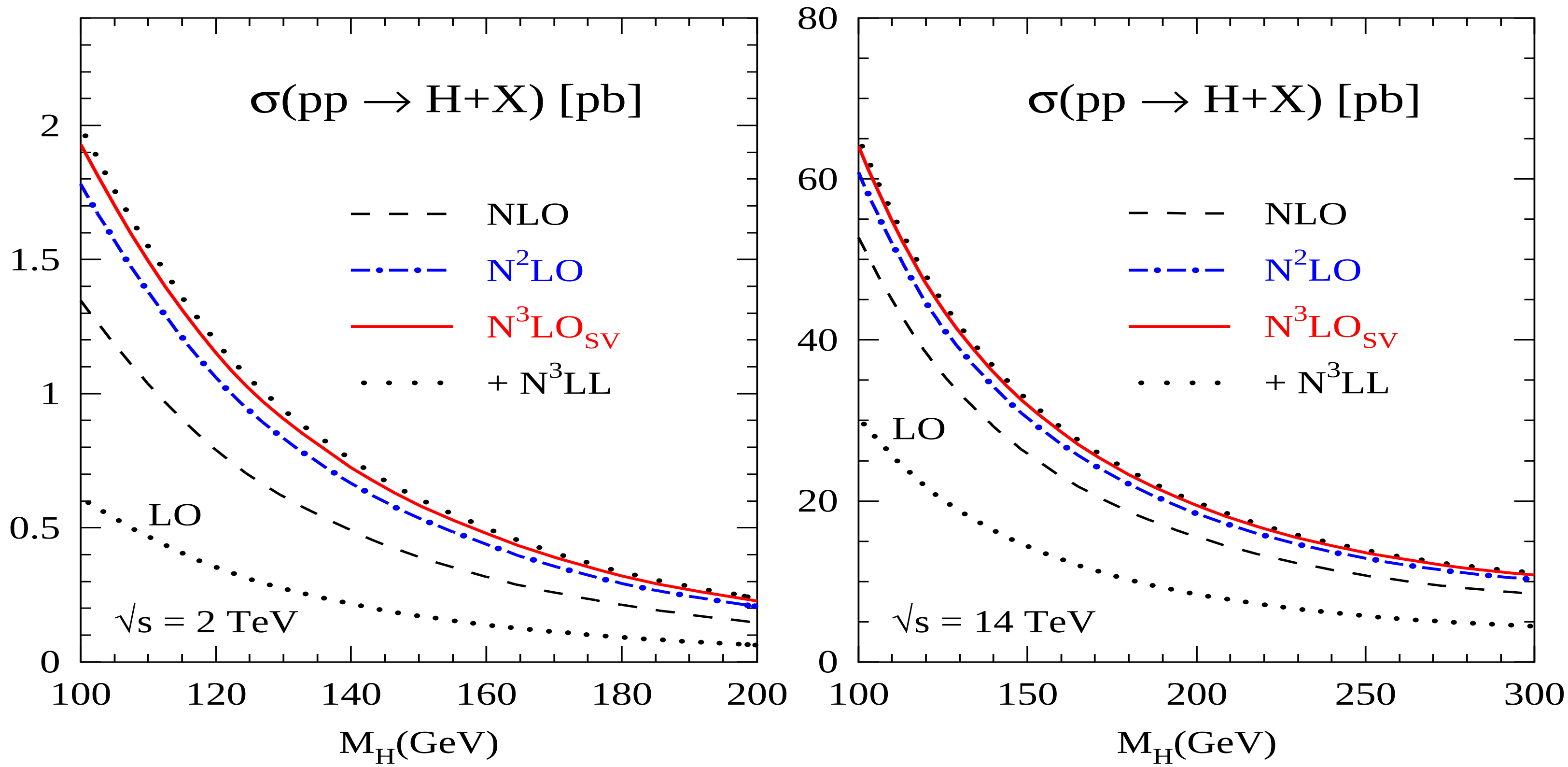

- N^3LL resummation exponents are available now.

Soft gluon Resummation beyond $NNLL$ for Higgs production

$S.Catani, P.Nason, D.DeFlorian, M.Grazzini;\ S.Moch, A.Vogt; E.Laenen, L.Magnea$

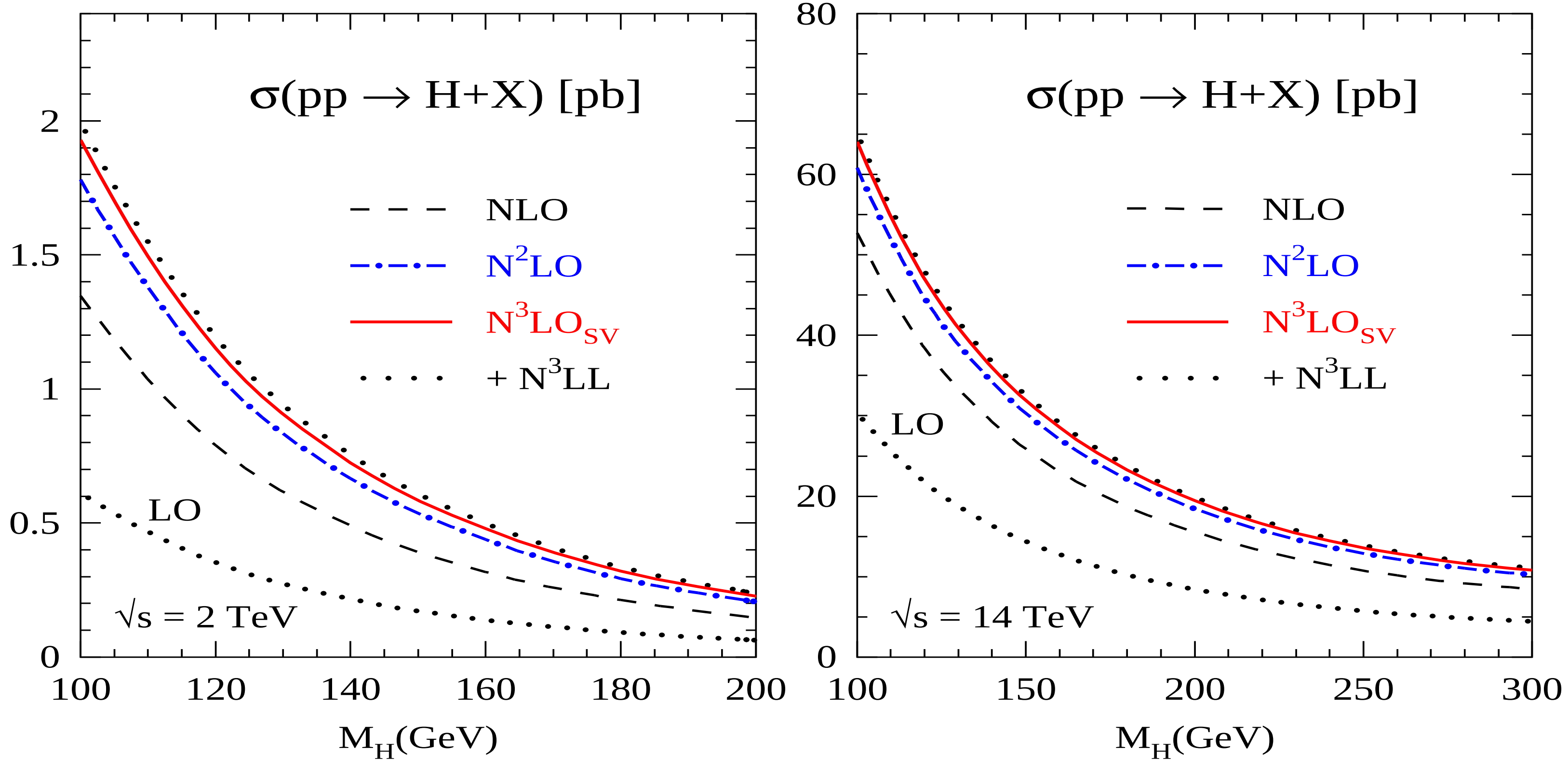

- $\boldsymbol{N^3LL}$ resummation exponents are available now.
- $\boldsymbol{N^3LL}$ resummation does not change the picture much. Fixed order $\boldsymbol{N^3LO_{pSV}}$ is very close to the $\boldsymbol{N^3LL}$ resummed result.

Soft gluon Resummation beyond $NNLL$ for Higgs production

S. Catani, P. Nason, D. DeFlorian, M. Grazzini; S. Moch, A. Vogt; E. Laenen, L. Magnea

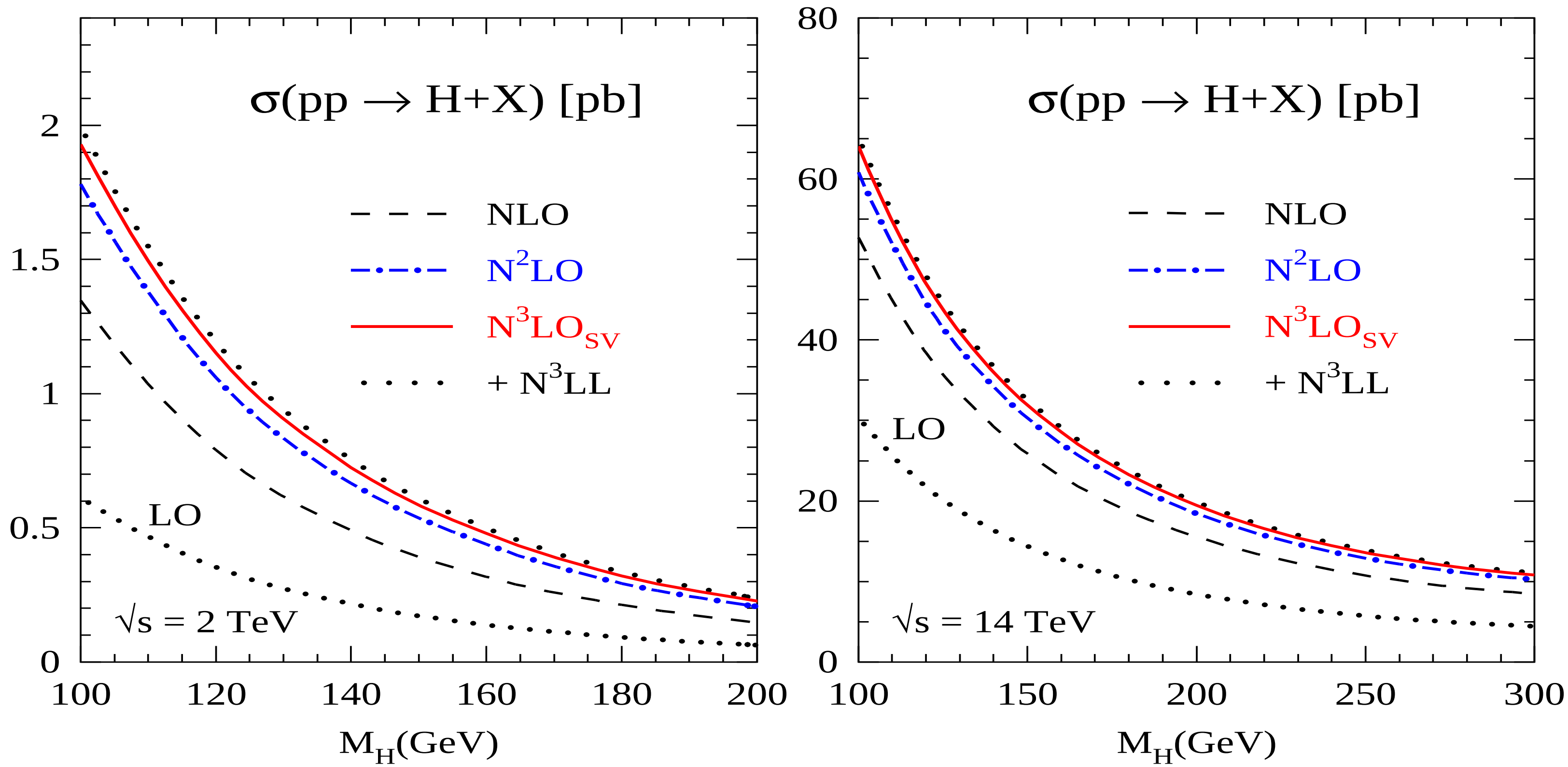

- N^3LL resummation exponents are available now.
- N^3LL resummation does not change the picture much. Fixed order N^3LO_{pSV} is very close to the N^3LL resummed result.
- Since QCD corrections can reduce the scale uncertainties only to $10\% - 20\%$, contributions from electroweak sector is also important.

2-loop Electroweak, Mixed QCD and Electroweak, b quark contributions:

U.Aglietti et al;G.Degrassi,F.Maltoni;G.Passarino et al;Anastasiou et al;W.Keung,F.Petriello,O.Brein

2-loop Electroweak, Mixed QCD and Electroweak, b quark contributions:

U.Aglietti et al;G.Degrassi,F.Maltoni;G.Passarino et al;Anastasiou et al;W.Keung,F.Petriello,O.Brein

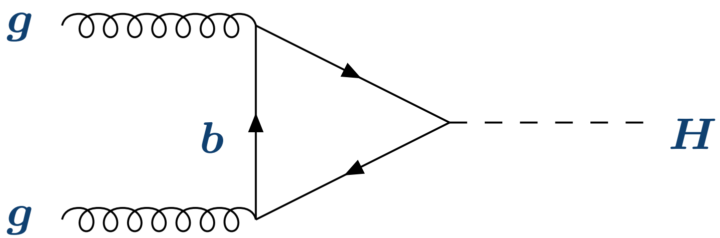

"interferece" with "t" loop + NLO QCD

2-loop Electroweak, Mixed QCD and Electroweak, b quark contributions:

U.Aglietti et al;G.Degrassi,F.Maltoni;G.Passarino et al;Anastasiou et al;W.Keung,F.Petriello,O.Brein

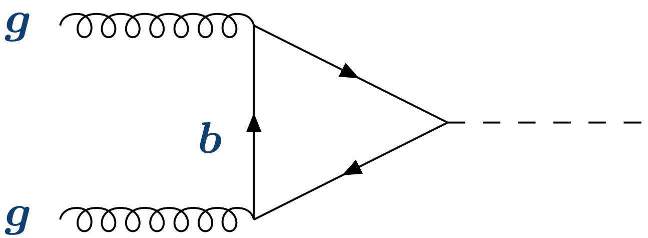

H "interferece" with "t" loop + NLO QCD

Pure QCD processes interference with Electroweak Processes:

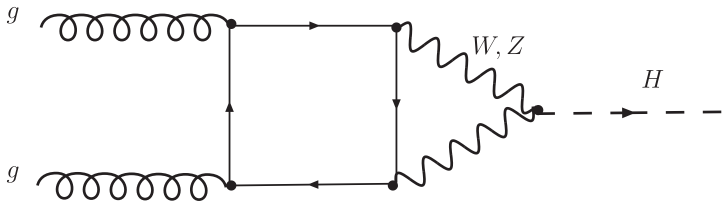

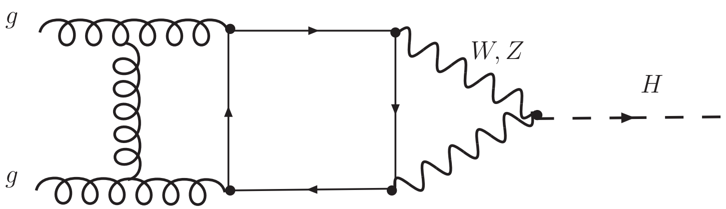

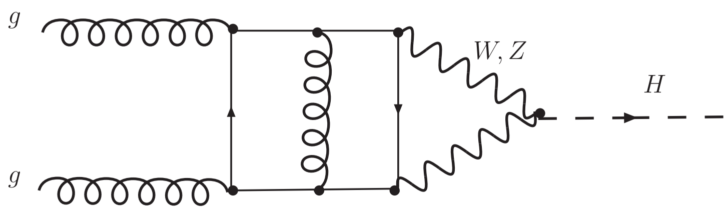

Electroweak: $5\%(m_H = 120$ Gev) and -2% ($m_H = 300$GeV); b quark loops contribute $5-6\%$ at $m_H = 120$ GeV at LHC

Renormalisation group improved result

Renormalisation group improved result

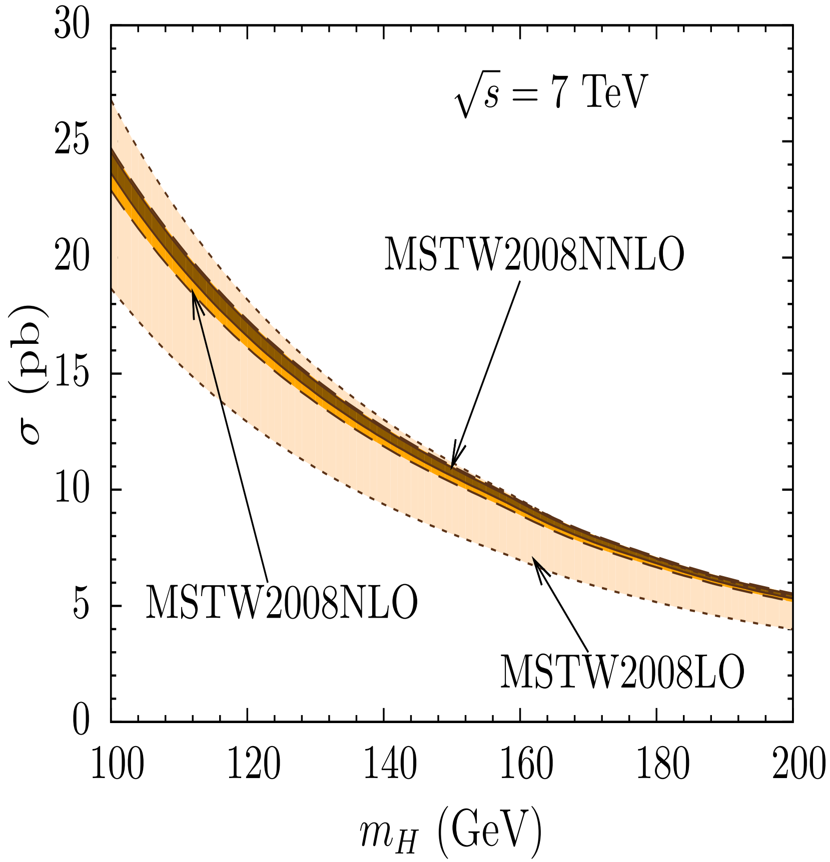

Renormalisation group improved result

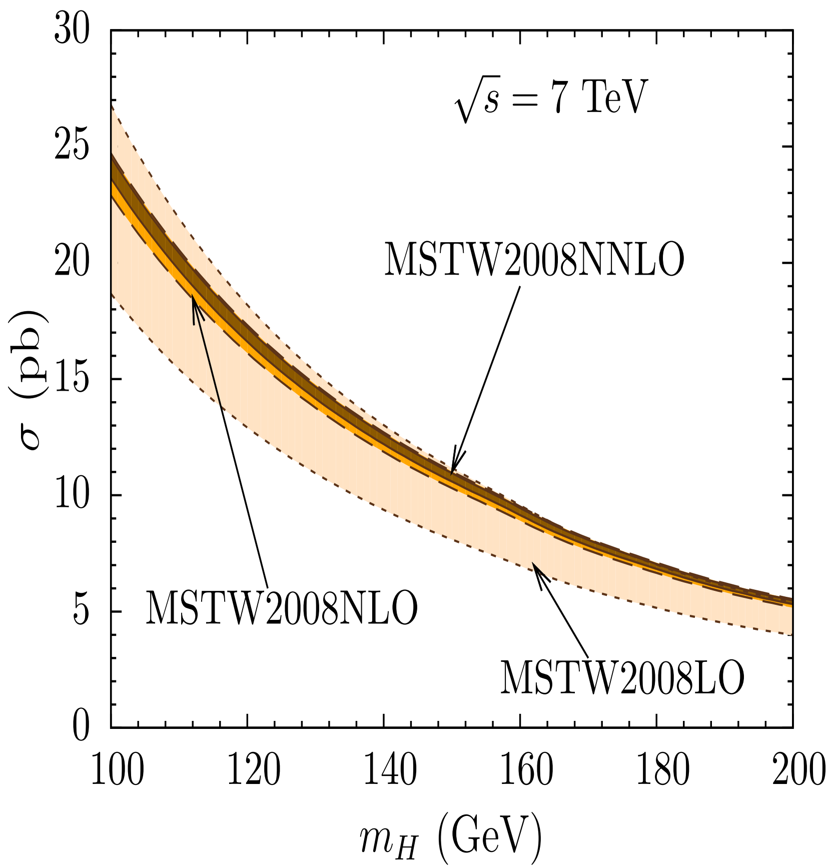

Ahrens, Becher, Neubert, Yang:

- NLO with exact top quark mass contributions,
- NNLO in the large top quark mass limit,
- EW corrections given by Passarino et al
- **use exact solutions to the RG equations of soft, collinear and hard pieces** of the cross section.

Renormalisation group improved result

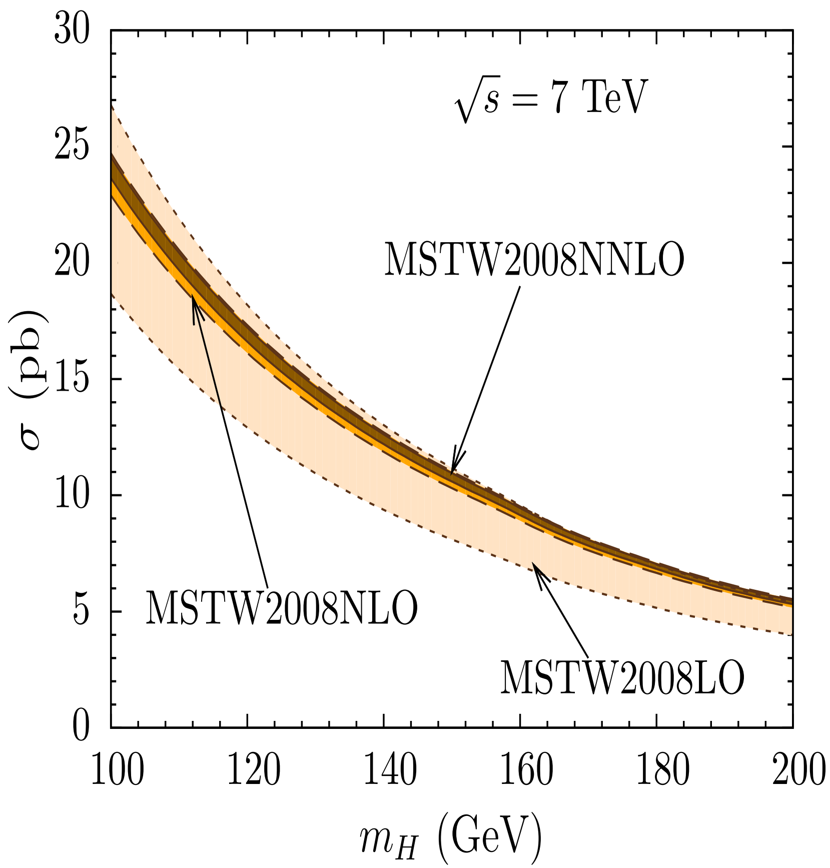

Ahrens, Becher, Neubert, Yang:

- NLO with exact top quark mass contributions,
- NNLO in the large top quark mass limit,
- EW corrections given by Passarino et al
- **use exact solutions to the RG equations of soft,collinear and hard pieces** of the cross section.

Good perturbative stability from LO onwards.

μ_R, μ_F and PDF dependence in Higgs production ($8\ TeV$)

MSTW PDF set (σ in pb and errors($\pm$) in %): $VR,\ J.\ Smith$

μ_R, μ_F and PDF dependence in Higgs production ($8\ TeV$)

MSTW PDF set (σ in pb and errors($\pm$) in %): *VR, J. Smith*

m_H	NNLO	μ_R	$\mu_{R,3}$	μ_F	μ	$\mathrm{NNLO}_{\overline{\mu}}$	PDF	$\mathrm{N^3LO}_{sv}$	μ_R
123	18.99	$+10.82$ -10.41	$+16.70$ -16.04	-0.43 $+0.53$	$+10.44$ -9.93	**20.97**	$+2.50$ -3.12	19.79	$+0.10$ -2.32
124	18.68	$+10.80$ -10.39	$+16.66$ -16.01	-0.41 $+0.51$	$+10.43$ -9.94	**20.62**	$+2.51$ -3.12	19.46	$+0.09$ -2.28
125	18.37	$+10.77$ -10.37	$+16.63$ -15.99	-0.39 $+0.50$	$+10.43$ -9.94	**20.28**	$+2.51$ -3.13	19.13	$+0.08$ -2.24
126	18.07	$+10.75$ -10.35	$+16.59$ -15.96	-0.37 $+0.47$	$+10.42$ -9.94	**19.95**	$+2.52$ -3.13	18.82	$+0.07$ -2.19
127	17.78	$+10.73$ -10.33	$+16.56$ -15.93	-0.35 $+0.45$	$+10.41$ -9.95	**19.63**	$+2.52$ -3.13	18.51	$+0.06$ -2.15

μ_R, μ_F and PDF dependence in Higgs production ($8\ TeV$)

MSTW PDF set (σ in pb and errors($\pm$) in %): *VR, J. Smith*

m_H	NNLO	μ_R	$\mu_{R,3}$	μ_F	μ	$\mathrm{NNLO}_{\overline{\mu}}$	PDF	$\mathrm{N^3LO}_{sv}$	μ_R
123	18.99	$^{+10.82}_{-10.41}$	$^{+16.70}_{-16.04}$	$^{-0.43}_{+0.53}$	$^{+10.44}_{-9.93}$	**20.97**	$^{+2.50}_{-3.12}$	19.79	$^{+0.10}_{-2.32}$
124	18.68	$^{+10.80}_{-10.39}$	$^{+16.66}_{-16.01}$	$^{-0.41}_{+0.51}$	$^{+10.43}_{-9.94}$	**20.62**	$^{+2.51}_{-3.12}$	19.46	$^{+0.09}_{-2.28}$
125	18.37	$^{+10.77}_{-10.37}$	$^{+16.63}_{-15.99}$	$^{-0.39}_{+0.50}$	$^{+10.43}_{-9.94}$	**20.28**	$^{+2.51}_{-3.13}$	19.13	$^{+0.08}_{-2.24}$
126	18.07	$^{+10.75}_{-10.35}$	$^{+16.59}_{-15.96}$	$^{-0.37}_{+0.47}$	$^{+10.42}_{-9.94}$	**19.95**	$^{+2.52}_{-3.13}$	18.82	$^{+0.07}_{-2.19}$
127	17.78	$^{+10.73}_{-10.33}$	$^{+16.56}_{-15.93}$	$^{-0.35}_{+0.45}$	$^{+10.41}_{-9.95}$	**19.63**	$^{+2.52}_{-3.13}$	18.51	$^{+0.06}_{-2.15}$

Uncertainty in NNLO result:

- μ_R variation ($m_h/2 < \mu_R < 2m_h$) gives 11%
- μ_R variation ($m_h/3 < \mu_R < 3m_h$) gives 17%
- μ_F variation ($m_h/2 < \mu_R < 2m_h$) gives 0.5%
- $\mu_R = \mu_F = 1/2 m_h$ resummes soft gluons
- MSTW PDF gives 3%
- N^3LO_{sv} gives around 3%

μ_R, μ_F and PDF dependence in Higgs production ($8\ TeV$)

VR, J. Smith

μ_R, μ_F and PDF dependence in Higgs production ($8\ TeV$)

ABM PDF set:($\boldsymbol{\sigma}$ in pb and errors($\pm$) in %): *VR, J. Smith*

m_H	NNLO	μ_R	$\mu_{R,3}$	μ_F	μ	NNLO$_{\overline{\mu}}$	PDF	N^{3}LO$_{sv}$	μ_R
123	17.58	$^{+10.13}_{-9.86}$	$^{+15.59}_{-15.25}$	$^{-0.18}_{+0.33}$	$^{+9.91}_{-9.63}$	19.33	± 4.40	19.97	$^{+0.10}_{-2.25}$
124	17.29	$^{+10.11}_{-9.85}$	$^{+15.57}_{-15.23}$	$^{-0.16}_{+0.31}$	$^{+9.90}_{-9.64}$	19.00	± 4.43	19.63	$^{+0.09}_{-2.21}$
125	16.99	$^{+10.08}_{-9.83}$	$^{+15.52}_{-15.20}$	$^{-0.12}_{+0.28}$	$^{+9.91}_{-9.65}$	18.67	± 4.75	19.28	$^{+0.12}_{-2.15}$
126	16.71	$^{+10.06}_{-9.81}$	$^{+15.49}_{-15.17}$	$^{-0.13}_{+0.25}$	$^{+9.87}_{-9.66}$	18.36	± 4.54	18.96	$^{+0.13}_{-2.11}$
127	16.43	$^{+10.04}_{-9.79}$	$^{+15.46}_{-15.15}$	$^{-0.03}_{+0.27}$	$^{+9.96}_{-9.63}$	18.07	± 4.26	18.64	$^{+0.14}_{-2.06}$

μ_R, μ_F and PDF dependence in Higgs production ($8\ TeV$)

ABM PDF set:(σ in pb and errors($\pm$) in %):

VR, J. Smith

m_H	NNLO	μ_R	$\mu_{R,3}$	μ_F	μ	$\mathrm{NNLO}_{\overline{\mu}}$	PDF	$\mathrm{N^3LO}_{sv}$	μ_R
123	17.58	$+10.13$ -9.86	$+15.59$ -15.25	-0.18 $+0.33$	$+9.91$ -9.63	19.33	± 4.40	19.97	$+0.10$ -2.25
124	17.29	$+10.11$ -9.85	$+15.57$ -15.23	-0.16 $+0.31$	$+9.90$ -9.64	19.00	± 4.43	19.63	$+0.09$ -2.21
125	16.99	$+10.08$ -9.83	$+15.52$ -15.20	-0.12 $+0.28$	$+9.91$ -9.65	18.67	± 4.75	19.28	$+0.12$ -2.15
126	16.71	$+10.06$ -9.81	$+15.49$ -15.17	-0.13 $+0.25$	$+9.87$ -9.66	18.36	± 4.54	18.96	$+0.13$ -2.11
127	16.43	$+10.04$ -9.79	$+15.46$ -15.15	-0.03 $+0.27$	$+9.96$ -9.63	18.07	± 4.26	18.64	$+0.14$ -2.06

Uncertainty in NNLO result:

- μ_R variation ($m_h/2 < \mu_R < 2m_h$) gives 10%
- μ_R variation ($m_h/3 < \mu_R < 3m_h$) gives 17%
- μ_F variation ($m_h/2 < \mu_R < 2m_h$) gives 0.5%
- $\mu_R = \mu_F = 1/2 m_h$ resummes soft gluons
- ABM PDF gives 5%
- N^3LO_{sv} gives around 2% due to μ_R

PDF dependence in Higgs production ($8\ TeV$)

$VR,\ J.\ Smith$

PDF dependence in Higgs production ($8\ TeV$)

Differnet PDF sets (m_h in GeV and cross sections in pb): *VR, J. Smith*

m_h	NNLO				$\mathbf{N^3LO_{sv}}$			
	MSTW	ABM	CT	NNPDF	MSTW	ABM	CT	NNPDF
120	19.98	18.51	19.86	21.00	20.83	21.04	20.26	20.91
121	19.64	18.18	19.52	20.65	20.47	20.62	19.91	20.56
122	19.31	17.89	19.20	20.30	20.13	20.32	19.57	20.21
123	18.99	17.58	18.88	19.96	19.79	19.97	19.24	19.87
124	18.68	17.29	18.57	19.63	19.46	19.63	18.92	19.54
125	18.37	16.99	18.27	19.31	19.13	19.28	18.61	19.21
126	18.07	16.71	17.97	18.99	18.82	18.96	18.31	18.89
127	17.78	16.43	17.68	18.66	18.51	18.64	18.01	18.53
128	17.49	16.16	17.39	18.52	18.21	18.32	17.72	18.61
129	17.21	15.91	17.12	18.09	17.91	18.04	17.43	17.99

PDF dependence in Higgs production ($8\ TeV$)

Differnet PDF sets (m_h in GeV and cross sections in pb): *$VR,\ J.\ Smith$*

m_h	NNLO				$\mathbf{N^3LO_{sv}}$			
	MSTW	ABM	CT	NNPDF	MSTW	ABM	CT	NNPDF
120	19.98	18.51	19.86	21.00	20.83	21.04	20.26	20.91
121	19.64	18.18	19.52	20.65	20.47	20.62	19.91	20.56
122	19.31	17.89	19.20	20.30	20.13	20.32	19.57	20.21
123	18.99	17.58	18.88	19.96	19.79	19.97	19.24	19.87
124	18.68	17.29	18.57	19.63	19.46	19.63	18.92	19.54
125	18.37	16.99	18.27	19.31	19.13	19.28	18.61	19.21
126	18.07	16.71	17.97	18.99	18.82	18.96	18.31	18.89
127	17.78	16.43	17.68	18.66	18.51	18.64	18.01	18.53
128	17.49	16.16	17.39	18.52	18.21	18.32	17.72	18.61
129	17.21	15.91	17.12	18.09	17.91	18.04	17.43	17.99

- ABM is $\mathbf{7.4\%}$ smaller than MSTW
- CT is just $\mathbf{0.5\%}$ smaller than MSTW
- NNPDF is $\mathbf{5\%}$ larger than MSTW
- All PDFs give almost same results for $\boldsymbol{N^3LO_{sv}}$ corrected cross section.

Soft gluons at N^3LO_{pSV} for Higgs production ($8\ TeV$)

VR, J. Smith

$$R = \frac{\sigma_{N^iLO}(\mu)}{\sigma_{N^iLO}(\mu_0)}$$

Soft gluons at N^3LO_{pSV} for Higgs production ($8\ TeV$)

VR, J. Smith

$$R = \frac{\sigma_{N^iLO}(\mu)}{\sigma_{N^iLO}(\mu_0)}$$

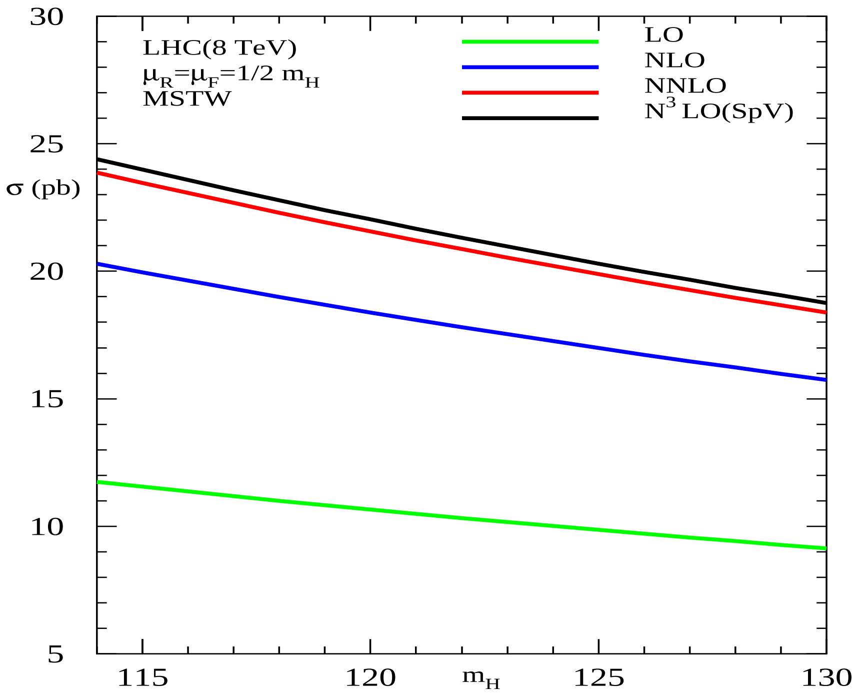

Soft gluons at N^3LO_{pSV} for Higgs production ($8\ TeV$)

VR, J. Smith

$$R = \frac{\sigma_{N^iLO}(\mu)}{\sigma_{N^iLO}(\mu_0)}$$

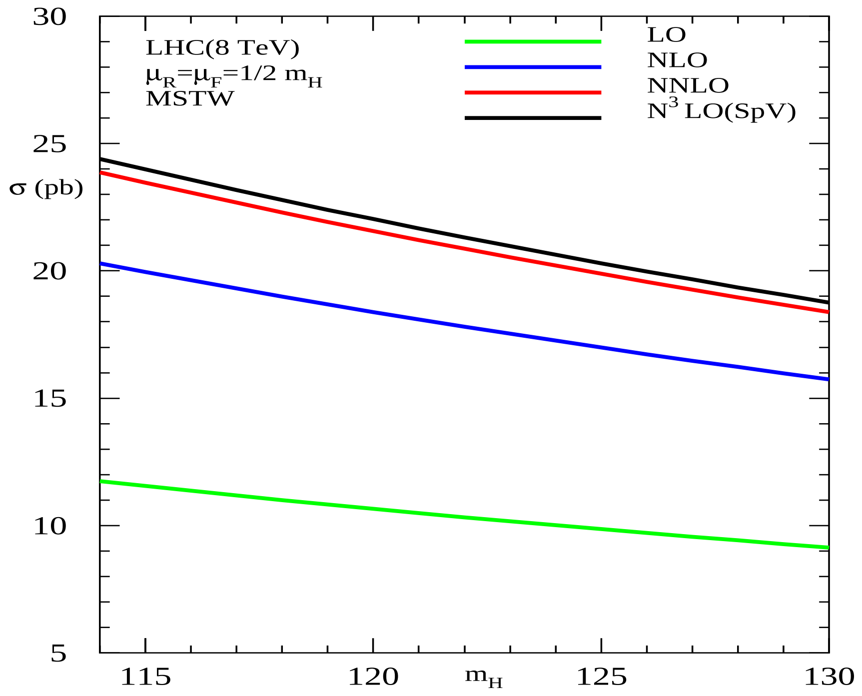

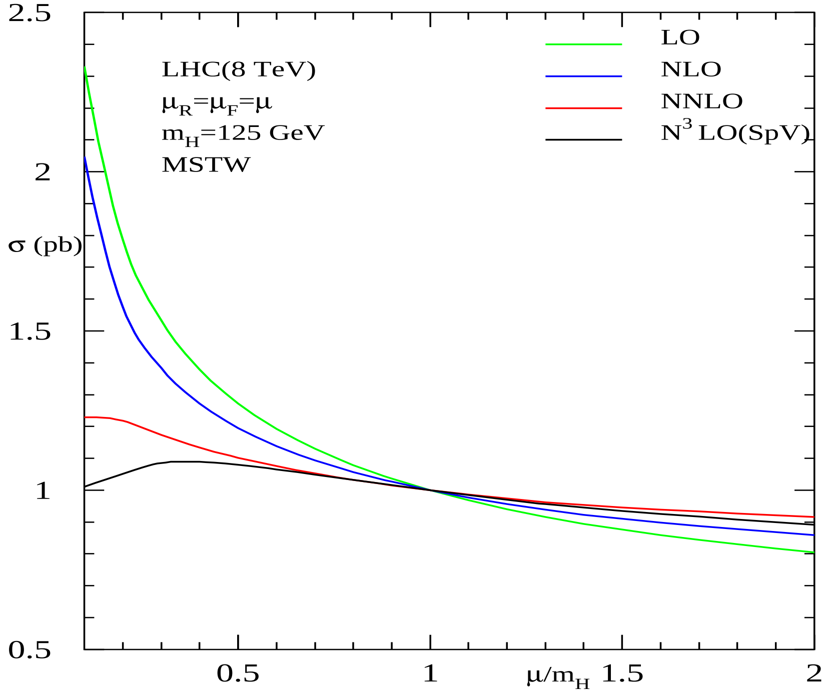

Soft gluons at N^3LO_{pSV} for Higgs production ($8\ TeV$)

VR, J. Smith

$$R = \frac{\sigma_{N^iLO}(\mu)}{\sigma_{N^iLO}(\mu_0)}$$

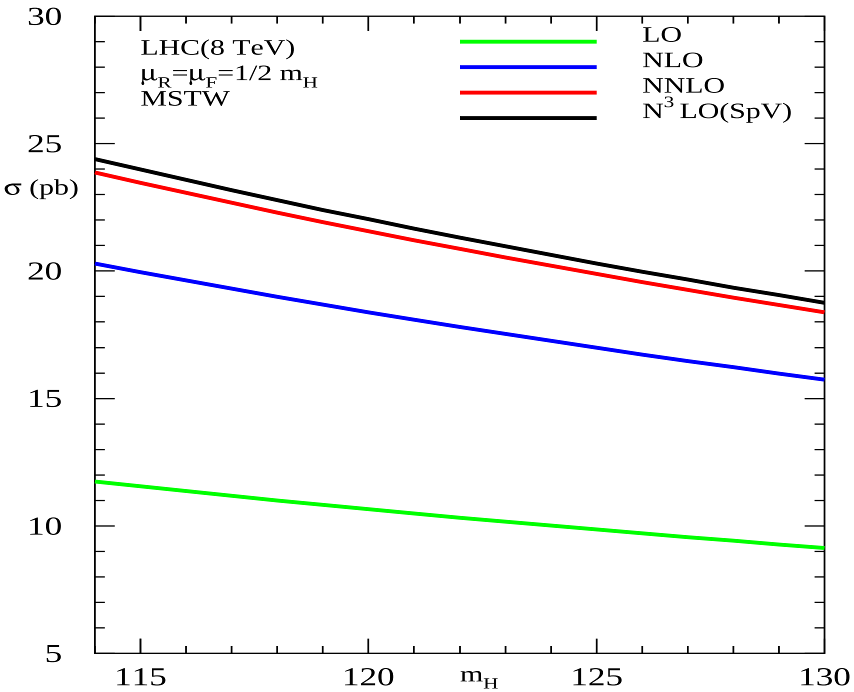

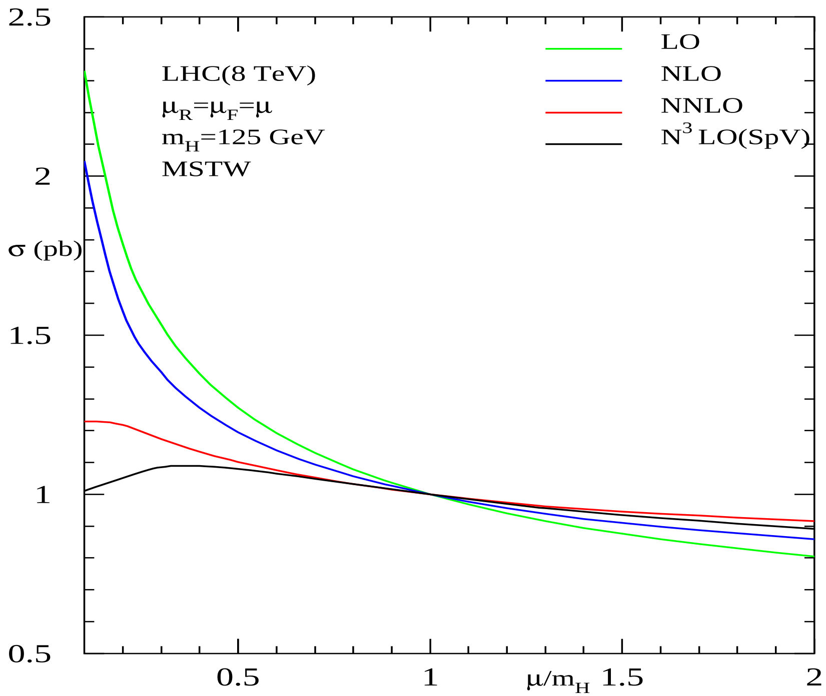

- NLO increases the cross section by 80%,
- NNLO to 30%,
- resummation to 10% and electoweak effects by 5%

Update-1: Anastasiou-Boughezal-Petriello-Stoeckli:

Update-1: Anastasiou-Boughezal-Petriello-Stoeckli:

- Exact NLO cross section with full dependence on the top- and bottom-quark masses
- NNLO cross section-Effective Field Theory, i.e., in the large-m_t limit
- EW contributions evaluated in the complete factorization scheme

$$\sigma = \sum_{i=0}^{\infty} \alpha_s^i \sigma_{QCD}^{(i)} \otimes (1 + \delta_{EW})$$

- Mixed QCD-EWcontributions are also accounted for, together with some effects from EW corrections at finite transverse momentum.
- The effect of soft-gluon resummation is mimicked by choosing the central value of the renormalization and factorization scales as $\mu_R = \mu_F = M_H/2$.

Update-2: de Florian-Grazzini:

Update-2: de Florian-Grazzini:

- Exact NLO cross section with full dependence on the top- and bottom-quark masses, computed with the program HIGLU,
- the NLL resummation of soft-gluons,
- the NNLL+NNLO corrections are consistently added in the large-mt limit
- corrected for EW contributions in the complete factorization scheme.
- The central value of factorization and renormalization scales is chosen to be $\mu_F = \mu_R = M_H$

Comparison

Comparison

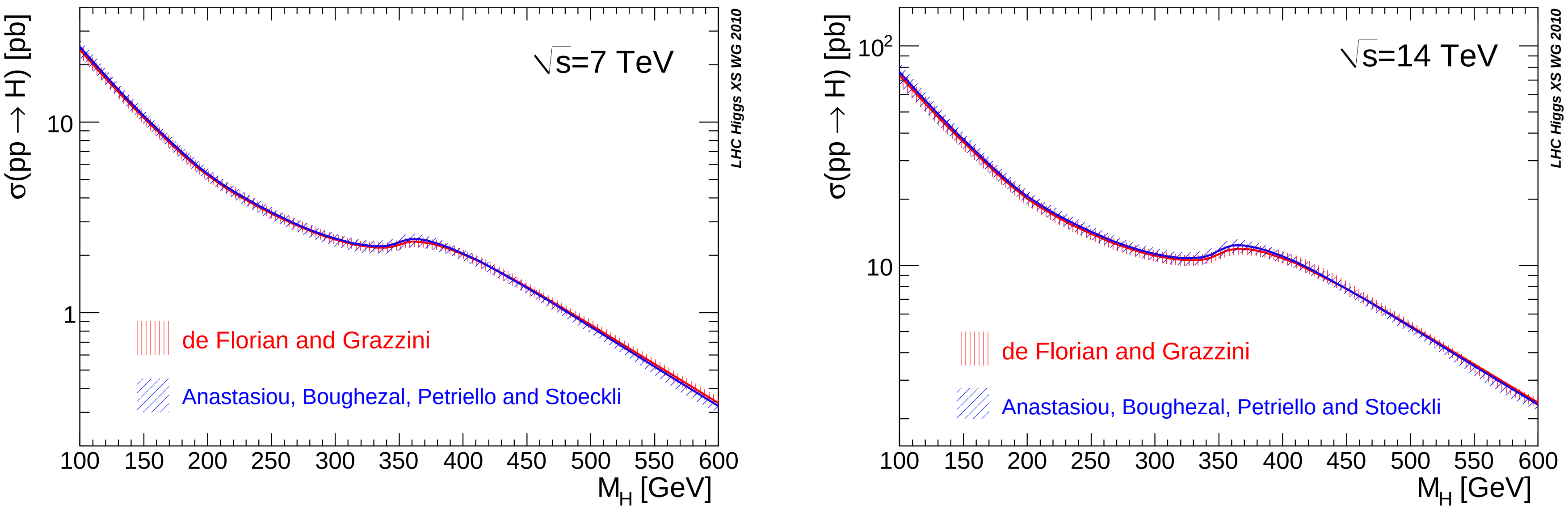

$\sigma(pp \to H)$ [pb]
$\sqrt{s}$=7 TeV
LHC Higgs XS WG 2010
10
1
de Florian and Grazzini
Anastasiou, Boughezal, Petriello and Stoeckli
100 150 200 250 300 350 400 450 500 550 600
M_H [GeV]
$\sigma(pp \to H)$ [pb]
$\sqrt{s}$=14 TeV
LHC Higgs XS WG 2010
10^2
10
de Florian and Grazzini
Anastasiou, Boughezal, Petriello and Stoeckli
100 150 200 250 300 350 400 450 500 550 600
M_H [GeV]

Fixed vs Resummed at 7 TeV

Fixed vs Resummed at 7 TeV

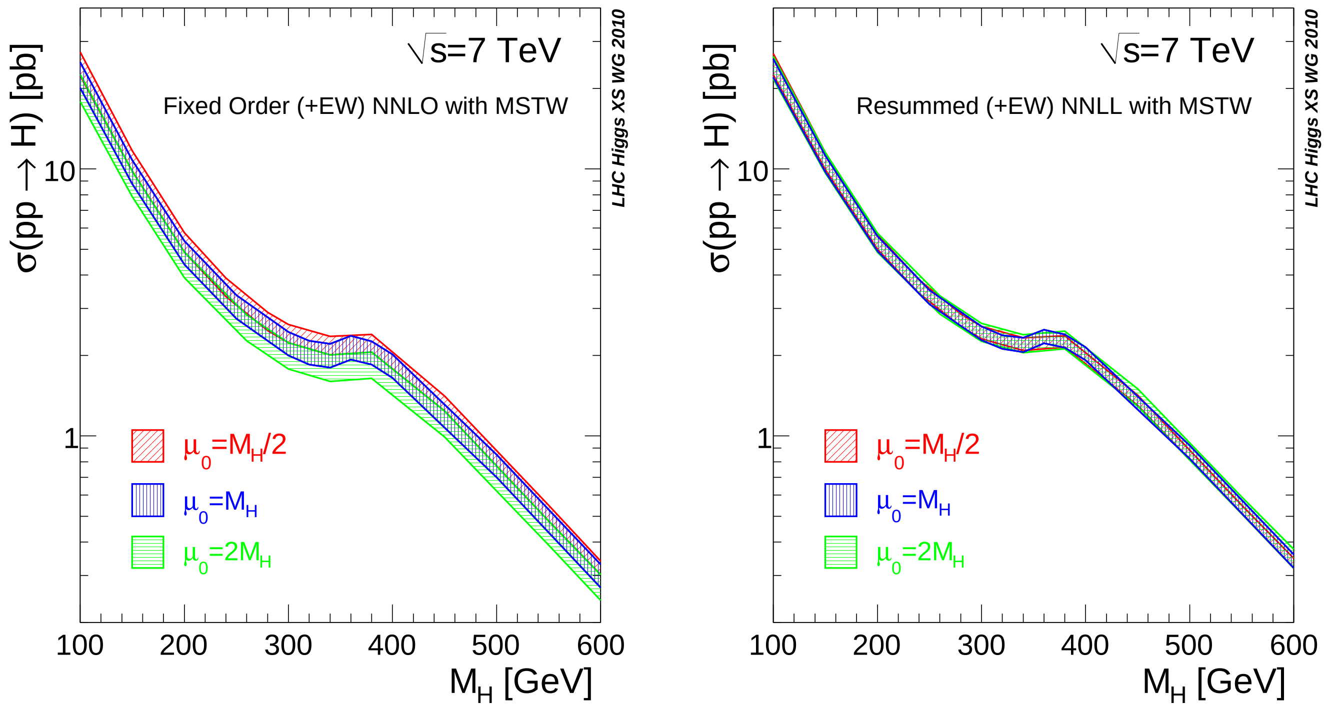

- Comparison of NNLO and NNLL bands with different choice of the central scale.

Final numbers for gluon fusion for $m_h = 125$ GeV

Final numbers for gluon fusion for $m_h = 125$ GeV

Production cross section at $\sqrt{s} = 7$ TeV with scale($\mu_R = \mu_F$) and PDF($+\alpha_s$) unctertainties:

$$\sigma = 15.31^{11.7\%}_{-7.8\%}(scale)^{+7.8\%}_{-7.3\%}(PDF + \alpha_s)pb$$

Production cross section at $\sqrt{s} = 8$ TeV:

- de Florian et al:

$$\sigma = 19.52^{7.2\%}_{-7.8\%}(\mathrm{scale})^{+7.5\%}_{-6.9\%}(\mathrm{PDF} + \alpha_\mathrm{s})pb$$

- Anastasiou et al:

$$\sigma = 20.69^{8.4\%}_{-9.3\%}(\mathrm{scale})^{+7.8\%}_{-7.5\%}(\mathrm{PDF} + \alpha_\mathrm{s})pb$$

Towards N^3LO corrected Higgs cross section

Anastasiou et.al

Towards N^3LO corrected Higgs cross section

Anastasiou et.al

- Square of one-loop virtuals to N^3LO

$$
\begin{aligned}
g(p_1) + g(p_2) &\rightarrow g(p_3) + H(p_4)\\
q(p_1) + g(p_2) &\rightarrow q(p_3) + H(p_4)\\
q(p_1) + \bar{q}(p_2) &\rightarrow g(p_3) + H(p_4)
\end{aligned}
$$

Towards N^3LO corrected Higgs cross section

$Anastasiou\ et.al$

- Square of one-loop virtuals to N^3LO

$$
\begin{aligned}
g(p_1) + g(p_2) &\rightarrow g(p_3) + H(p_4) \\
q(p_1) + g(p_2) &\rightarrow q(p_3) + H(p_4) \\
q(p_1) + \bar{q}(p_2) &\rightarrow g(p_3) + H(p_4)
\end{aligned}
$$

- Performing a loop-expansion of the amplitudes

$$\mathcal{A}_X = \sum_{j=0}^{\infty} \mathcal{A}_X^{(j)}$$

in the effective theory with j being the number of loops, we have:

$$|\mathcal{A}_X|^2 = \left|\mathcal{A}_X^{(0)}\right|^2 + 2\Re\left(\mathcal{A}_X^{(0)}\mathcal{A}_X^{(1)^*}\right) + \left[\left|\mathcal{A}_X^{(1)}\right|^2 + 2\Re\left(\mathcal{A}_X^{(0)}\mathcal{A}_X^{(2)^*}\right)\right] + \ldots$$

Towards N^3LO corrected Higgs cross section

Anastasiou et.al

- Square of one-loop virtuals to N^3LO

$$\begin{aligned} g(p_1) + g(p_2) &\to g(p_3) + H(p_4) \\ q(p_1) + g(p_2) &\to q(p_3) + H(p_4) \\ q(p_1) + \bar{q}(p_2) &\to g(p_3) + H(p_4) \end{aligned}$$

- Performing a loop-expansion of the amplitudes

$$\mathcal{A}_X = \sum_{j=0}^{\infty} \mathcal{A}_X^{(j)}$$

in the effective theory with j being the number of loops, we have:

$$|\mathcal{A}_X|^2 = \left|\mathcal{A}_X^{(0)}\right|^2 + 2\Re\left(\mathcal{A}_X^{(0)}\mathcal{A}_X^{(1)*}\right) + \left[\left|\mathcal{A}_X^{(1)}\right|^2 + 2\Re\left(\mathcal{A}_X^{(0)}\mathcal{A}_X^{(2)*}\right)\right] + \dots$$

$$\sigma_X^{1\otimes 1} = s^{-1-\varepsilon}\,\frac{\mathcal{N}_X\,(4\pi)^{\varepsilon}}{16\pi\,\Gamma(1-\varepsilon)}\,\delta^{1-2\varepsilon}\int_0^1 d\lambda\,[\lambda\,(1-\lambda)]^{-\varepsilon}\sum\left|\mathcal{A}_X^{(1)}\right|^2 .$$

Towards N^3LO corrected Higgs cross section

$Anastasiou\ et.al$

- Square of one-loop virtuals to N^3LO

$$\begin{aligned} g(p_1) + g(p_2) &\to g(p_3) + H(p_4) \\ q(p_1) + g(p_2) &\to q(p_3) + H(p_4) \\ q(p_1) + \bar{q}(p_2) &\to g(p_3) + H(p_4) \end{aligned}$$

- Performing a loop-expansion of the amplitudes

$$\mathcal{A}_X = \sum_{j=0}^{\infty} \mathcal{A}_X^{(j)}$$

in the effective theory with j being the number of loops, we have:

$$|\mathcal{A}_X|^2 = \left|\mathcal{A}_X^{(0)}\right|^2 + 2\Re\left(\mathcal{A}_X^{(0)}\mathcal{A}_X^{(1)*}\right) + \left[\left|\mathcal{A}_X^{(1)}\right|^2 + 2\Re\left(\mathcal{A}_X^{(0)}\mathcal{A}_X^{(2)*}\right)\right] + \ldots$$

$$\sigma_X^{1\otimes 1} = s^{-1-\varepsilon}\,\frac{\mathcal{N}_X\,(4\pi)^{\varepsilon}}{16\pi\,\Gamma(1-\varepsilon)}\,\delta^{1-2\varepsilon}\int_0^1 d\lambda\,[\lambda\,(1-\lambda)]^{-\varepsilon}\sum\left|\mathcal{A}_X^{(1)}\right|^2 .$$

- Reverse Unitarity and Integration parts lead to 19 master integrals
- Differential equation method is used to solve the master integrals

Alternate approach towards N^3LO

Kilgore

Alternate approach towards N^3LO

Kilgore

- Threshold expansion

- Square of the one-loop contribution to the cross section as an extended threshold expansion.

- Obtain enough terms to invert the series and determine the closed functional form through order ε.

- The method has been applied to get earlier results at NLO and NNLO level for inclusive cross sections in closed form, in terms of G-functions and the hypergeometric functions $2F_1$ and $3F_2$.

- These functions can be readily expanded to all orders in ε

Alternate approach towards N^3LO

Kilgore

- Threshold expansion

- Square of the one-loop contribution to the cross section as an extended threshold expansion.

- Obtain enough terms to invert the series and determine the closed functional form through order ε.

- The method has been applied to get earlier results at NLO and NNLO level for inclusive cross sections in closed form, in terms of G-functions and the hypergeometric functions $2F_1$ and $3F_2$.

- These functions can be readily expanded to all orders in ε

$$2F_1(1,-\varepsilon;1-\varepsilon;-xy/\overline{y}) = \sum_{n=0}^{\infty} \frac{\overline{x}}{n!} \frac{(-\varepsilon)_n}{n!} \left(2F_1(1,-\varepsilon,1-\varepsilon,-y/\overline{y}) - \overline{y} \sum_{m=0}^{n-1} y^m \frac{m!}{(1-\varepsilon)_m} \right)$$

Higgs with $0, 1, 2$ jets

Petriello et al

Higgs with $0, 1, 2$ jets

Petriello et al

- $\sigma_{\rm tot}$ - Inclusive cross section
- $\sigma_0(p_T^{\rm cut})$ - the 0-jet cross section: no jets with $p_T^{\rm jet} > p_T^{\rm cut}$ NNLO in QCD
- $\sigma_{\geq 1}(p_T^{\rm cut})$- the inclusive 1-jet cross section, with at least 1 jet with $p_T^{\rm jet} > p_T^{\rm cut}$ NLO in QCD
- $\sigma_1([p_{Ta}, p_{Tb}]; p_T^{\rm cut})$- the exclusive 1-jet cross section, with $p_{Tb} > p_{TJ} > p_{Ta}$ NLO
- $\sigma_{\geq 2}(p_T^{\rm cut})$ - the inclusive 2-jet cross section, with at least 2 jets with $p_T^{\rm jet} > p_T^{\rm cut}$ LO

Consistency conditions:

$$\begin{aligned} \sigma_{\rm tot} &= \sigma_0(p_T^{\rm cut}) + \sigma_{\geq 1}(p_T^{\rm cut})\,, \\ \sigma_{\geq 1}(p_T^{\rm cut}) &= \sigma_1([p_T^{\rm cut}, \infty]; p_T^{\rm cut}) + \sigma_{\geq 2}(p_T^{\rm cut})\,. \end{aligned}$$

- This leads to correlated errors

Theory Uncertainties

Petriello et al

Theory Uncertainties

Petriello et al

rate [pb]	ATLAS ($p_T^{\mathrm{cut}} = 25\mathrm{GeV},\ R = 0.4$)	CMS ($p_T^{\mathrm{cut}} = 30\mathrm{GeV},\ R = 0.5$)
$\sigma_{\mathrm{tot}}^{\mathrm{NNLO}}$	19.27 ± 1.50	19.27 ± 1.50
$\sigma_{\geq 1}^{\mathrm{NLO}}$	7.85 ± 1.41	6.47 ± 1.27
$\sigma_{\geq 2}^{\mathrm{LO}}$	2.42 ± 1.80	1.73 ± 1.31
$\sigma_{0}^{\mathrm{NNLO}}$	11.69 ± 2.06	12.80 ± 1.97
$\sigma_{1}^{\mathrm{NLO}}$	5.16 ± 2.29	4.75 ± 1.82

- Fixed order cross sections and their uncertainties for ATLAS and CMS parameters. The central scale is $\mu = m_H/2$.

Theory Uncertainties

Petriello et al

rate [pb]	ATLAS ($p_T^{\mathbf{cut}} = \mathbf{25GeV},\ \boldsymbol{R} = \mathbf{0.4}$)	CMS ($p_T^{\mathbf{cut}} = \mathbf{30GeV},\ \boldsymbol{R} = \mathbf{0.5}$)
$\boldsymbol{\sigma}_{\mathrm{tot}}^{\mathrm{NNLO}}$	19.27 ± 1.50	19.27 ± 1.50
$\boldsymbol{\sigma}_{\geq \mathbf{1}}^{\mathrm{NLO}}$	7.85 ± 1.41	6.47 ± 1.27
$\boldsymbol{\sigma}_{\geq \mathbf{2}}^{\mathrm{LO}}$	2.42 ± 1.80	1.73 ± 1.31
$\boldsymbol{\sigma}_{\mathbf{0}}^{\mathrm{NNLO}}$	11.69 ± 2.06	12.80 ± 1.97
$\boldsymbol{\sigma}_{\mathbf{1}}^{\mathrm{NLO}}$	5.16 ± 2.29	4.75 ± 1.82

- Fixed order cross sections and their uncertainties for ATLAS and CMS parameters. The central scale is $\boldsymbol{\mu} = \boldsymbol{m_H/2}$.

rate [pb]	ATLAS ($p_T^{\mathbf{cut}} = \mathbf{25GeV},\ \boldsymbol{R} = \mathbf{0.4}$)	CMS ($p_T^{\mathbf{cut}} = \mathbf{30GeV},\ \boldsymbol{R} = \mathbf{0.5}$)
$\boldsymbol{\sigma}_{\mathrm{tot}}$	21.69 ± 1.49	21.69 ± 1.49
$\boldsymbol{\sigma}_{\mathbf{0}}$	$12.67 \pm 0.87_{\boldsymbol{\mu}} \pm 0.86_{\boldsymbol{res}}$ ($\pm\ \mathbf{1.22}_{\mathrm{tot}}$)	$13.86 \pm 0.70_{\boldsymbol{\mu}} \pm 0.52_{\boldsymbol{res}}$ ($\pm\ \mathbf{0.87}_{\mathrm{tot}}$)
$\boldsymbol{\sigma}_{\mathbf{1}}$	$5.68 \pm 0.30_{\boldsymbol{\mu}} \pm 0.89_{\boldsymbol{res}}$ ($\pm\ \mathbf{0.94}_{\mathrm{tot}}$)	$4.97 \pm 0.43_{\boldsymbol{\mu}} \pm 0.61_{\boldsymbol{res}}$ ($\pm\ \mathbf{0.74}_{\mathrm{tot}}$)
$\boldsymbol{\sigma}_{\geq \mathbf{2}}$	$3.34 \pm 0.32_{\boldsymbol{\mu}} \pm 0.47_{\boldsymbol{res}}$ ($\pm\ \mathbf{0.57}_{\mathrm{tot}}$)	$2.86 \pm 0.36_{\boldsymbol{\mu}} \pm 0.44_{\boldsymbol{res}}$ ($\pm\ \mathbf{0.57}_{\mathrm{tot}}$)

- The total, 0-jet, 1-jet, and inclusive 2-jet cross sections and their uncertainties.

Higgs + 2 jets at NLO

H. van Deurzen et al.

Higgs + 2 jets at NLO

H. van Deurzen et al.

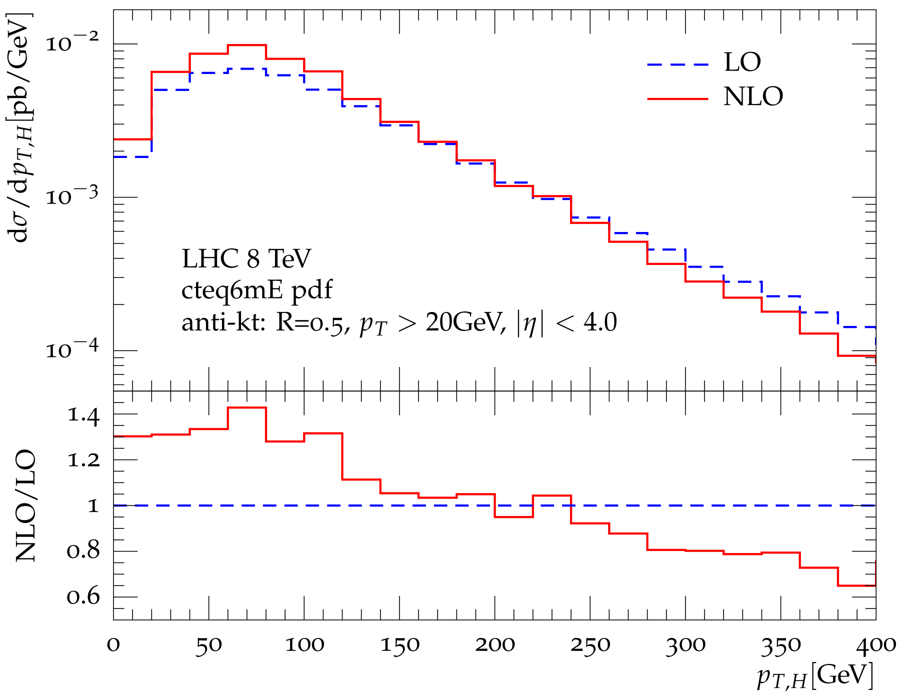

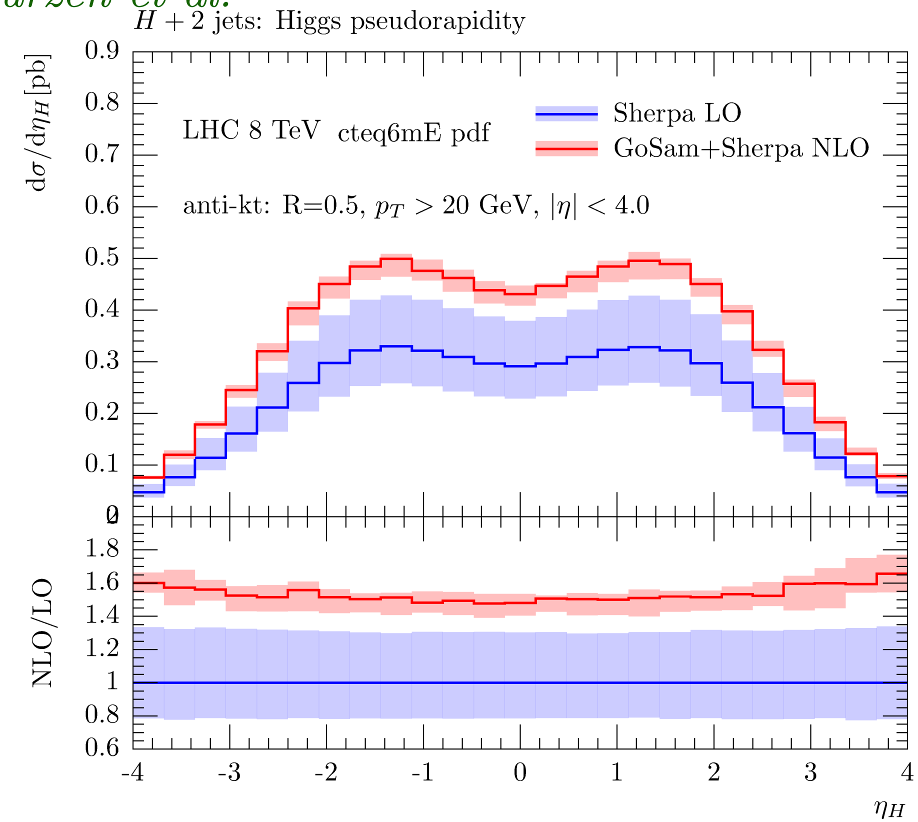

Higgs + 2 jets at NLO

H. van Deurzen et al.

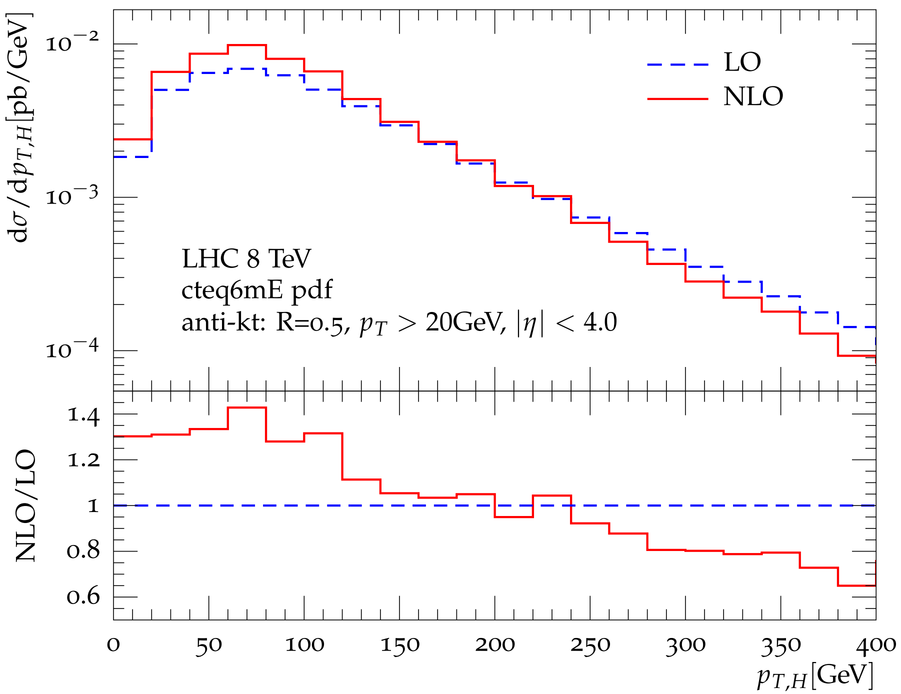

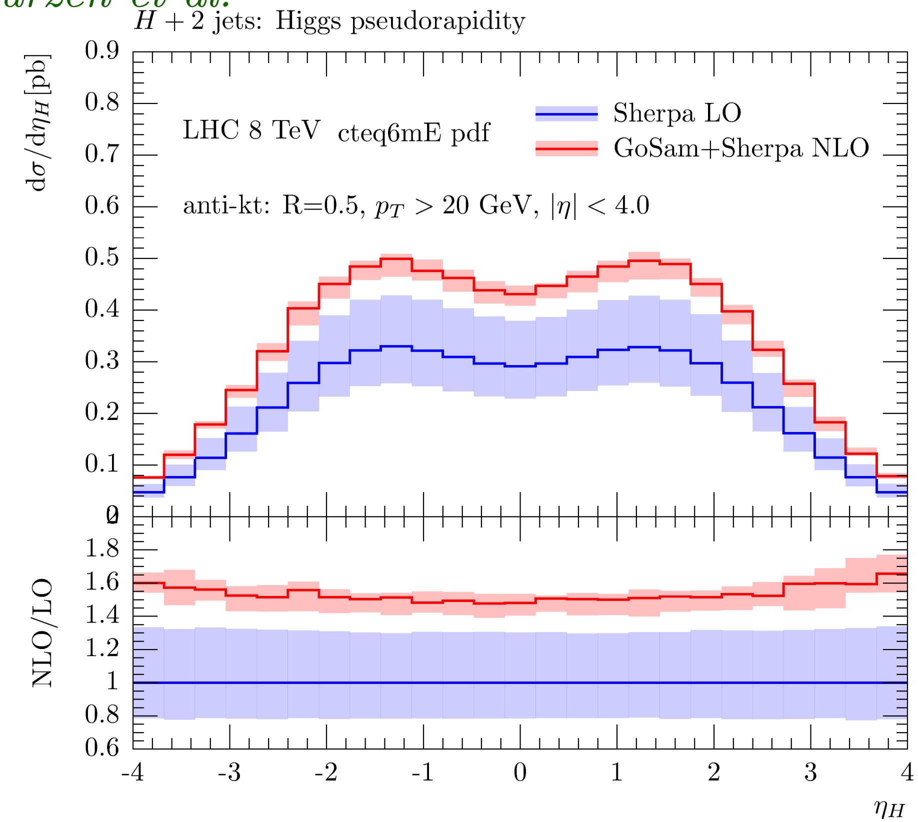

- Transverse momentum p_T and Pseudorapidity η of the Higgs boson are plotted.
- The jets are clustered by using the anti-k_T algorithm provided by the FastJet package:

$$p_{t,j} \geq 20GeV, \quad |\eta_j| \leq 4.0, \quad R = 0.5\,.$$

- The factorization and the renormalization scale are set to be

$$\hat{H}_t = \sqrt{M_H^2 + p_{t,H}^2} + \sum_j p_{t,j}\,.$$

Higgs + 2 jets at NLO

H. van Deurzen et al.

Higgs + 2 jets at NLO

H. van Deurzen et al.

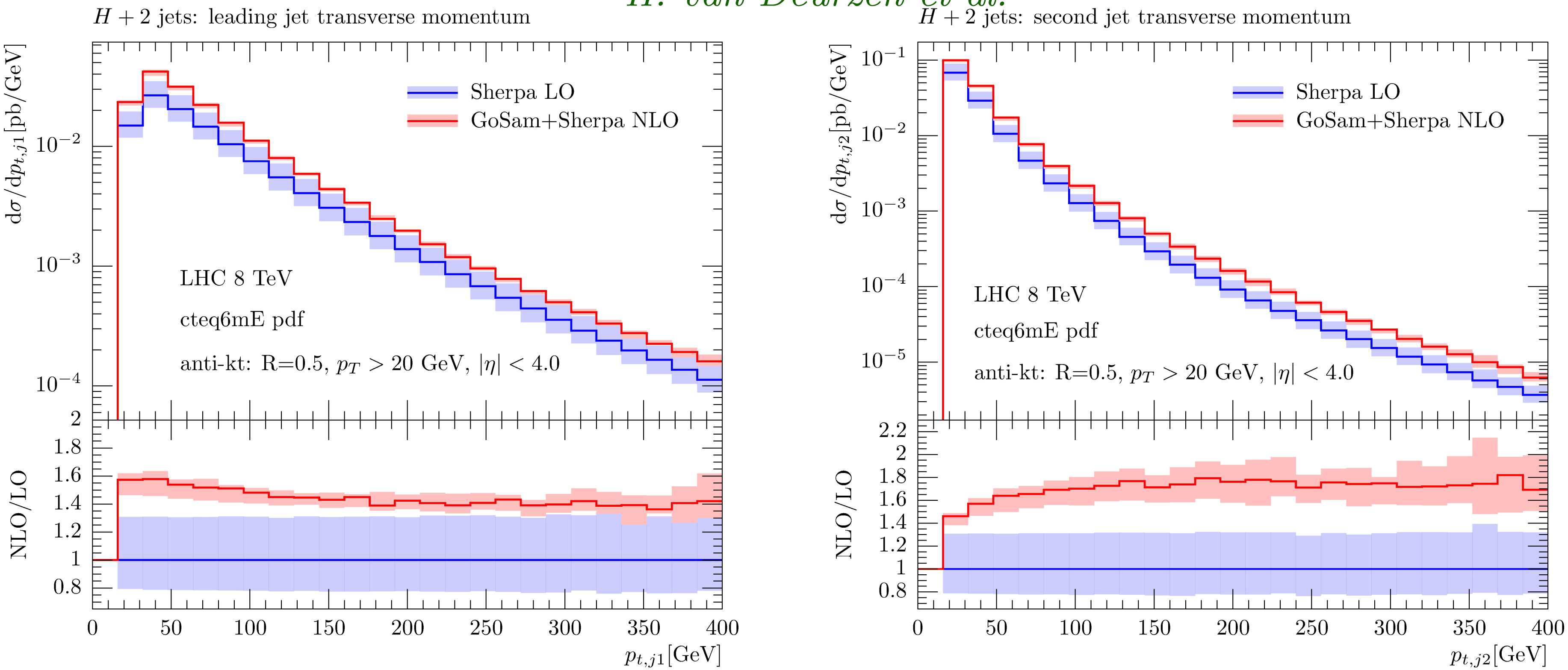

Higgs + 2 jets at NLO

H. van Deurzen et al.

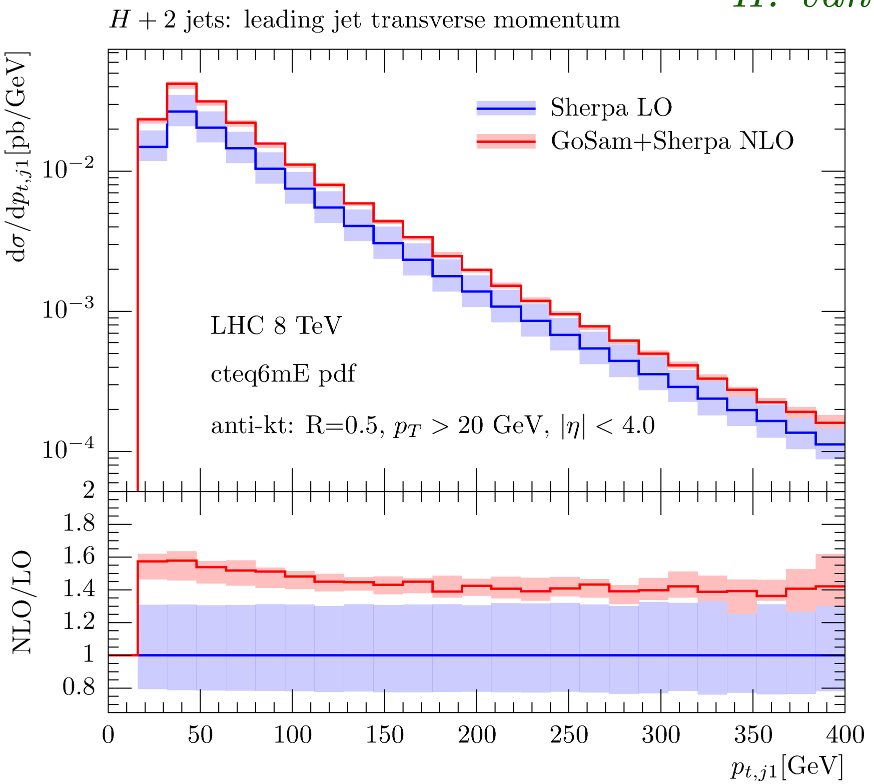

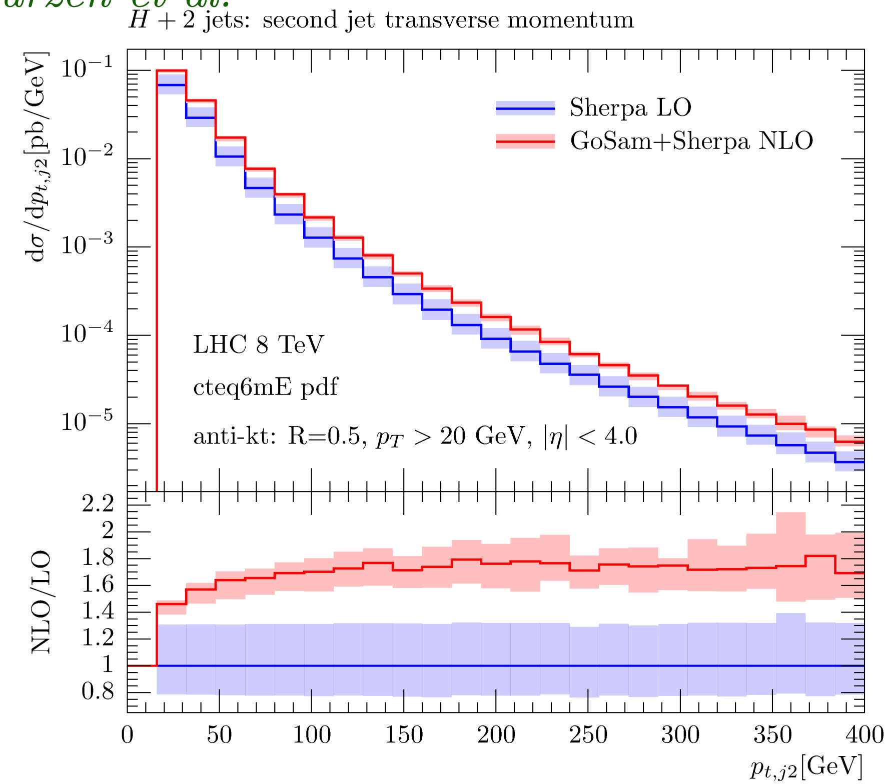

- Transverse momentum p_T of the first and the second jet.

$$\sigma_{\rm LO}[\rm pb] = 1.90^{+0.58}_{-0.41}\,, \qquad \sigma_{\rm NLO}[\rm pb] = 2.90^{+0.05}_{-0.20}\,,$$

- Scale variation:

$$\frac{1}{2}\hat{H}_t < \mu < 2\hat{H}_t\,.$$

GOSAM framework

GOSAM framework

G. Heinrich et al.

- GoSam performs one-loop virtual contributions to physical processes automatically.
- Amplitudes are generated via Feynman diagrams, using QGRAF, FORM, SPINNEY and HAGGIES.

- The input required:

  - the $process$, such as a list of initial and final state particles, the order in the coupling constants, and the model;
  - the $scheme$ employed, such as the regularization and renormalization schemes;
  - the $system$, such as paths to libraries or compiler options;
  - optional information to control the code generation.

- the virtual corrections are evaluated using the $\boldsymbol{d}$-dimensional integrand-level reduction method, as implemented in SAMURAI library, which allows for the combined determination of both cut-constructible and rational terms at once.

- Embedding the virtual corrections within a Monte Carlo framework (MC), such as SHERPA, POWHEG, MADGRAPH,HERWIG, or aMC@NLO, that can take care of the phase-space integration and showering.

GOSAM framework

G. Heinrich et al.

- GoSam performs one-loop virtual contributions to physical processes automatically.
- Amplitudes are generated via Feynman diagrams, using QGRAF, FORM, SPINNEY and HAGGIES.

- The input required:

  - the *process*, such as a list of initial and final state particles, the order in the coupling constants, and the model;
  - the *scheme* employed, such as the regularization and renormalization schemes;
  - the *system* , such as paths to libraries or compiler options;
  - optional information to control the code generation.

- the virtual corrections are evaluated using the $\boldsymbol{d}$-dimensional integrand-level reduction method, as implemented in SAMURAI library, which allows for the combined determination of both cut-constructible and rational terms at once.

- Embedding the virtual corrections within a Monte Carlo framework (MC), such as SHERPA, POWHEG, MADGRAPH,HERWIG, or aMC@NLO, that can take care of the phase-space integration and showering.

GOSAM framework

G. Heinrich et al.

- GoSam performs one-loop virtual contributions to physical processes automatically.
- Amplitudes are generated via Feynman diagrams, using QGRAF, FORM, SPINNEY and HAGGIES.
- The input required:
  - the $process$, such as a list of initial and final state particles, the order in the coupling constants, and the model;
  - the $scheme$ employed, such as the regularization and renormalization schemes;
  - the $system$, such as paths to libraries or compiler options;
  - optional information to control the code generation.
- the virtual corrections are evaluated using the $\boldsymbol{d}$-dimensional integrand-level reduction method, as implemented in SAMURAI library, which allows for the combined determination of both cut-constructible and rational terms at once.
- Embedding the virtual corrections within a Monte Carlo framework (MC), such as SHERPA, POWHEG, MADGRAPH,HERWIG, or aMC@NLO, that can take care of the phase-space integration and showering.

Higgs + 3-jets in gluon-gluon fusion

G. Cullen et al.

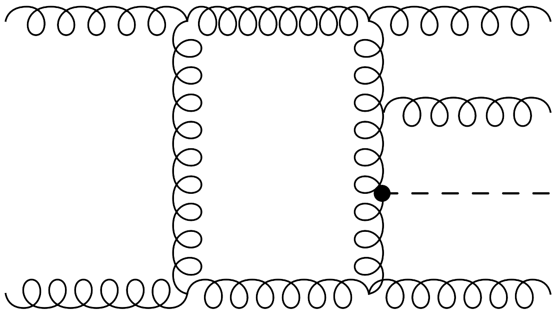

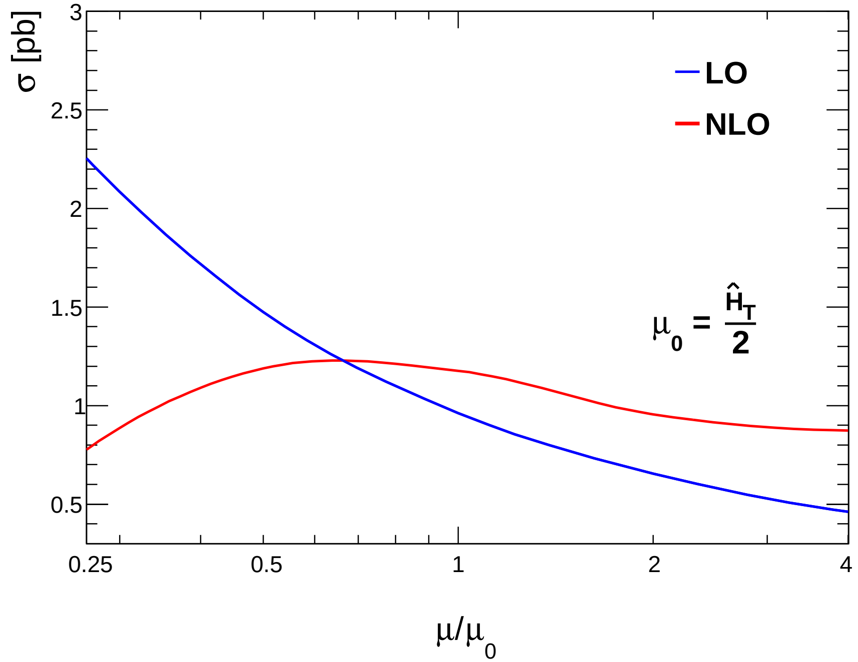

Higgs + 3-jets in gluon-gluon fusion

G. Cullen et al.

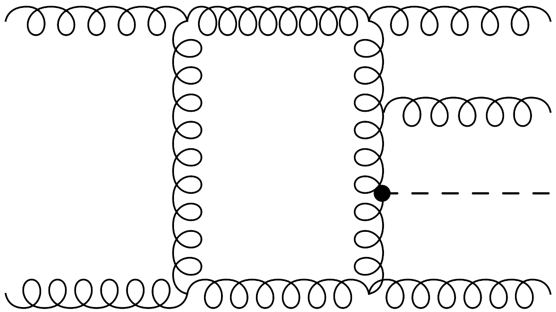

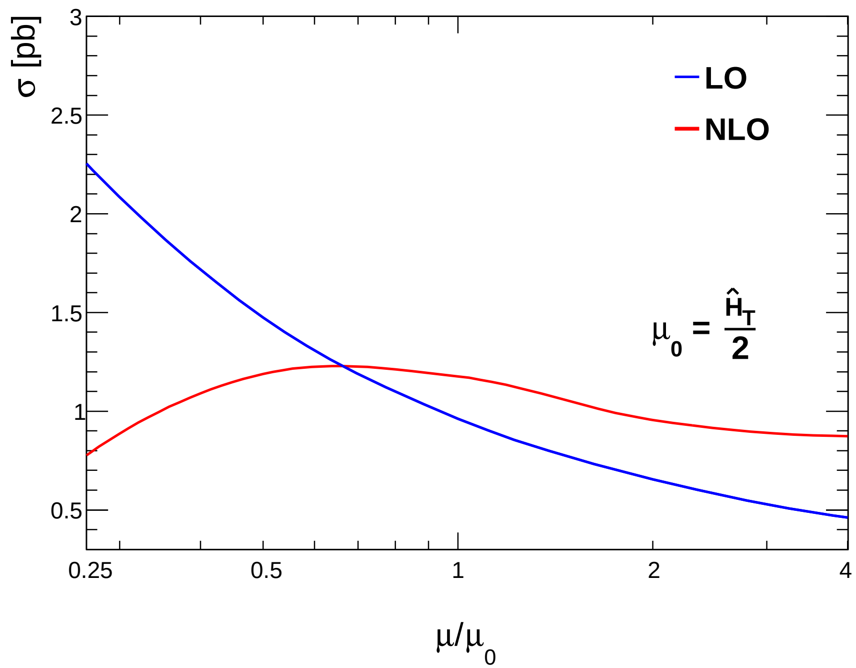

- Jets are clustered using the anti-k_t-algorithm implemented in FastJet with radius $R = 0.5$ and a minimum transverse momentum of $p_{T,jet} > 20$ GeV and pseudorapidity $|\eta| < 4.0$.
- The renormalization and factorization scales are set to

$$\mu_F = \mu_R = \frac{\hat{H}_T}{2} = \frac{1}{2}\left(\sqrt{m_H^2 + p_{T,H}^2} + \sum_i |p_{T,i}|\right) ,$$

- The strong coupling is therefore evaluated at different scales according to $\alpha_s^5 \to \alpha_s^2(m_H)\alpha_s^3(\hat{H}_T/2)$.

Higgs + 3-jets in gluon-gluon fusion

Higgs + 3-jets in gluon-gluon fusion

G. Cullen et al.

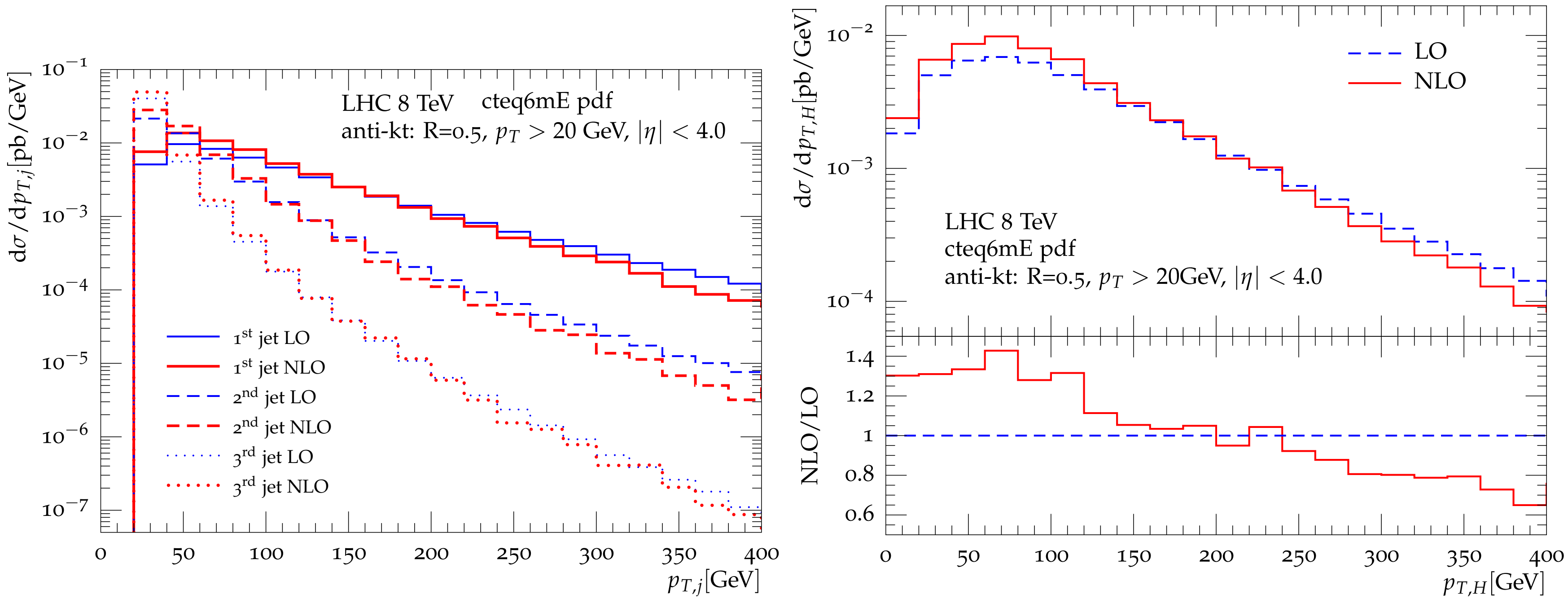

Higgs + 3-jets in gluon-gluon fusion

G. Cullen et al.

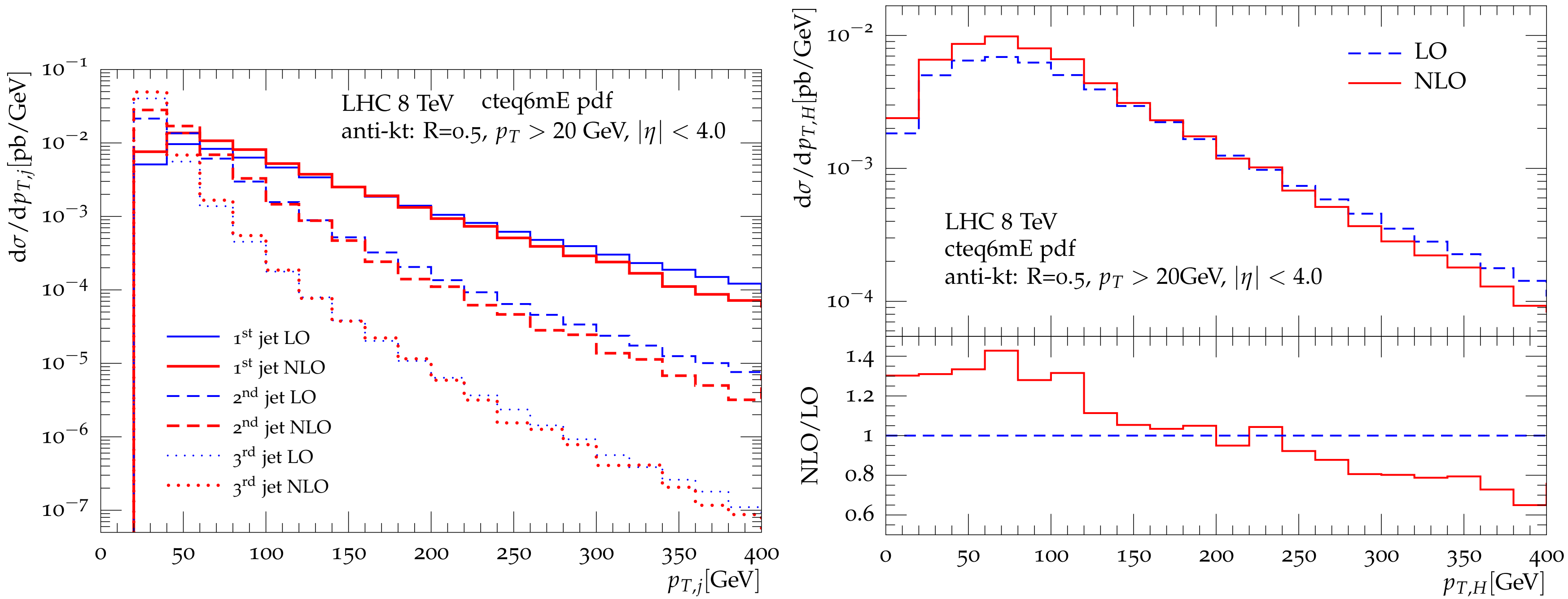

- Transverse momentum (p_T) distributions for the first, second, and third leading jet and the Higgs boson
- The theoretical uncertainties are estimated by varying the scales by factors of 0.5 and 2.0.
- In the effective coupling the scale is kept at m_H.

$$\sigma_{\mathrm{LO}}[\mathrm{pb}] = 0.962^{+0.51}_{-0.31}\,, \quad \sigma_{\mathrm{NLO}}[\mathrm{pb}] = 1.18^{+0.01}_{-0.22}\,.$$

- The scale dependence of the total cross section is strongly reduced by the inclusion of the NLO contributions.

Higgs + 3-jets via vector boson fusion (VBF)

F. Campanario et al.

Higgs + 3-jets via vector boson fusion (VBF)

F. Campanario et al.

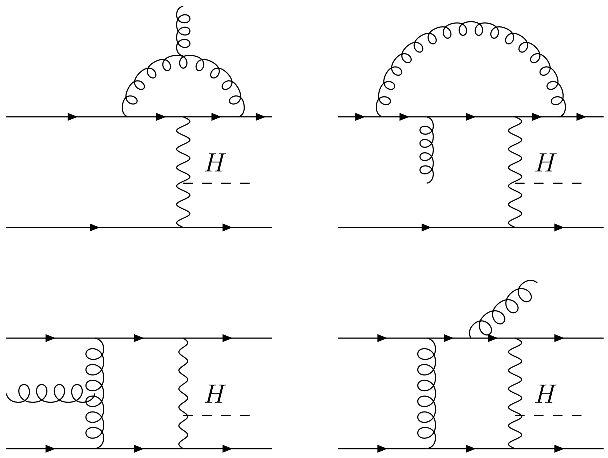

- Higgs production via Vector Boson Fusion (VFB) can disentangle the Higgs boson's coupling to fermionns and gauge bosons.
- Taging two jets with Higgs and vetoing soft jets in the central region can significantly reduce the QCD background as well as Higgs plus two jets from gluon-gluon fusion.
- Ratio of Higgs+3 jets to Higgs+2 jets need to known accurately.

Method:

- Spin helicity package MATCHBOX provides real emission amplitudes, spin summation, subtraction terms for IR singularities
- ColorFull and ColurMath packages to do color algebra
- Passarino-Veltman reduction and Denner-Dittmaier scheme to do one-loop reduction and evaluation.

Higgs + 3-jets via vector boson fusion (VBF)

F. Campanario et al.

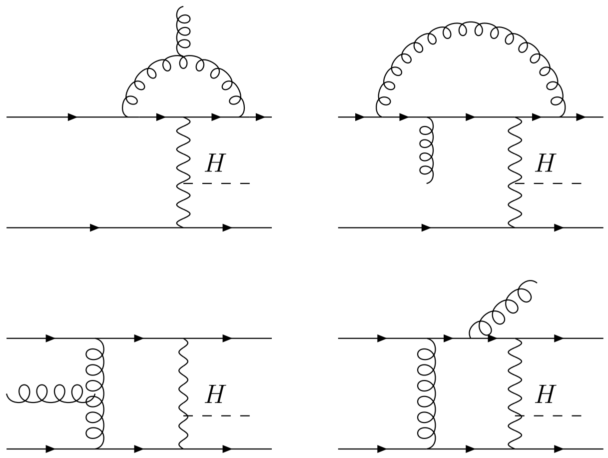

- Higgs production via Vector Boson Fusion (VFB) can disentangle the Higgs boson's coupling to fermionns and gauge bosons.

- Taging two jets with Higgs and vetoing soft jets in the central region can significantly reduce the QCD background as well as Higgs plus two jets from gluon-gluon fusion.

- Ratio of Higgs+3 jets to Higgs+2 jets need to known accurately.

Method:

- Spin helicity package MATCHBOX provides real emission amplitudes, spin summation, subtraction terms for IR singularities

- ColorFull and ColurMath packages to do color algebra

- Passarino-Veltman reduction and Denner-Dittmaier scheme to do one-loop reduction and evaluation.

Higgs+3 jets via VBF

F. Campanario et al.

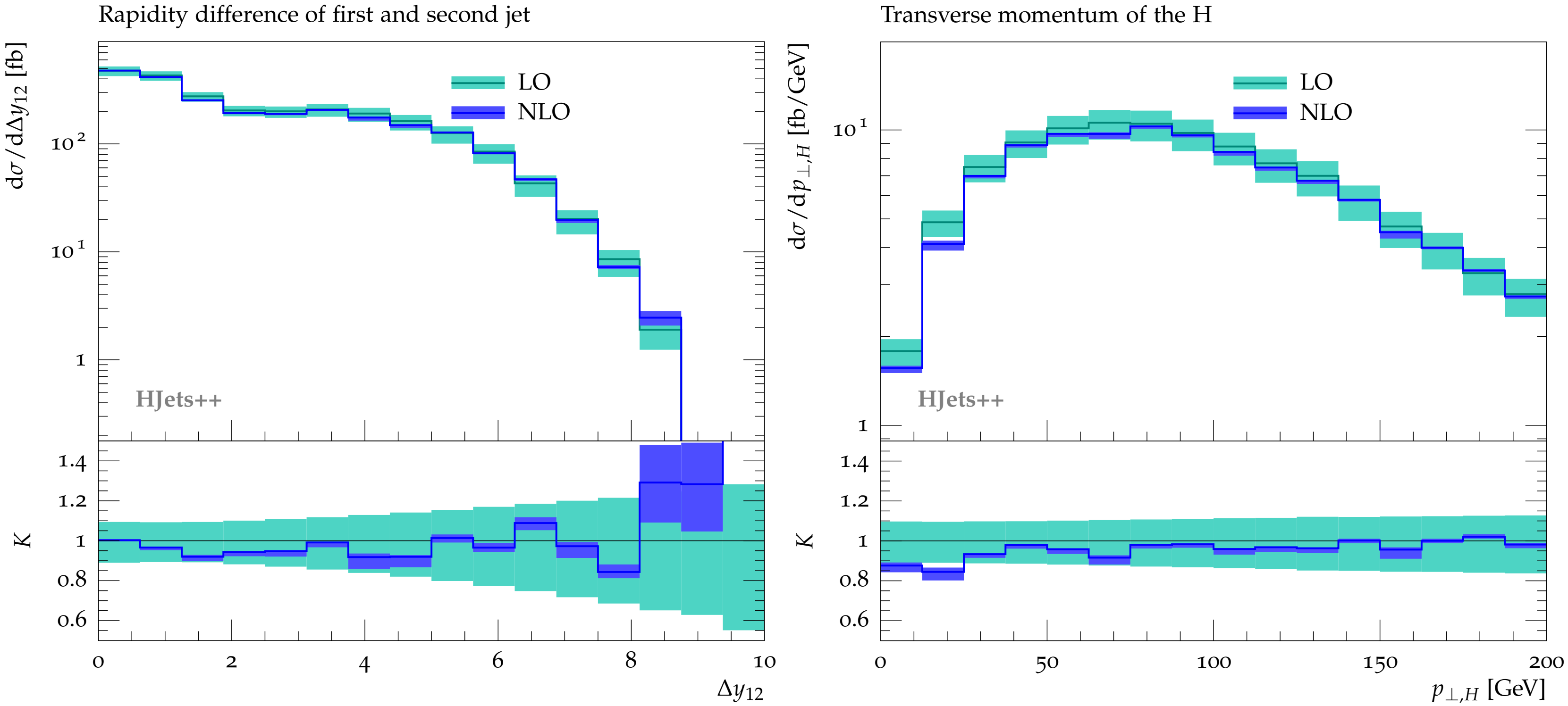

- Cluster jets with the anti-k_T algorithm using FastJet with $D = 0.4$, E-scheme recombination and require at least three jets with transverse momentum $p_{T,j} \geq 20$ GeV and rapidity $|y_j| \leq 4.5$. Jets are ordered in decreasing transverse momenta.
- The bands correspond to varying $\mu_F = \mu_R$ by factors 1/2 and 2 around the central value $H_T/2$.
- Differential cross section and K factor for the p_T of the Higgs. The bands correspond to varying $\mu_F = \mu_R$ by factors 1/2 and 2 around the central value $H_T/2$.

Higgs+3 jets via VBF

F. Campanario et al.

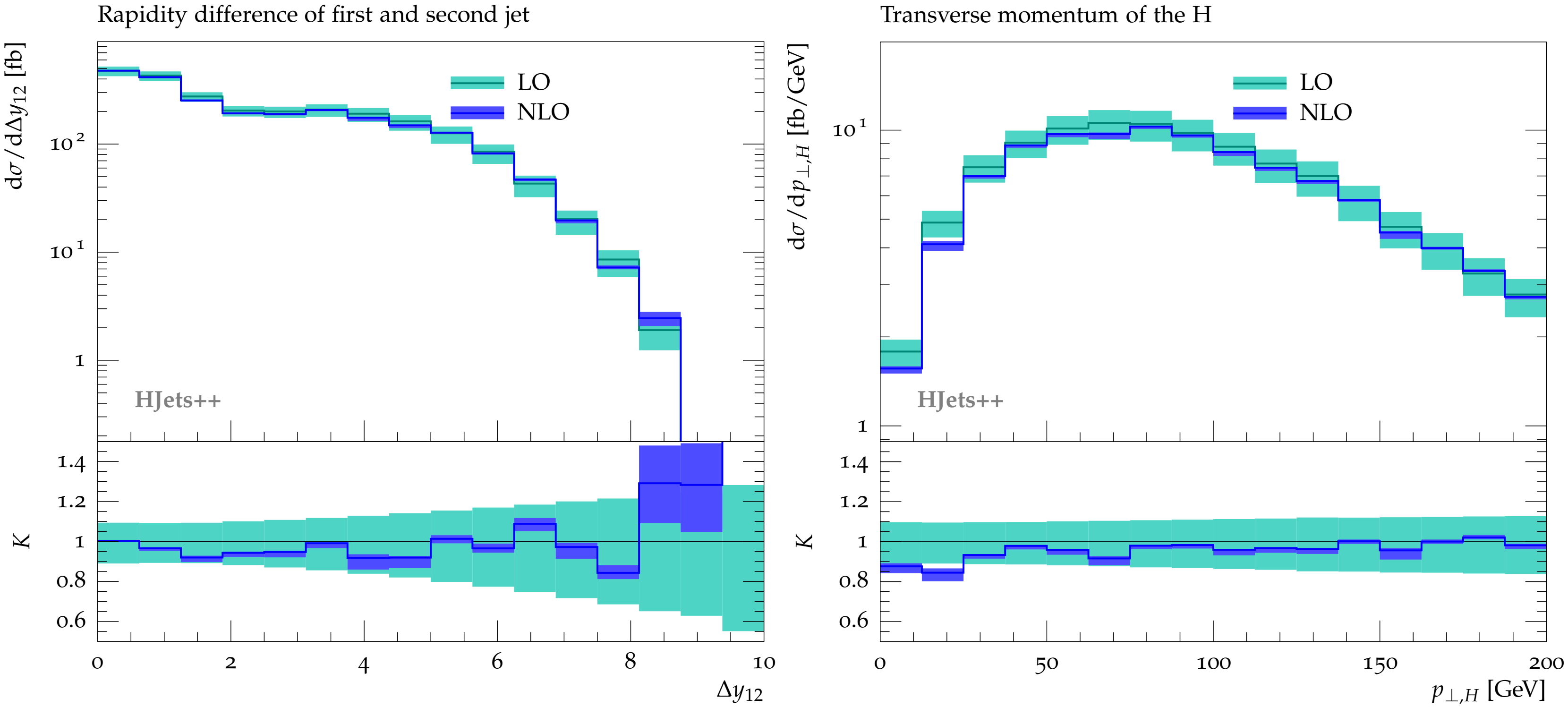

- Cluster jets with the anti-k_T algorithm using FastJet with $D = 0.4$, E-scheme recombination and require at least three jets with transverse momentum $p_{T,j} \geq 20$ GeV and rapidity $|y_j| \leq 4.5$. Jets are ordered in decreasing transverse momenta.
- The bands correspond to varying $\mu_F = \mu_R$ by factors 1/2 and 2 around the central value $H_T/2$.
- Differential cross section and K factor for the p_T of the Higgs. The bands correspond to varying $\mu_F = \mu_R$ by factors 1/2 and 2 around the central value $H_T/2$.

Higgs+3 jets via VBF

F. Campanario et al.

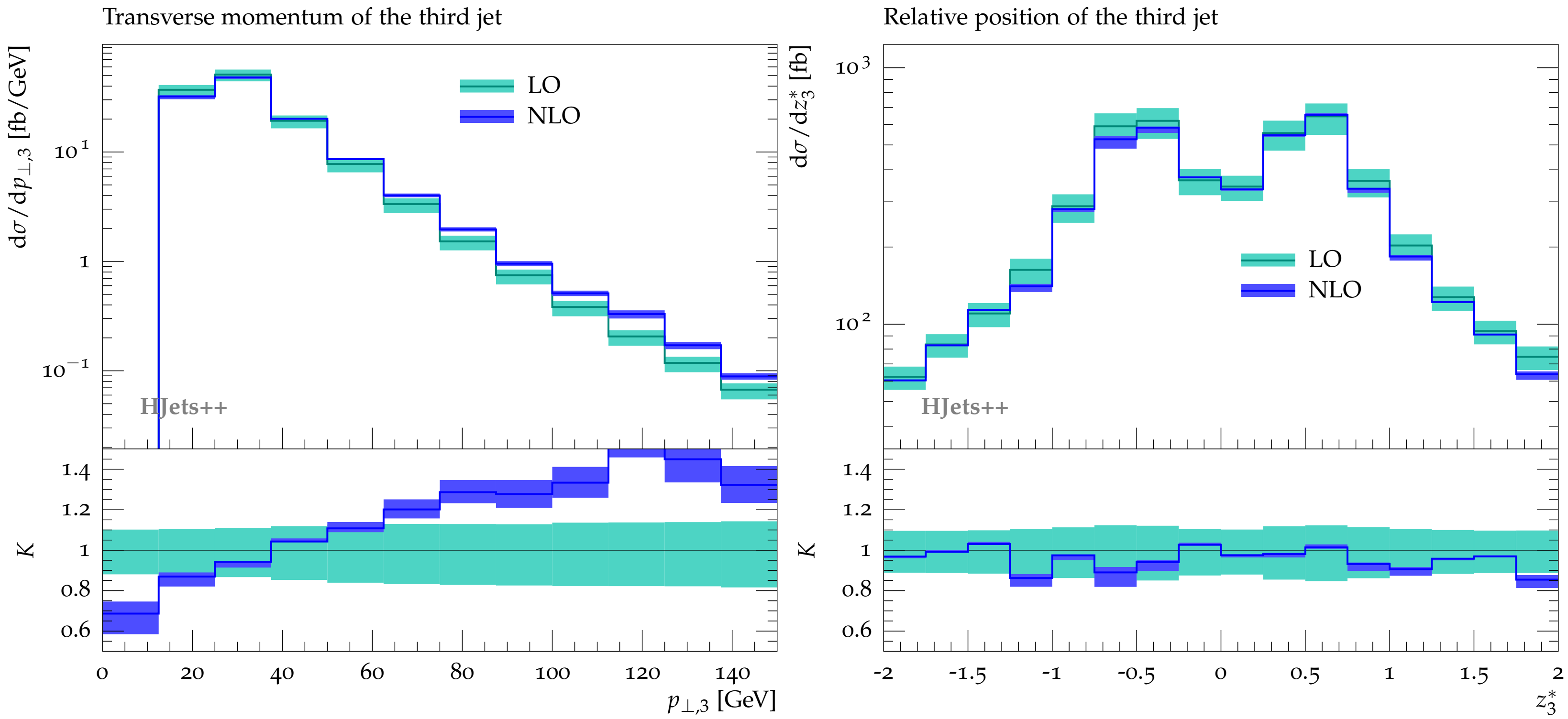

- Differential cross section and K factor for the p_T of the third hardest jet.

- Differential cross section and K factor for the normalized centralized rapidity distribution of the third jet w.r.t. the tagging jets.

- The bands correspond to varying $\mu_F = \mu_R$ by factors 1/2 and 2 around the central value $H_T/2$.

Higgs+3 jets via VBF

F. Campanario et al.

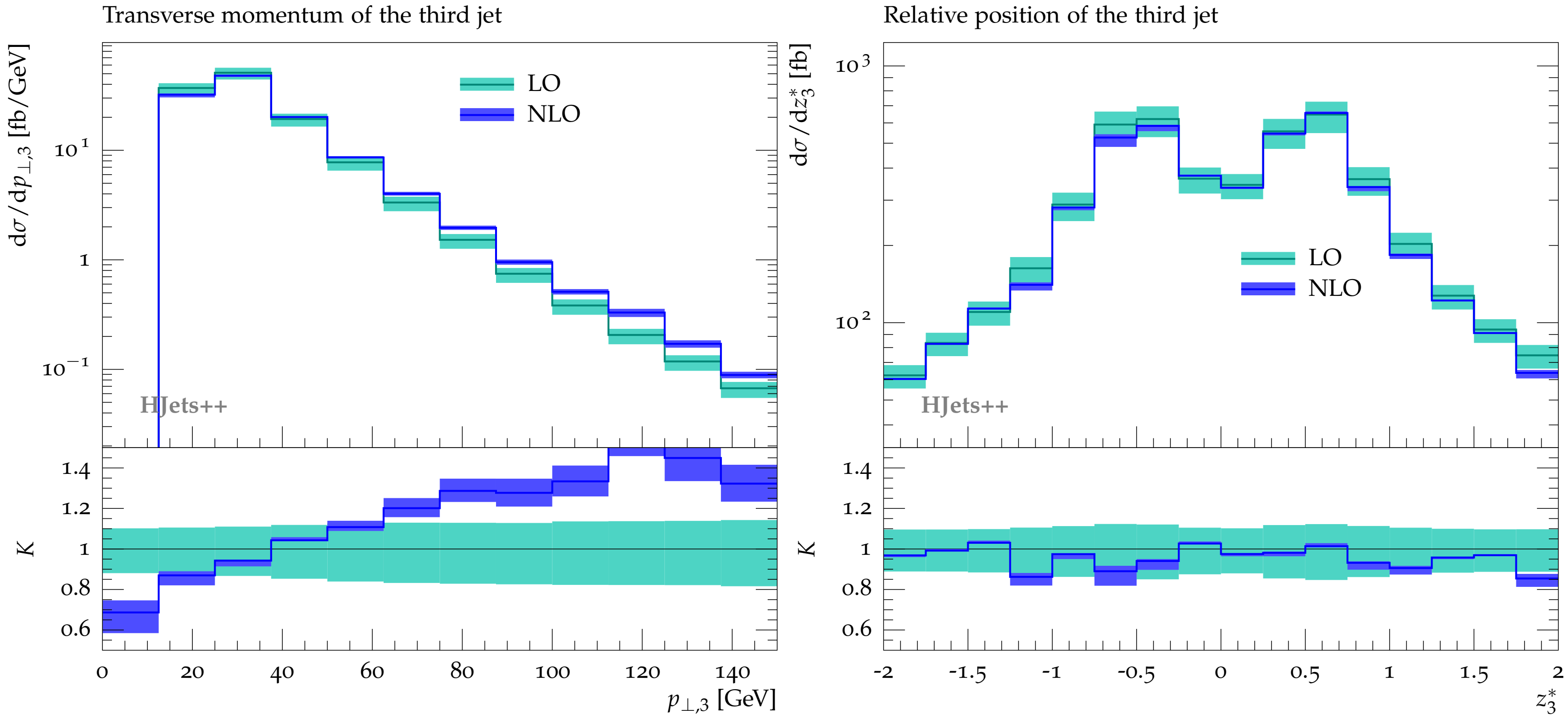

- Differential cross section and K factor for the p_T of the third hardest jet.

- Differential cross section and K factor for the normalized centralized rapidity distribution of the third jet w.r.t. the tagging jets.

- The bands correspond to varying $\mu_F = \mu_R$ by factors 1/2 and 2 around the central value $H_T/2$.

$t\bar{t}H+$ jet at NLO

H. van Deurzen et al.

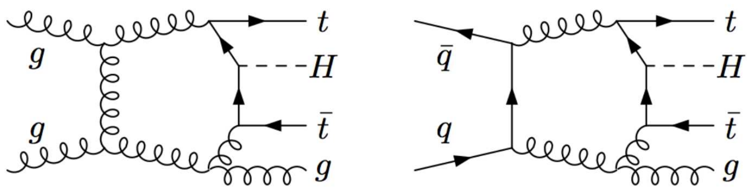

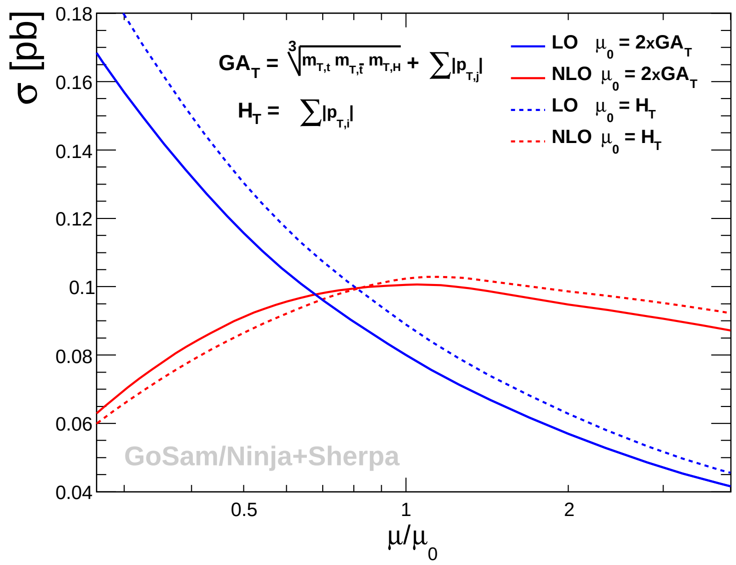

$t\bar{t}H+$ jet at NLO

H. van Deurzen et al.

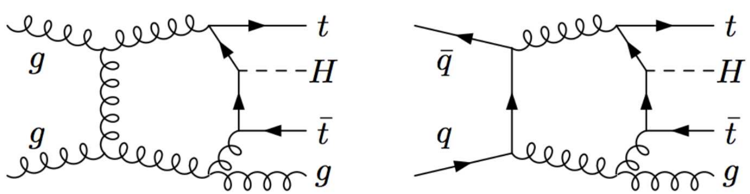

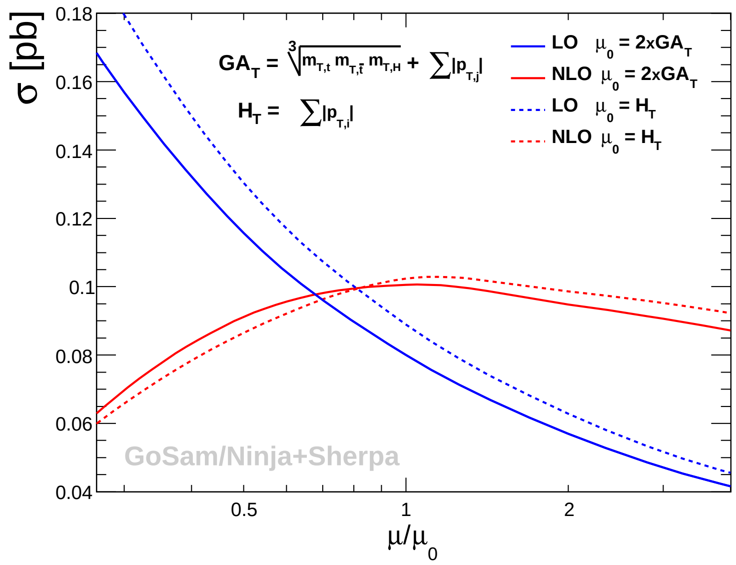

- The Born and the real emission matrix elements are computed using SHERPA and the library AMEGIC which implements the Catani-Seymour dipole formalism. SHERPA also performs the integration over the phase space and the analysis.
- The virtual corrections are generated with the GOSAM which combines automated diagram generation and algebraic manipulation with d-dimensional integrand-level reduction.
- The virtual amplitudes of $t\bar{t}Hj$ have been decomposed in terms of MIs using for the first time the *integrand reduction via Laurent expansion*, implemented in the $C++$ library NINJA.

$t\bar{t}H+$ jet at NLO

H. van Deurzen et al.

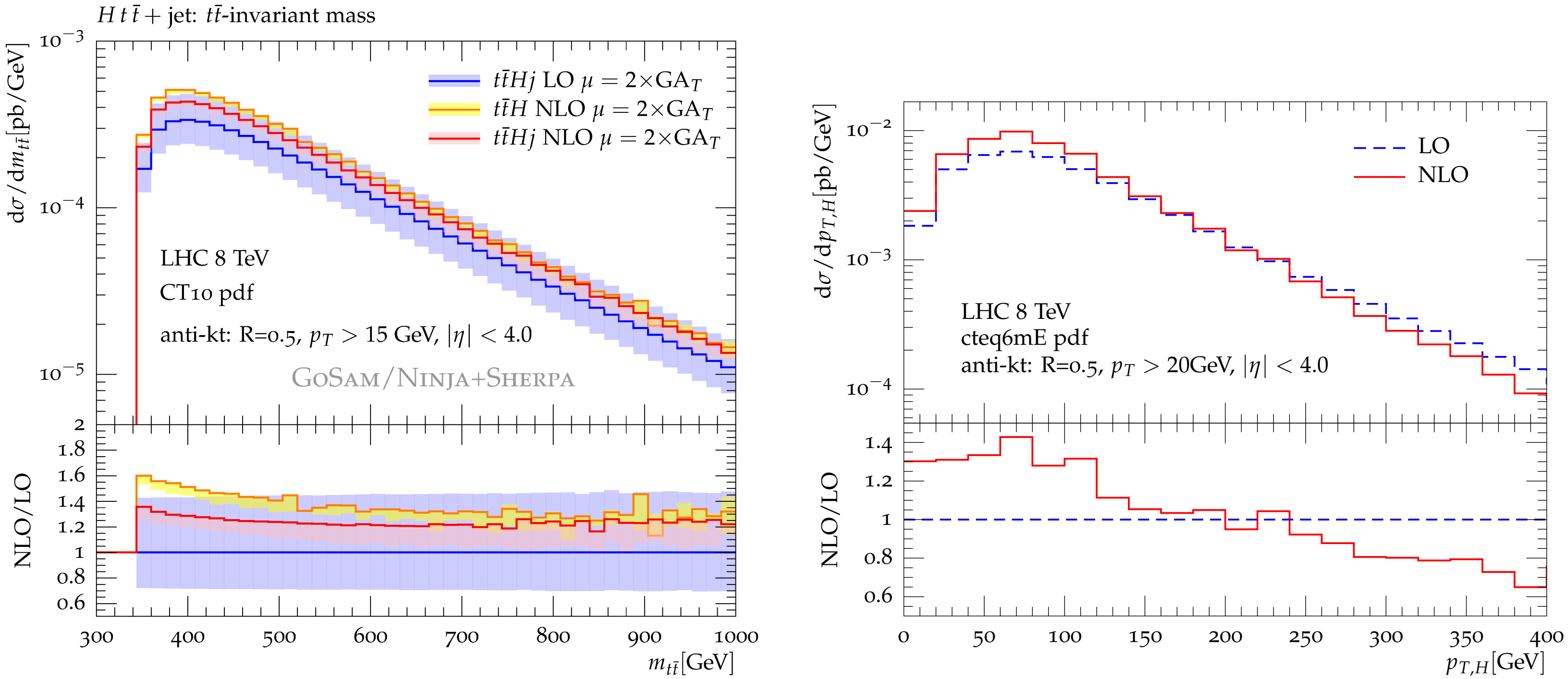

$t\bar{t}H+$ jet at NLO

H. van Deurzen et al.

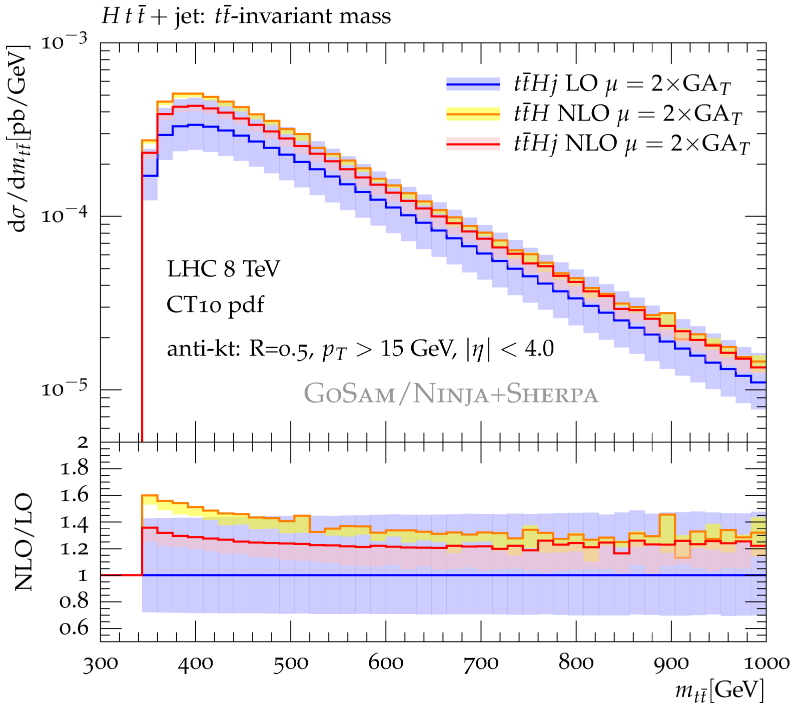

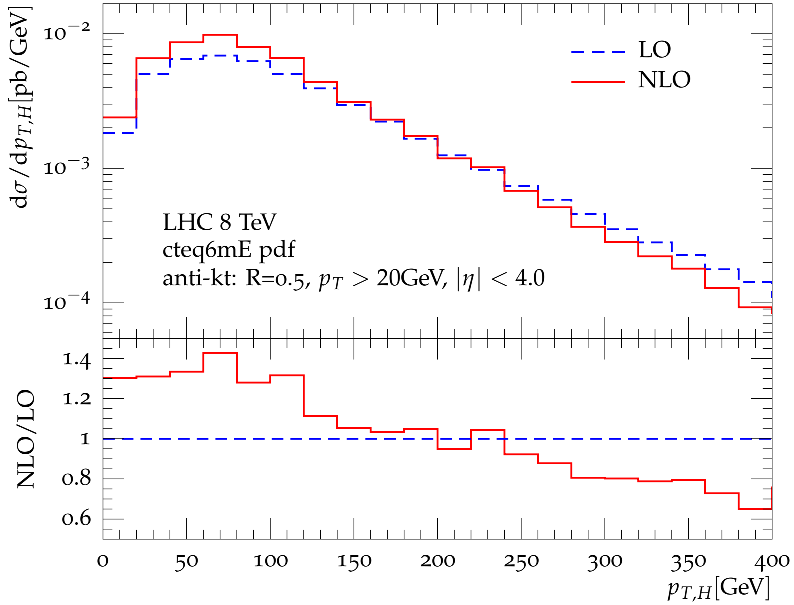

- To cluster the jets the anti-k_t-algorithm is implemented in FASTJET with radius $R = 0.5$, a minimum transverse momentum of $p_{T,jet} > 15$ GeV and pseudorapidity $|\eta| < 4.0$.
- In order to study the scale dependence of the total cross section, two different choices of the renormalization and factorizationt scales $\mu_R = \mu_F = \mu_0$, namely $\mu_0 = H_T$ and $\mu_0 = 2 \times \mathrm{GA}_T$ with

$$H_T = \sum_{\text{final states } f} |p_{T,f}| \,, \mathrm{GA}_T = \sqrt[3]{m_{T,H}\, m_{T,t}\, m_{T,\bar{t}}} + \sum_{\text{jets } j} |p_{T,j}| \,.$$

Higgs Characterisation at NLO

F. Maltoni, Prakash Mathews, VR et al.

- Effective Field Theory (EFT) approach to study the nature of interaction of Higgs with the other SM particles.
- Not only useful for SM electroweak precision physics, but also pin down BSM effects.

Higgs Characterisation at NLO

F. Maltoni, Prakash Mathews, VR et al.

- Effective Field Theory (EFT) approach to study the nature of interaction of Higgs with the other SM particles.
- Not only useful for SM electroweak precision physics, but also pin down BSM effects.
- EFT contains only SM particles and the symmetries at the EW scale.

$$\mathcal{L}_{HC,J} = \mathcal{L}_{SM-H} + \mathcal{L}_J \ ,$$

  - reduces significantly the possible interaction terms in the Lagrangian
  - Higgs boson with various spin-partiy assignment

Higgs Characterisation at NLO

F. Maltoni,Prakash Mathews, VR et al.

- Effective Field Theory (EFT) approach to study the nature of interaction of Higgs with the other SM particles.
- Not only useful for SM electroweak precision physics, but also pin down BSM effects.
- EFT contains only SM particles and the symmetries at the EW scale.

$$\mathcal{L}_{HC,J} = \mathcal{L}_{SM-H} + \mathcal{L}_{J} \ ,$$

  - reduces significantly the possible interaction terms in the Lagrangian
  - Higgs boson with various spin-partiy assignment
- EFT has been implemented in FeynRules and passed to the Madgraph5 and aMC@NLO framework by means of UFO model file.
  - improvable with new operators,
  - higher order QCD effects can be incorporated systematically.
  - multi-parton tree-level computation with parton shower,
  - next to leading order calculations matched with parton sowers.

Higgs Characterisation for spin-0 Higgs

Buchmuller et al, Grzadkowski et al

Higgs Characterisation for spin-0 Higgs

Buchmuller et al, Grzadkowski et al

dimension-6 operators with pair of fermions

$$\mathcal{L}_0^f = -\sum_{f=t,b,\tau} \bar{\psi}_f \left(c_\alpha \kappa_{Hff} g_{Hff} + i s_\alpha \kappa_{Aff} g_{Aff} \gamma_5\right) \psi_f X_0 \,,$$

Higgs Characterisation for spin-0 Higgs

Buchmuller et al, Grzadkowski et al

dimension-6 operators with pair of fermions

$$\mathcal{L}_0^f = -\sum_{f=t,b,\tau} \bar{\psi}_f \left(c_\alpha \kappa_{Hff} g_{Hff} + i s_\alpha \kappa_{Aff} g_{Aff} \gamma_5\right) \psi_f X_0 \,,$$

dimension-6 operators with pair of vector bosons

$$\begin{aligned}
\mathcal{L}_0^V = \Big\{ & c_\alpha \kappa_{\rm SM} \big[\tfrac{1}{2} g_{HZZ}\, Z_\mu Z^\mu + g_{HWW}\, W_\mu^+ W^{-\mu}\big] \\
& - \frac{1}{4}\big[c_\alpha \kappa_{H\gamma\gamma} g_{H\gamma\gamma}\, A_{\mu\nu} A^{\mu\nu} + s_\alpha \kappa_{A\gamma\gamma} g_{A\gamma\gamma}\, A_{\mu\nu} \widetilde{A}^{\mu\nu}\big] \\
& - \frac{1}{2}\big[c_\alpha \kappa_{HZ\gamma} g_{HZ\gamma}\, Z_{\mu\nu} A^{\mu\nu} + s_\alpha \kappa_{AZ\gamma} g_{AZ\gamma}\, Z_{\mu\nu} \widetilde{A}^{\mu\nu}\big] \\
& - \frac{1}{4}\big[c_\alpha \kappa_{Hgg} g_{Hgg}\, G^a_{\mu\nu} G^{a,\mu\nu} + s_\alpha \kappa_{Agg} g_{Agg}\, G^a_{\mu\nu} \widetilde{G}^{a,\mu\nu}\big] \\
& - \frac{1}{4}\frac{1}{\Lambda}\big[c_\alpha \kappa_{HZZ}\, Z_{\mu\nu} Z^{\mu\nu} + s_\alpha \kappa_{AZZ}\, Z_{\mu\nu} \widetilde{Z}^{\mu\nu}\big] \\
& - \frac{1}{2}\frac{1}{\Lambda}\big[c_\alpha \kappa_{HWW}\, W^+_{\mu\nu} W^{-\mu\nu} + s_\alpha \kappa_{AWW}\, W^+_{\mu\nu} \widetilde{W}^{-\mu\nu}\big] \\
& - \frac{1}{\Lambda} c_\alpha \big[\kappa_{H\partial\gamma}\, Z_\nu \partial_\mu A^{\mu\nu} + \kappa_{H\partial Z}\, Z_\nu \partial_\mu Z^{\mu\nu} + \big(\kappa_{H\partial W}\, W_\nu^+ \partial_\mu W^{-\mu\nu} + h.c.\big)\big] \Big\} X_0 \,,
\end{aligned}$$

$$c_\alpha \equiv \cos\alpha \,, \quad s_\alpha \equiv \sin\alpha \,,$$

Higgs Characterisation with spin-2 Higgs

J. Ellis et al

Minimal coupling to spin-2 Higgs with fermions:

$$\mathcal{L}_2^f = -\frac{1}{\Lambda} \sum_{f=q,\ell} \kappa_f \, T_{\mu\nu}^f X_2^{\mu\nu} \,,$$

Higgs Characterisation with spin-2 Higgs

J. Ellis et al

Minimal coupling to spin-2 Higgs with fermions:

$$\mathcal{L}_2^f = -\frac{1}{\Lambda} \sum_{f=q,\ell} \kappa_f \, T^f_{\mu\nu} X_2^{\mu\nu} \, ,$$

Minimal coupling to spin-2 Higgs with fermions:

$$\mathcal{L}_2^V = -\frac{1}{\Lambda} \sum_{V=Z,W,\gamma,g} \kappa_V \, T^V_{\mu\nu} X_2^{\mu\nu} \, .$$

where $T^{\mu\nu}$ is the energy momentum tensor of SM fields.

$$\begin{aligned} T^f_{\mu\nu} =& - g_{\mu\nu}\Big[\bar{\psi}_f(i\gamma^\rho D_\rho - m_f)\psi_f - \frac{1}{2}\partial^\rho(\bar{\psi}_f i\gamma_\rho\psi_f)\Big] \\ &+ \Big[\frac{1}{2}\bar{\psi}_f i\gamma_\mu D_\nu\psi_f - \frac{1}{4}\partial_\mu(\bar{\psi}_f i\gamma_\nu\psi_f) + (\mu\leftrightarrow\nu)\Big] \, , \\ T^\gamma_{\mu\nu} =& - g_{\mu\nu}\Big[-\frac{1}{4}A^{\rho\sigma}A_{\rho\sigma} + \partial^\rho\partial^\sigma A_\sigma A_\rho + \frac{1}{2}(\partial^\rho A_\rho)^2\Big] \\ &- A_\mu^\rho A_{\nu\rho} + \partial_\mu\partial^\rho A_\rho A_\nu + \partial_\nu\partial^\rho A_\rho A_\mu \, , \end{aligned}$$

Higgs Characterisation

F. Maltoni, Prakash Mathews, VR et al.

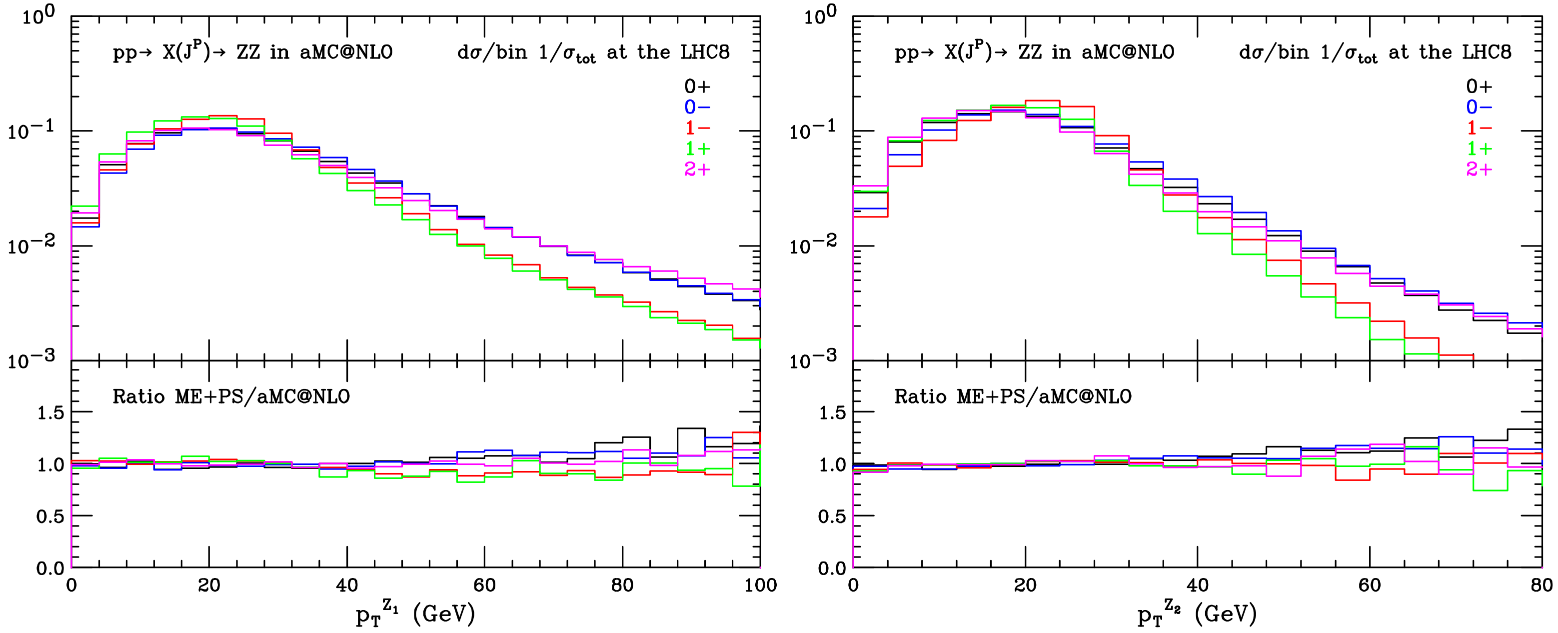

The transverse momentum of the Z boson with the highest and lowest reconstructed mass, $p_T^{Z_1}$ and $p_T^{Z_2}$, in $X(\to ZZ^*) \to \mu^+\mu^-e^+e^-$.

Higgs Characterisation

F. Maltoni,Prakash Mathews, VR et al.

Higgs Characterisation

F. Maltoni, Prakash Mathews, VR et al.

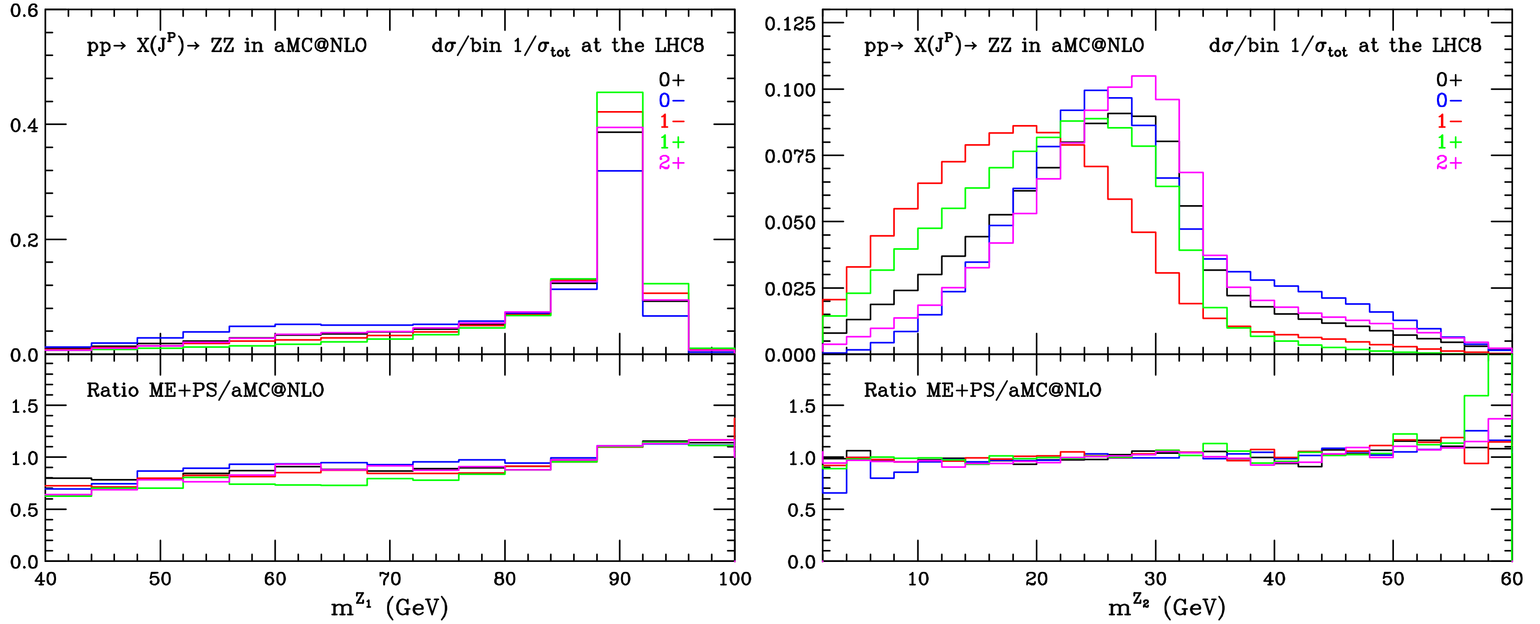

The invariant mass of the two leptons $m_{\ell\ell}$ from Z bosons

Higgs Characterisation: Non-universal couplings

F. Maltoni,Prakash Mathews, VR et al.

Higgs Characterisation: Non-universal couplings

F. Maltoni, Prakash Mathews, VR et al.

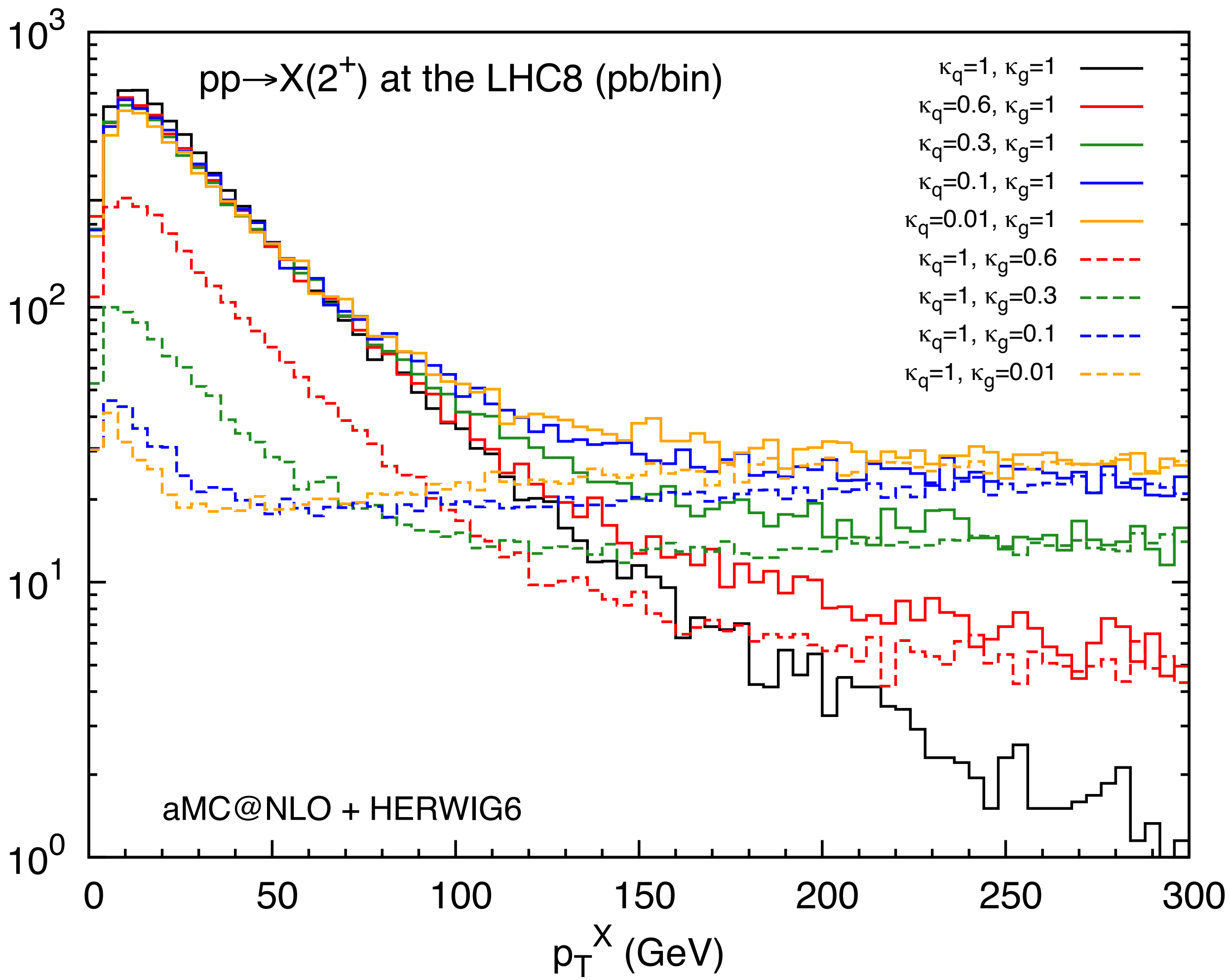

The transverse momentum p_T^X of a spin-2 state with non universal couplings to quarks and gluons $\kappa_q \neq \kappa_g$ as obtained from aMC@NLO. • It violates unitarity.

Conclusions

Conclusions

- Fixed order QCD corrections to gluon fusion contribute bulk of the cross section

Conclusions

- Fixed order QCD corrections to gluon fusion contribute bulk of the cross section

- Two loop EW corrections, mixed QCD-electroweak and $\boldsymbol{b}$ quark contributions account for $\mathbf{5\%}$ to gluon fusion

Conclusions

- Fixed order QCD corrections to gluon fusion contribute bulk of the cross section

- Two loop EW corrections, mixed QCD-electroweak and $\boldsymbol{b}$ quark contributions account for $\mathbf{5\%}$ to gluon fusion

- $\boldsymbol{NNLL}$ resummation effects can be included through suitable central scale choice.

Conclusions

- Fixed order QCD corrections to gluon fusion contribute bulk of the cross section

- Two loop EW corrections, mixed QCD-electroweak and $\boldsymbol{b}$ quark contributions account for $\mathbf{5\%}$ to gluon fusion

- $\boldsymbol{NNLL}$ resummation effects can be included through suitable central scale choice.

- At $\sqrt{\boldsymbol{S}} = \mathbf{8\%}$ TeV, the scale uncertainty varies between $\pm\mathbf{9\%}$ at $\boldsymbol{m_H} = \mathbf{125}$ GeV.
- the PDF $+\boldsymbol{\alpha_s}$ uncertainty varies between $\pm\mathbf{7\%}$ at $\boldsymbol{m_H} = \mathbf{125}$ GeV.

Conclusions

- Fixed order QCD corrections to gluon fusion contribute bulk of the cross section

- Two loop EW corrections, mixed QCD-electroweak and b quark contributions account for 5% to gluon fusion

- $NNLL$ resummation effects can be included through suitable central scale choice.

- At $\sqrt{S} = 8\%$ TeV, the scale uncertainty varies between $\pm 9\%$ at $m_H = 125$ GeV.
- the PDF +α_s uncertainty varies between $\pm 7\%$ at $m_H = 125$ GeV.

- Higgs with 1,2 and 3 jets; Higgs with top +one jet are known upto NLO level

Conclusions

- Fixed order QCD corrections to gluon fusion contribute bulk of the cross section

- Two loop EW corrections, mixed QCD-electroweak and $\boldsymbol{b}$ quark contributions account for $\mathbf{5\%}$ to gluon fusion

- $\boldsymbol{NNLL}$ resummation effects can be included through suitable central scale choice.

- At $\sqrt{\boldsymbol{S}} = \mathbf{8\%}$ TeV, the scale uncertainty varies between $\pm\mathbf{9\%}$ at $\boldsymbol{m_H} = \mathbf{125}$ GeV.
- the PDF $+\boldsymbol{\alpha_s}$ uncertainty varies between $\pm\mathbf{7\%}$ at $\boldsymbol{m_H} = \mathbf{125}$ GeV.

- Higgs with 1,2 and 3 jets; Higgs with top +one jet are known upto NLO level ● Higgs

Characterisation with MADGRAF frame work is a new tool in the market to analyse Higgs boson's spin-partity and its coupling to SM particles in a model independent way.